Università degli Studi di Napoli "Federico II"

Scuola Politecnica e delle Scienze di Base

Ph.D. in Chemical Sciences-XXVIII Cycle

Physico-chemical characterization of model bio-membranes and their interaction with potential therapeutic peptides

Ph.D. student

Stellato Marco Ignazio

Tutors

Prof.a Del Vecchio Pompea

Prof. Petraccone Luigi

Supervisor

Prof. Merlino Antonello

Ph.D. Coordinator

Prof. Paduano Luigi

Alla mia famiglia

“La natura non fa nulla invano”

Aristotele

Index

Chapter 3- Material and Methods

Chapter 4- Results and Discussion: Physico-chemical characterization of the interaction of the antimicrobial peptide Myxinidin and its mutant WMR with liposomes mimicking *P.aeruginosa* and *E.coli* cell membranes

Chapter 5- Structural characterization of Myxinidin and WMR in micelles and bicelles

Chapter 6- Effect of an unusual lipid A covalently linked to a hopanoid moiety on the stability of model bio-membranes

Abbreviations

AMPs = Antimicrobial Peptides

Arg = Arginine

CD = Circular Dichroism

CL= Cardiolipin

CMC = Critical Micellar Concentration

DihepPC =1,2-diheptanoyl-*sn*-glycero-3-phosphocholine

DLS = Dynamic Light Scattering

DMPC-d_{54}= 1,2-dimyristoyl-d_{54}-*sn*-glycero-3-phosphocholine

DMPG = 1,2-dimyristoyl-*sn*-glycero-3-phospho-(1'-rac-glycerol) (sodium salt)

DOPE = 1,2-dioleoyl-*sn*-glycero-3-phosphoethanolamine

DOPG = 1,2-dioleoyl-*sn*-glycero-3-phospho-(1'-*rac*-glycerol) (sodium salt)

DPPC = 1,2-dipalmitoyl-*sn*-glycero-3-phosphocholine

DPPE = 1,2-dipalmitoyl-*sn*-glycero-3-phosphoethanolamine

DPPG = 1,2-dipalmitoyl-*sn*-glycero-3-phospho-(1'-*rac*-glycerol) (sodium salt)

DSC = Differential Scanning Calorimetry

EPR= Electron Paramagnetic Resonance

Fig. = Figure

GUVs=Giant Unilamellar Vesicles

HoLA = Hopanoid covalently linked to BTAi1 lipid A

ITC = Isothermal Titration Calorimetry

Lys = Lysine

LPS = Lipopolysaccharide

LUVs = Large Unilamellar Vesicles

MHC = Maximum Hemolytic Concentration

MIC = Minimum Inhibitory Concentration

MLVs= MultiLamellar Vesicles

NMR = Nuclear Magnetic Resonance

PBS = buffer 0.010M Na_2HPO_4; 0.002M KH_2PO_4; 0.135M NaCl; 0.0027M KCl; pH=7.4.

n-PCSL = 1-acyl-2-[*n*-(4,4-dimethyloxazolidine-*N*-oxyl)]stearoyl-*sn*-glycero-3-phosphocholine

POPE = 1-palmitoyl-2-oleoyl-*sn*-glycero-3phosphoethanolamine

POPG = 1-palmitoyl-2-oleoyl-*sn*-glycero-3-phospho-(1'-*rac*-glycerol) (sodium salt)

SDS-d_{25}= sodium dodecyl sulfate-d_{25}

SUVs= Small Unilamellar Vesicles

TFE = 2,2,2-trifluoroethanol

UV-VIS = Ultraviolet-Visible

Trp = Tryptophan

Tyr = Tyrosine

VLCFA = Very Long-Chain Fatty Acids

Preface

In the present Ph.D. thesis an extensive structural and functional study on model bio-membranes is presented. The first part of my research has been focused to understand how the lipid composition of the bio-membranes affects their biophysical properties and modulates their interactions with peptides. One of the biological processes involving lipid composition is the interaction between antimicrobial peptides (AMPs) and biological membranes. In fact, the selective interaction of AMPs with prokaryotic cells arises from the difference in the chemical composition between prokaryotic and eukaryotic membranes. The interest for detailed studies of these interaction processes has an important biological relevance because AMPs are potential candidate drugs that could resolve the emergence of the antibiotic resistance caused by pathogenic bacteria. Different mechanisms of membrane destruction induced by AMPs have been proposed, depending on physico-chemical properties of both the peptides and the target bio-membranes. Among the large number of AMPs present in nature, Myxinidin, from hagfish (*Myxine glutinosa L.*), is a promising antimicrobial candidate due to its antibacterial activity against different pathogenic Gram negative and Gram positive bacteria (*1, 2*). Starting from the natural hagfish peptide, some analogues were designed to enhance the antibacterial activity and one of these, named WMR, have shown excellent antimicrobial activity on different bacterial strains (*2*). This thesis reports a comparative study of the interaction between Myxinidin and its mutant WMR with two model bio-membranes at different composition and complexity. In particular, in order to understand the role of lipid composition in the peptide-membrane interaction, two different models of bio-membranes have been studied mimicking *P. aeruginosa* and *E. coli* cell cytoplasmic membranes. The final goal was to elucidate the effect of amino acid residues substitutions of the peptides and the role of lipid composition on the antibacterial activity of Myxinidin and WMR against these two model bio-membranes. The collected data have allowed to recognize the AMPs specificity for a particular lipid composition and to propose a mechanism of membrane destabilization.

In order to study the role of lipid composition in biological processes, another important model of bio-membrane has been studied. In particular the work has been focused on a particular model of bio-membrane representative of *Bradyrhizobium BTAi1* Gram negative bacterium, containing an unusual lipopolysaccharide (LPS) in which the lipid A is covalently linked to a hopanoid moiety(*3*). The aim of this study was to understand the effect of this unique lipid A in modulating the stability and rigidity of the outer membrane of *Bradyrhizobium BTAi1*strain .

To obtain a wide physico-chemical characterization of the analyzed systems, a combined experimental strategy has been adopted including spectroscopic and calorimetric techniques such as Circular Dichroism (CD) to study the secondary structure of peptides and its changes in lipid environment; Fluorescence to estimate the microenvironment of the peptides in the vesicles; Dynamic Light Scattering (DLS) to estimate the size and distribution of the liposomes in the absence and in the presence of peptides; (NMR) to obtain information about the conformation of the peptides in membrane environment; Electron Paramagnetic Resonance (EPR) to investigate the dynamics of the lipid hydrophobic tail in the bilayer; Differential Scanning Calorimetry (DSC) to understand the thermotropic behavior of liposomes and the effect of peptides on their phase transition; Isothermal Titration Calorimetry (ITC) to study the energetic of the interaction process between peptides and liposomes.

References

(1) Subramanian, S., Ross, N. W., and MacKinnon, S. L. (2009) Myxinidin, a novel antimicrobial peptide from the epidermal mucus of hagfish, Myxine glutinosa L. *Mar Biotechnol (NY) 11*, 748-57.

(2) Cantisani, M., Leone, M., Mignogna, E., Kampanaraki, K., Falanga, A., Morelli, G., Galdiero, M., and Galdiero, S. (2013) Structure-activity relations of myxinidin, an antibacterial peptide derived from the epidermal mucus of hagfish. *Antimicrob Agents Chemother 57*, 5665-73.

(3) Silipo, A., Vitiello, G., Gully, D., Sturiale, L., Chaintreuil, C., Fardoux, J., Gargani, D., Lee, H. I., Kulkarni, G., Busset, N., Marchetti, R., Palmigiano, A., Moll, H., Engel, R., Lanzetta, R., Paduano, L., Parrilli, M., Chang, W. S., Holst, O., Newman, D. K., Garozzo, D., D'Errico, G., Giraud, E., and Molinaro, A. (2014) Covalently linked hopanoid-lipid A improves outer-membrane resistance of a Bradyrhizobium symbiont of legumes. *Nat Commun 5*, 5106.

Chapter 1

Biological membranes

1.1 Introduction

The biological membranes are essential and common components of different cell types and they define the barrier between inner components (organelles) and the surrounding environment of the cells (plasma membrane). Due to its position of interface, the plasma membrane plays an important role of selective filter, favoring the passage of some substances rather than others. In particular liposoluble molecules move across the membrane by diffusion, whereas those not soluble are unable to cross this barrier without the contribute of specific proteic channel or specific transport proteins(carrier).In fact, the plasma membrane surface is a cellular communication area, thanks to the presence of specific receptors that allow the exchange information between intracellular and extracellular environment. In particular, cellular membranes are constituted by many proteins embedded in a bilayer of phospholipids according to the fluid-mosaic model (*1*).The basic concept of this model, introduced by Singer and Nicolson, suggests that lipids have only a barrier and communication function between the interior and outside cell world. On the contrary the heterogeneity and the non-random mixing of the lipids in a bilayer underline an active role of the lipid composition on the bio-membranes function and domains formation (*2*).

1.2 Lipid components in the membranes

An interesting question about cellular membranes is: Why does the nature use many different lipids in various bio-membranes? The answer for the great variety of lipids found in different types of biological membranes is an unsolved problem that many researcher are studying in the last years.

Although the basic structure of biological membranes is the lipid bilayer with a thickness of around 5 nm (Gorter and Grendel 1925) containing dynamic proteins with specific functions and some carbohydrates (Fig.1.2.1), a large amount of different lipids is present(*3*).

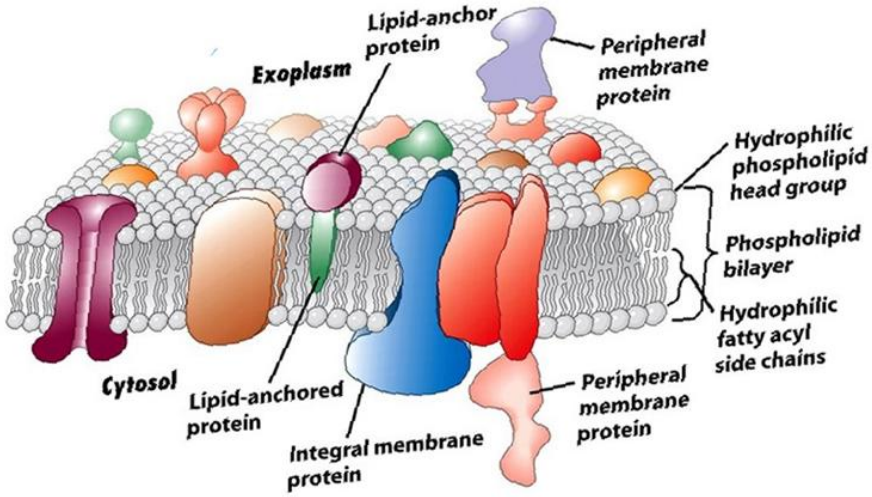

Fig.1.2.1 Biological membrane structure. Taken and modified by:
(Lodish et al. Molecular Cell Biology, Sixth Edition , 2008, W.H. Freeman and company)

The principal classes of lipids present in the membranes are: glycerophospholipids, sphingolipids and closely-related sterols.

The glycerophospholipids are the main components of biological membranes formed by a glycerol backbone, two ester-linked fatty acyl chains and a phosphorylated alcohol, typically phosphorylcholine (PC), phosphorylethanolamine (PE), phosphorylserine (PS), phosphorylglycerol (PG). All the glycerophospholipids are derived by phosphatic acid and they take the name by the

polar head group. The fatty acyl chains usually present an even and variable number of carbon atoms, typically between 16 and 20 in total, with one hydrocarbon chain being saturated and the other unsaturated in different eukaryotic and prokaryotic membranes. The chemical structures of two representative glycerophospholipids are reported in Fig.1.2.2.

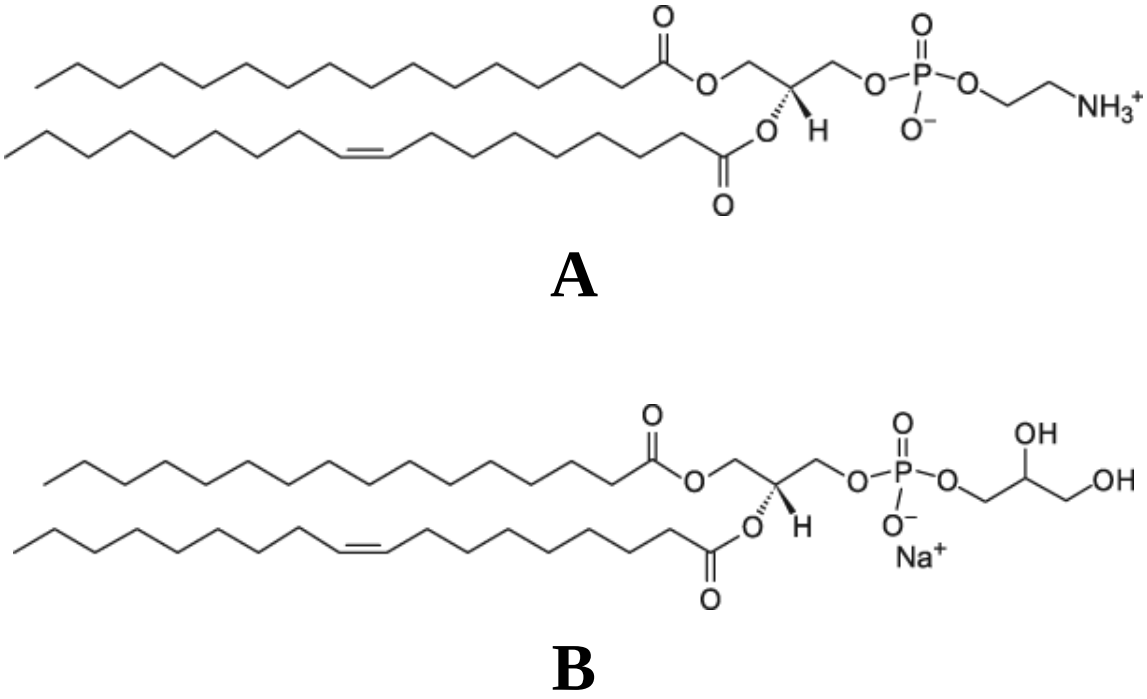

Fig.1.2.2 The chemical structures of two representative glycerophospholipids: A)1-palmitoyl-2-oleoyl-*sn*-glycero-3-phosphoethanolamine (POPE); B) 1-palmitoyl-2-oleoyl-*sn*-glycero-3-phospho-(1'-*rac*-glycerol) (sodium salt)(POPG)

Interestingly, a different lipid composition has been found in Archaeabacteria. In fact, in these microorganisms the nonpolar saturated isoprenyl groups (phytanyl) are connected to the glycerol backbone by ether rather than ester linkage at the 2- and 3- position (archeol) (Fig.1.2.3).These structural properties may help these bacteria to resist the extreme conditions, such as low pH, high temperature (*4*).

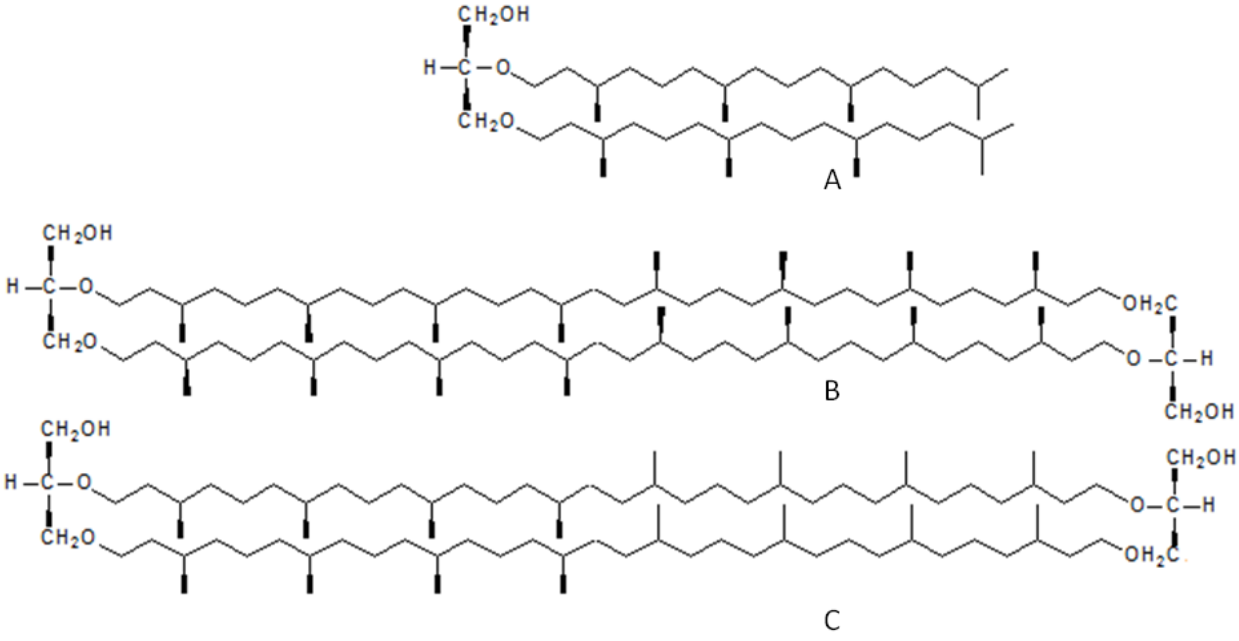

Fig.1.2.3 The chemical structures of representative phospholipids in Archeabacteria: A) 2,3-diphytanyl-O-sn-glycerol (archaeol), B) caldarchaeol, C) isocaldarchaeol. Taken and modified by the website: http://www.lipidhome.co.uk/lipids/complex/archaea/index.htm

The sphingolipids are another important class of lipids present in the eukaryotic membranes, they are aliphatic amino alcohol sphingosine derivates. They contain a single amide-linked fatty acyl chain, which is usually saturated and may contain up to 24 carbon atoms, and either a phosphorylated alcohol, or one or more sugar molecules linked to the hydroxyl terminus of the sphingosine backbone. The most important example of sphingolipids is the sphingomyelin, indispensable for neuronal cells (Fig.1.2.4).

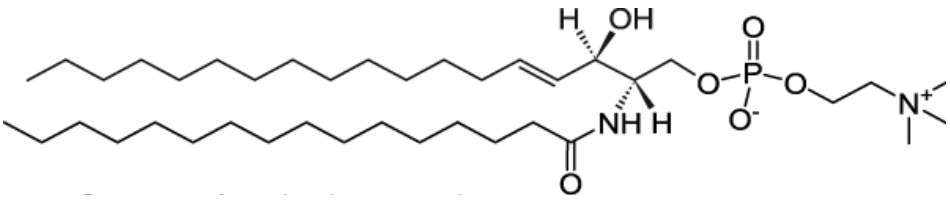

Fig.1.2.4 Chemical structure of the sphingomyelin

Finally, sterols and other structurally similar molecules have been found in eukaryotic and prokaryotic membranes. They are synthesized via the mevalonate pathway of isoprenoid metabolism (*5*). Cholesterol is the most known sterol present in the animal membranes and its structure consists of four linked hydrocarbon rings forming the bulky steroid structure, containing a single polar hydroxyl group and an isooctyl side chain (Fig.1.2.5).

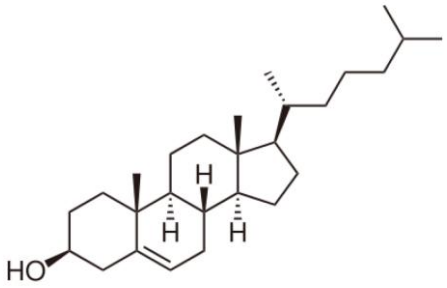

Fig.1.2.5 Chemical structure of the Cholesterol

In contrast to animal membranes, the main sterols present in the plant membranes are sitesterols, stigmasterol, campesterols, whereas fungi membranes contain mainly ergosterol. These sterols differ from cholesterol in their side chain and in the presence of additional double bonds in the ring system. (*6*)(Fig.1.2.6).

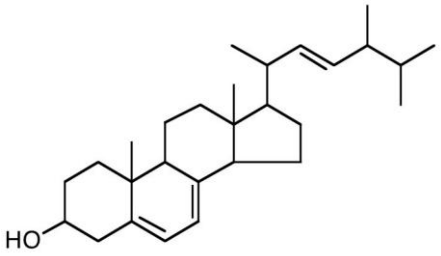

Fig.1.2.6 Chemical structure of the ergosterol

In prokaryotic membranes different unusual kinds of lipids similar to cholesterol have been found. These sterol analogues are named hopanoids, which belong to the wide group of triterpenoids, comprising a great variety of compounds (*7*). A more accurate description of a particular hopanoid (Fig.1.2.7) found in a bacterial membrane will be discussed in the Chapter 6.

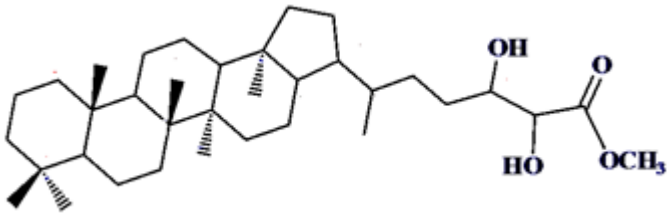

Fig.1.2.7. Chemical structure of the hopanoid of *Bradyrhizobium* BTAi1 bacterium

1.3 Difference between eukaryotic and prokaryotic membranes

Eukaryotic (mammalian) and prokaryotic (bacterial) membranes are formed by two leaflets (inner and outer) that differ in the lipid composition. The outer leaflet of eukariotic membranes is rich in zwitterionic lipids, mainly phosphatidylcholine (PC), sphingolipids and cholesterol. Their relative proportions vary depending on the species and cell type in vertebrates, but typically the percentages (mol/mol) of different classes of lipids found in the mammalian plasma membranes are: 40-60% for glycerophospholipids, 10-20% sphingolipids and 30-40% cholesterol (*8*). Although the phospholipids are asymmetrically present in the inner and outer leaflets of the membranes, in human red blood cells the inner leaflet is formed mainly by phosphatidylethanolamine (PE), phosphatidylserine (PS) and phosphatidylinositol (PI), whereas phosphatidylcoline (PC) and sphingomyelin have been found in the outer leaflet.

In contrast to eukaryotic membranes, bacterial cytoplasmic membranes have a high percentage of anionic lipids such as phosphatidylglycerol (PG), -serine (PS), diphosphatidylglycerol (Cardiolipin), besides their zwitterionic phosphoethanolamine (PE). The ratio between anionic and zwitterionic lipids depends on the type of bacteria (*9*) and the relative amount of the lipids dramatically change during the bacteria's life cycle (*10*).

Cardiolipin, which is present in many types of Gram negative and Gram positive bacteria, plays an interesting role in bacterial membranes (*9*). The presence of Cardiolipin has been also found in the inner mitochondrial eukaryotic membranes, where it serves as a proton source in proton-pumping during ATP synthesis and in transduction processes (*11, 12*). Cardiolipin is an unique anionic monovalent phospholipid, that was first found in the beef heart by Mary Pangborn in 1947 (*13*). It has a dimeric structure in which two phosphatidyl moieties are linked by a glycerol. At physiological pH it is not fully ionized due to the intra-molecular hydrogen bonding between the protonated phosphate and the free hydroxyl of the central glycerol and for this reason it has a single negative charge at pH 7.0 (*14*). In addition, the acyl chain composition of the Cardiolipin strongly varies depending on the species, tissues and cell types of the organism. The reason of this variability has been attributed to the environmental conditions adaptation (salt concentration, percentage of bivalent cations, temperature) of the species (*15*). It also appears to be dependent on the organism age. Further, the high Cardiolipin turnover rate in mitochondrial and bacterial membranes quickly changes the level and redistribution of this lipid in the membranes (*16*).

1.4 Two different bacterial membranes: Gram positive and Gram negative bacteria

Bacteria have developed a complex cell envelope composed by a series of layers. Their organization allows to distinct two different classes of bacteria: Gram positive and Gram negative bacteria (Fig.1.4.1).

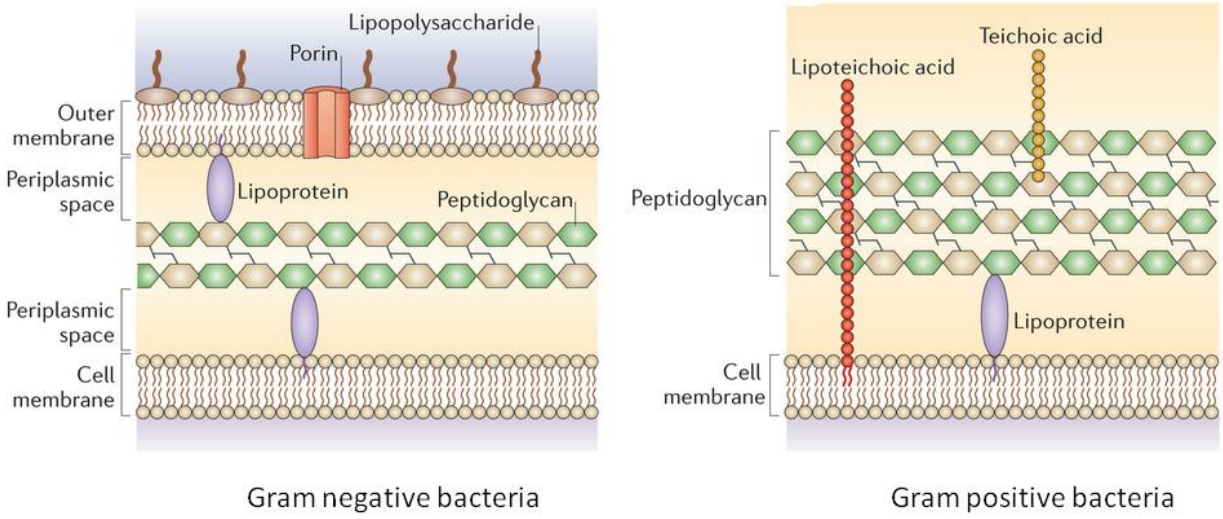

Fig.1.4.1 Difference between Gram negative and Gram positive bacteria. Taken and modified by: (Lisa Brown et al. Nat Rev Microbiol 2015, 13(10):620-30.)

In the Gram-positive bacteria, cytoplasmic membrane is formed by a lipid bilayer hosting proteins and has a higher percentage of anionic lipids (PG and Cardiolipin) respect to Gram negative bacteria membrane. Further, it is in turn surrounded by a thick cell wall (20 ÷ 80 nm) composed by peptidoglycan (or murein), that confers mechanical resistance to the cell. From this cell wall, protrude polyanionic molecules named Teichoic Acids (TAs) and Lipoteichoic Acids (LTAs) with antigenic function (*17*).In particular, LTAs are embedded in the cytoplasmic membrane through a lipid anchor (acylated glycerol), while TA are directly linked to muramic acid of the peptidoglycan through a phosphodiester bond (*18*).

On the contrary, the cell envelope of Gram negative bacteria is formed by a cytoplasmic membrane, composed by a high percentage of zwitterionic lipids (PE).

In this case, the murein layer thickness is lower and a second membrane, the outer membrane (OM), encloses the cell wall. The outer membrane is composed by glyceropospholipids and lipoproteins in the inner leaflet and by lipopolisaccharides (LPS) in the outer leaflet. Lipopolisaccharides (LPS) contribute to the integrity and the protection of bacterial cell envelope, covering about 75% of bacterial surface area (*19*).

The LPS architecture is organized into three biogenetically and chemically distinct regions:

1) the Lipid A
2) the Core, hetero-oligosaccharide
3) the O-chain, hydrophilic hetero-polysaccharide

In Figure 1.4.2 is reported a schematic structure of a lipopolysaccharide (LPS).

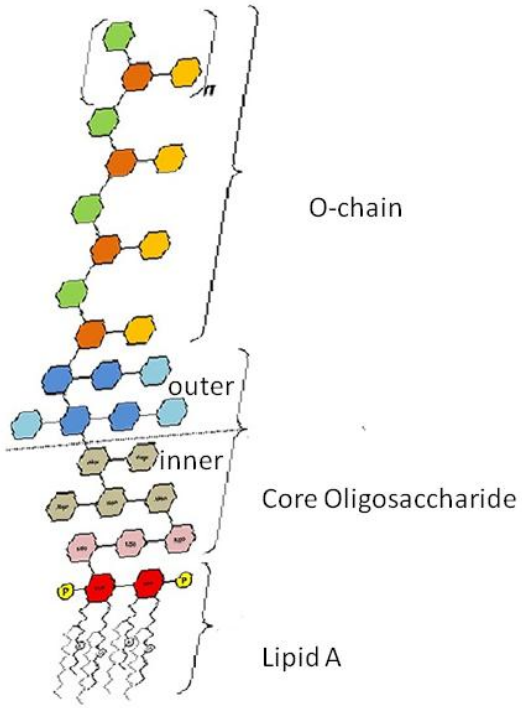

Fig. 1.4.2 Structure of a lipopolysaccharide.

Taken and modified by: (Serrato RV. Front. Cell. Infect. Microbiol., 2014 (3);4:119)

Moving from the inside of the cell, the first portion of a LPS is the glycolipid named lipid A, to which the Core oligosaccharide is covalently linked. Lipid A is the most conservative part of a LPS and consists of a disaccharide backbone with multiple fatty acid tails. On the contrary the Core oligosaccharide consist of two regions: Inner and Outer Core. The Inner Core is more conservative and contains peculiar monosaccharides, whereas the Outer Core has a higher structural variability. The structural element common to all bacterial Core oligosaccharide regions is the presence of a distinctive acid monosaccharide, the 3-deoxy-D-manno-oct-2-ulo pyranosonic acid (Kdo) residue, which is always present and allows the linkage of the Core to the lipid A.

Finally, the O-chain represents the most variable part of the LPS and constitutes the antigenic determinant, specifically recognized by the host acquired immune system, that produces antibodies against them.

These three part of LPS are strongly influenced by external factors and their response confers to the bacteria a specific resistance to particular molecules such as antibiotics.

1.5 Fluidity of the membranes

The variety of the lipid composition confers a different fluidity to the bio-membranes. It has been shown that the function of integral proteins can be regulate by the local fluidity of the lipid bilayer and by the lipid composition at the protein-lipid interface (*3, 20*). In fact, the presence of particular lipids provides a local membrane environment of appropriate viscosity, pivotal to the protein function. Different factors influence bio-membrane fluidity: length fatty acids, degree of unsaturation of fatty acid tails of phospholipids, temperature, characteristics of polar head group and the presence of sterols (such as cholesterol for eukaryotic membranes). The principal lipid lamellar phases are the gel (L_β), the fluid or liquid crystalline (L_α) and the liquid ordered (L_o) phases. Cells contain commonly the lipids in the gel or liquid-crystalline phase, which are characterized by a different motional freedom, mobility and spatial arrangement of each lipid (*21*).

The gel phase (L_β) is characterized by the presence of phospholipids chains in a fully extended all-trans conformation, the order parameter (S value) of acyl chain segment is high, the thickness of the bilayer is maximum, the mobility of the phospholipids is restricted and the cross-sectional area of the phospholipid molecule is minimal. On the contrary, the fluid or liquid-crystalline (L_α) phase is characterized by some gauche rotational conformers, the intra and intermolecular motions are fast, the S value is low. Fig. 1.5.1 shows the schematic arrangement of lipids into the gel (L_β) and liquid crystalline (L_α) phases.

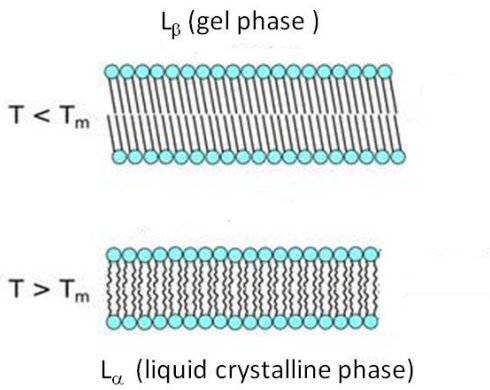

Fig.1.5.1 Representation of the gel (L_β) and liquid crystalline (L_α) phase of the liposomes. Take and modified by the website: http://physwiki.ucdavis.edu/Wikitexts/UCD_BPH241/The_fluid_phase

In the presence of sterols such as cholesterol for eukaryotic membranes, a liquid ordered (L_o) phase takes place. This phase has intermediate properties between gel (L_β) and liquid crystalline (L_α) phase (*22*, *23*).

Lipid bilayers have definite melting temperature (T_m), depending on the type of phospholipids, such as the nature of polar head, the length of acyl chains, the degree of unsaturation. The melting temperature is directly proportional to the length of the fatty acids and inversely correlated to the number of unsaturation present in acyl chain lipids. The increase of T_m at increasing of the length of carbon chain is due to the major number of the van der Waals interactions between the carbon chains, whereas the decrease of melting temperature on the increase of number of unsaturation is due to lower packing between lipids acyl chain.

At temperatures lower than the melting ones, the bilayer is present in gel phase (L_β), whereas at higher temperature the liquid crystalline (L_α) phase occurs. A large number of studies demonstrated that, at physiological temperature, the gel phase is not dominant in biological membranes (*24*), due to the presence of high number of unsaturated lipids in the inner mitochondrial and endoplasmic

reticulum membranes (*25*) (*26*). In addition, the preference of membrane proteins to exert their activity in the fluid phase than that in gel phase confirms the importance of the lipid phase in proteins regulatory functions in the membranes (*27, 28*). These studies confirm the importance of lipid composition and phase in biological processes in which the membranes play a key function.

Other different lipid phases have been found in addition to two main gel (L_β) and liquid crystalline (L_α) phases. In particular, lipids with small head group and large hydrophobic core (cone shape) such as phosphatidylethanolamine (PE) have the ability to form a hexagonal (H_{II}) phase at high temperatures (*4*). Other lipids with the same molecular shape can exist in this exotic phase in the presence of cationic bivalent ions. This is the case of the Cardiolipin in the presence of Ca^{2+} ions. The reason of the formation of this exotic phase is due to the capture of the internal aqueous core by the polar head groups and the resulting exterior orientation of the hydrophobic tails (inverted micelle). On the contrary lipids with a head group and hydrophobic tail of the similar size (cylinder shape), such as phosphatidylcholine (PC), and phosphatidylglycerol (PG), usually form gel (L_β) and liquid crystalline (L_α) phases (*4*).

1.6 Lipid rafts

It is well known that sphingolipids have different structures than most biological glycerophospholipids. In fact, sphyngolipids have saturated acyl chains that confer them a higher melting temperature than glyceropospholipids. The different lipids acyl chain packing between sphingolipids and phospholipids leads to phase separation in the membranes. In addition, the existence of lipid rafts in the membranes containing sphingomyelin and cholesterol has been shown. The lipid raft concept, introduced by Simon and van Meer in 1988, explains the existence of micro-domains enriched in glycolipids in the epithelial cells (*29*). The lipid rafts were later defined as nanoscale sterol-, sphingolipid-enriched ordered assemblies of proteins in which lipid-lipid, protein-protein, lipid-protein interactions occur (*30*). Further, an important function of these micro-domains in signal transduction has been shown (*31-34*). Recent studies stressed that lipid rafts in eukaryotic membranes are target of proteins such as Reggie or Flotillin-1, involved in the regulation of vesicle trafficking, cytoskeleton rearrangement (*35*). These micro-domains are capable to bind glycosylphosphatidylinositol (GPI)-anchored proteins, transmembrane proteins and acylated tyrosine kinases of the Src family (*36-38*). To evidence that also bacterial membranes contain lipid rafts with similar function to those of eukaryotic membranes, Daniel Lopez and collegues showed

the existence of these micro-domains containing polyisoprenoids in *B. subtilis* and *S. aureus* strains (*39*). In addition, an important paper on the lipid rafts published in Neuroscience field has shown the crucial role of these lipid raft for neural development and function, confirming their importance and universal presence in different cell types (*40*).

1.7 Model of membranes: Liposomes, micelles and bicelles

The high complexity of bio-membranes composition has forced the scientists to develop simply models in order to mimic the membranes. Liposomes (or vesicles) are the most common bio-mimetic systems including the lipid bilayers.

Liposomes are spherical vesicles formed by one of more phospholipid bilayers (*41*). They were discovered by Bangham and Horne by electron microscope in the early 1960's (*42*). It is possible to explain the formation of the liposomes considering the amphiphilic nature of the lipid molecules. In fact, lipids have hydrophilic (polar) head groups and hydrophobic (apolar) tails and in aqueous solution they spontaneously form structures with internal aqueous medium bounded by lipid bilayer, forming the liposomes (Fig.1.7.1).

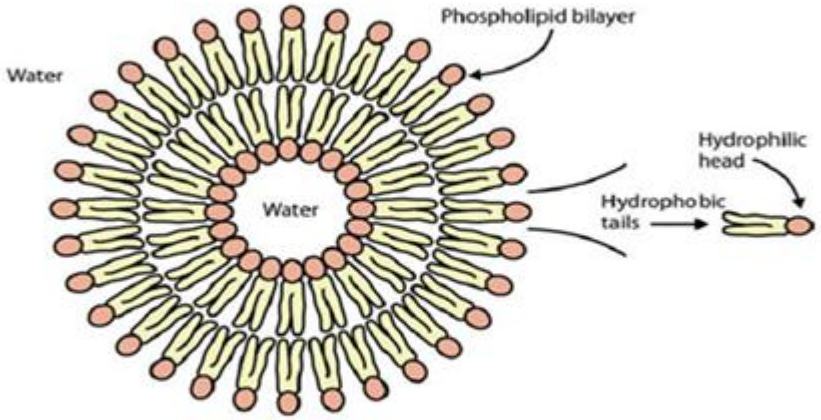

Fig.1.7.1 Schematic representation of a liposome. Taken and modified by: (Helen Watson. Biological membranes Essays Biochem. (2015) 59, 43–70)

The great advantage of the liposomes is the flexibility on the preparation method. In this way liposomes of different size, lamellarity, charge and composition can be prepared in order to mimic both eukaryotic and prokaryotic membranes.

Based on size and lamellarity, the liposomes can be classified in four main classes:

- ✓ GUVs (Giant Unilamellar Vesicles)
- ✓ MLVs (MultiLamellar Vesicles)
- ✓ LUVs (Large Unilamellar Vesicles)
- ✓ SUVs (Small Unilamellar Vesicles)

Giant Unilamellar Vesicles (GUVs) are the best model to visualize the lipid rafts and the phase separation in the membranes, due to their average diameter of 100 μm. (*43*). The most frequently used protocol to obtain these vesicles is termed electroformation, that consists in the application of a static electric field to a phospholipid deposit (*44*).

MultiLamellar Vesicles (MLVs) are formed by concentric bilayers and they have a large average diameter > 500 nm. These MLVs are quickly prepared, but their lamellarity depend on the lipid composition and hydration method.

Large Unilamellar Vesicles (LUVs) are liposomes with an average diameter between 100 and 500 nm and they are prevalently produced by extrusion method (*45*). To obtain LUVs of specific size, MLVs have to pass through a pore of specific diameter and the size of the liposome obtained depend on the filter pore used in the extrusion procedure.

Small Unilamellar Vesicles (SUVs) are similar to LUVs with an average diameter in the range 20-100 nm. They are produced by sonication process, which uses the pulsed, high frequency sound waves that disrupt MLVs and produce SUVs (*46*).

The variety of the nature and physico-chemical properties of the lipids can induce the formation of different lipid structures in aqueous solution. In fact, phosholipids with short alkyl chains (<14 atoms of carbon) and detergents do not form liposomes in aqueous solution, but they self associate in micelles (*4*). Differently from liposomes, micelles are closed structures without the internal aqueous medium. Lipids with a high propensity to form micelles instead of liposomes in aqueous solution are those containing a large polar head group and small hydrophobic tails. Sodium dodecyl sulfate (SDS) is the most studied lipid capable to form micelles in aqueous solution.

The micelle formation in aqueous solution is a phenomenon depending on the lipid concentration and this process is facilitated above a threshold concentration, typical of each lipid. This lipid concentration is the Critical Micellar Concentration (CMC) and depends on the type of lipid, dielectric constant of medium and temperature. The CMC value for SDS is 8.2 mM in pure water at 25°C (*47*). The disadvantages of micelles as model membranes are the high curvature and the content of detergents. More recently, bicelles have been introduced in order to develop more accurate model membranes (Fig.1.7.2).

Fig.1.7.2 Comparison between micelles and bicelles. Taken and modified by: (C. O. Rangel-Yagui et al. J. Chem. Eng. 2004 (21) 4)

Bicelles mimic membranes surface better than micelles, in fact they have a disk-shape, containing a central and planar bilayer formed by long chain phospholipids that is surrounded by detergent molecules or short chain phospholipids (*48*). These models of bio-membranes have been used in solution and solid state NMR, thanks to their propensity to align their axis in the presence of a magnetic field.

All these models are largely used as membrane mimetics and the choice of each than others depends on the nature and the physico-chemical properties of the phospholipids that mimic the lipid composition of the studied membrane and on the experimental technique used .

1.8 Lipid-peptide interactions

The interaction between lipids and peptides plays a pivotal role in different cellular processes such as the lipid transport in biological fluid (*49*), amyloid fiber formation(*50*), raft segregation in lipid bilayer (*51*), selective ion/molecule transport and signal trafficking across membranes (*52*), drug bioavailability across blood-brain barrier, antimicrobial defense mechanism, signal reception and transduction, viral fusion, membrane-membrane interactions (*53-55*). From the peptide side, it is well-established that a combination of molecular features drives the membrane interaction, including the amino acid sequence, the residue spatial distribution as determined by folding, conformational changes and aggregation at the membrane site (*56*). In essence peptide-membrane interactions depend on physico-chemical properties of the peptides and the lipid composition of the target cell membrane. It is well known that the bilayer composition regulates the physico-chemical properties of the different types of the membrane, such as curvature, elasticity, surface charge and this reflects on the attitude to interact with peptides. An important example of biological process based on the fine protein/lipid interplay is the fusion of the phospholipid membrane enveloping a virus with target cell, which is a fundamental step in viral infection (*57*). A sequence of energetically unfavorable events between the envelope and the target membranes for entry into the cells are facilitated by the action of specific viral membrane glycoproteins that undergo conformational changes favoring micro- and mesoscopic lipid rearrangements (*58, 59*). Different protein domains cooperate, according to a concerted mechanism, in driving membrane fusion. In particular, in the case of the human immunodeficiency virus (HIV) and the feline analogue (FIV), a key role is played by the membrane-proximal external region (MPER) of the ectodomain of the respective fusion proteins, gp41 and gp36 (*60, 61*). Both MPER domains are unusually Trp-rich and are expected to show a marked tendency to reside at the viral envelope interface once exposed during the cascade of protein conformational changes promoting the fusion event (*62*). Another important process involving bio-membranes is the interaction with antimicrobial peptides (*63*), which is the principal object of this research project.

References

(1) Singer, S. J., and Nicolson, G. L. (1972) The fluid mosaic model of the structure of cell membranes. *Science 175*, 720-31.

(2) Wisniewska, A., Draus, J., and Subczynski, W. K. (2003) Is a fluid-mosaic model of biological membranes fully relevant? Studies on lipid organization in model and biological membranes. *Cell Mol Biol Lett 8*, 147-59.

(3) Cronan, J. E., Jr., and Gelmann, E. P. (1975) Physical properties of membrane lipids: biological relevance and regulation. *Bacteriol Rev 39*, 232-56.

(4) De Rosa, M., Gambacorta, A., and Gliozzi, A. (1986) Structure, biosynthesis, and physicochemical properties of archaebacterial lipids. *Microbiol Rev 50*, 70-80.

(5) Schaller, H. (2003) The role of sterols in plant growth and development. *Prog Lipid Res 42*, 163-75.

(6) Matyash, V., Entchev, E. V., Mende, F., Wilsch-Brauninger, M., Thiele, C., Schmidt, A. W., Knolker, H. J., Ward, S., and Kurzchalia, T. V. (2004) Sterol-derived hormone(s) controls entry into diapause in Caenorhabditis elegans by consecutive activation of DAF-12 and DAF-16. *PLoS Biol 2*, e280.

(7) Sessions, A. L., Zhang, L., Welander, P. V., Doughty, D., Summons, R. E., and Newman, D. K. (2013) Identification and quantification of polyfunctionalized hopanoids by high temperature gas chromatography-mass spectrometry. *Org Geochem 56*, 120-130.

(8) van Meer, G. (1989) Lipid traffic in animal cells. *Annu Rev Cell Biol 5*, 247-75.

(9) Epand, R. F., Savage, P. B., and Epand, R. M. (2007) Bacterial lipid composition and the antimicrobial efficacy of cationic steroid compounds (Ceragenins). *Biochim Biophys Acta 1768*, 2500-9.

(10) Gidden, J., Denson, J., Liyanage, R., Ivey, D. M., and Lay, J. O. (2009) Lipid Compositions in Escherichia coli and Bacillus subtilis During Growth as Determined by MALDI-TOF and TOF/TOF Mass Spectrometry. *Int J Mass Spectrom 283*, 178-184.

(11) Junge, W., Panke, O., Cherepanov, D. A., Gumbiowski, K., Muller, M., and Engelbrecht, S. (2001) Inter-subunit rotation and elastic power transmission in F0F1-ATPase. *FEBS Lett 504*, 152-60.

(12) Oster, G., and Wang, H. (2000) Why is the mechanical efficiency of F(1)-ATPase so high? *J Bioenerg Biomembr 32*, 459-69.

(13) Pangborn, M. C. (1947) The composition of cardiolipin. *J Biol Chem 168*, 351-61.

(14) Kates, M., Syz, J. Y., Gosser, D., and Haines, T. H. (1993) pH-dissociation characteristics of cardiolipin and its 2'-deoxy analogue. *Lipids 28*, 877-82.

(15) Houtkooper, R. H., and Vaz, F. M. (2008) Cardiolipin, the heart of mitochondrial metabolism. *Cell Mol Life Sci 65*, 2493-506.

(16) Wahjudi, P. N., J, K. Y., Martinez, S. R., Zhang, J., Teitell, M., Nikolaenko, L., Swerdloff, R., Wang, C., and Lee, W. N. (2011) Turnover of nonessential fatty acids in cardiolipin from the rat heart. *J Lipid Res 52*, 2226-33.

(17) Archibald, A. R., Baddiley, J., and Shaukat, G. A. (1968) The glycerol teichoic acid from walls of Staphylococcus epidermidis I2. *Biochem J 110*, 583-8.

(18) Neuhaus, F. C., and Baddiley, J. (2003) A continuum of anionic charge: structures and functions of D-alanyl-teichoic acids in gram-positive bacteria. *Microbiol Mol Biol Rev 67*, 686-723.

(19) Lerouge, I., and Vanderleyden, J. (2002) O-antigen structural variation: mechanisms and possible roles in animal/plant-microbe interactions. *FEMS Microbiol Rev 26*, 17-47.

(20) Cullis, P. R., and de Kruijff, B. (1979) Lipid polymorphism and the functional roles of lipids in biological membranes. *Biochim Biophys Acta 559*, 399-420.

(21) van Meer, G., Voelker, D. R., and Feigenson, G. W. (2008) Membrane lipids: where they are and how they behave. *Nat Rev Mol Cell Biol 9*, 112-24.

(22) Brown, D. A., and London, E. (1998) Structure and origin of ordered lipid domains in biological membranes. *J Membr Biol 164*, 103-14.

(23) Brown, D. A., and London, E. (2000) Structure and function of sphingolipid- and cholesterol-rich membrane rafts. *J Biol Chem 275*, 17221-4.

(24) Cullis, P. R., and de Kruijff, B. (1978) The polymorphic phase behaviour of phosphatidylethanolamines of natural and synthetic origin. A 31P NMR study. *Biochim Biophys Acta 513*, 31-42.
(25) Gulik-Krzywicki, T., Rivas, E., and Luzzati, V. (1967) [Structure and polymorphism of lipids: x-ray diffraction study of the system formed from beef heart mitochondria lipids and water]. *J Mol Biol 27*, 303-22.
(26) Lee, T. C., and Snyder, F. (1973) Phospholipid metabolism in rat liver endoplasmic reticulum. Structural analyses, turnover studies and enzymic activities. *Biochim Biophys Acta 291*, 71-82.
(27) Grant, C. W., and McConnell, H. M. (1974) Glycophorin in lipid bilayers. *Proc Natl Acad Sci U S A 71*, 4653-7.
(28) Kleemann, W., and McConnell, H. M. (1976) Interactions of proteins and cholesterol with lipids in bilayer membranes. *Biochim Biophys Acta 419*, 206-22.
(29) Simons, K., and van Meer, G. (1988) Lipid sorting in epithelial cells. *Biochemistry 27*, 6197-202.
(30) Jiang, L., Bechtel, M. D., Galeva, N. A., Williams, T. D., Michaelis, E. K., and Michaelis, M. L. (2012) Decreases in plasma membrane Ca(2)(+)-ATPase in brain synaptic membrane rafts from aged rats. *J Neurochem 123*, 689-99.
(31) Brown, D. A., and Rose, J. K. (1992) Sorting of GPI-anchored proteins to glycolipid-enriched membrane subdomains during transport to the apical cell surface. *Cell 68*, 533-44.
(32) Brown, D. A., and London, E. (1998) Functions of lipid rafts in biological membranes. *Annu Rev Cell Dev Biol 14*, 111-36.
(33) Ikonen, E. (2001) Roles of lipid rafts in membrane transport. *Curr Opin Cell Biol 13*, 470-7.
(34) van Meer, G. (2002) Cell biology. The different hues of lipid rafts. *Science 296*, 855-7.
(35) Langhorst, M. F., Reuter, A., and Stuermer, C. A. (2005) Scaffolding microdomains and beyond: the function of reggie/flotillin proteins. *Cell Mol Life Sci 62*, 2228-40.
(36) Skibbens, J. E., Roth, M. G., and Matlin, K. S. (1989) Differential extractability of influenza virus hemagglutinin during intracellular transport in polarized epithelial cells and nonpolar fibroblasts. *J Cell Biol 108*, 821-32.
(37) Sargiacomo, M., Sudol, M., Tang, Z., and Lisanti, M. P. (1993) Signal transducing molecules and glycosyl-phosphatidylinositol-linked proteins form a caveolin-rich insoluble complex in MDCK cells. *J Cell Biol 122*, 789-807.
(38) Danielsen, E. M., and van Deurs, B. (1995) A transferrin-like GPI-linked iron-binding protein in detergent-insoluble noncaveolar microdomains at the apical surface of fetal intestinal epithelial cells. *J Cell Biol 131*, 939-50.
(39) Lopez, D., and Kolter, R. (2010) Functional microdomains in bacterial membranes. *Genes Dev 24*, 1893-902.
(40) Tsui-Pierchala, B. A., Encinas, M., Milbrandt, J., and Johnson, E. M., Jr. (2002) Lipid rafts in neuronal signaling and function. *Trends Neurosci 25*, 412-7.
(41) Sessa, G., and Weissmann, G. (1968) Phospholipid spherules (liposomes) as a model for biological membranes. *J Lipid Res 9*, 310-8.
(42) Bangham, A. D., and Horne, R. W. (1964) Negative Staining of Phospholipids and Their Structural Modification by Surface-Active Agents as Observed in the Electron Microscope. *J Mol Biol 8*, 660-8.
(43) Wesolowska, O., Michalak, K., Maniewska, J., and Hendrich, A. B. (2009) Giant unilamellar vesicles - a perfect tool to visualize phase separation and lipid rafts in model systems. *Acta Biochim Pol 56*, 33-9.
(44) Montes, L. R., Ahyayauch, H., Ibarguren, M., Sot, J., Alonso, A., Bagatolli, L. A., and Goni, F. M. (2010) Electroformation of giant unilamellar vesicles from native membranes and organic lipid mixtures for the study of lipid domains under physiological ionic-strength conditions. *Methods Mol Biol 606*, 105-14.
(45) Mui, B., Chow, L., and Hope, M. J. (2003) Extrusion technique to generate liposomes of defined size. *Methods Enzymol 367*, 3-14.

(46) Akbarzadeh, A., Rezaei-Sadabady, R., Davaran, S., Joo, S. W., Zarghami, N., Hanifehpour, Y., Samiei, M., Kouhi, M., and Nejati-Koshki, K. (2013) Liposome: classification, preparation, and applications. *Nanoscale Res Lett 8*, 102.

(47) Stanley, F. E., Warner, A. M., Schneiderman, E., and Stalcup, A. M. (2009) Rapid determination of surfactant critical micelle concentrations using pressure-driven flow with capillary electrophoresis instrumentation. *J Chromatogr A 1216*, 8431-4.

(48) Vestergaard, M., Kraft, J. F., Vosegaard, T., Thogersen, L., and Schiott, B. (2015) Bicelles and Other Membrane Mimics: Comparison of Structure, Properties, and Dynamics from MD Simulations. *J Phys Chem B 119*, 15831-43.

(49) Kalish, B. T., Fell, G. L., Nandivada, P., and Puder, M. (2015) Clinically Relevant Mechanisms of Lipid Synthesis, Transport, and Storage. *JPEN J Parenter Enteral Nutr 39*, 8S-17S.

(50) Berthelot, K., Cullin, C., and Lecomte, S. (2013) What does make an amyloid toxic: morphology, structure or interaction with membrane? *Biochimie 95*, 12-9.

(51) Harder, T., Rentero, C., Zech, T., and Gaus, K. (2007) Plasma membrane segregation during T cell activation: probing the order of domains. *Curr Opin Immunol 19*, 470-5.

(52) Clay, A. T., and Sharom, F. J. (2013) Lipid bilayer properties control membrane partitioning, binding, and transport of p-glycoprotein substrates. *Biochemistry 52*, 343-54.

(53) Marsh, D. (2008) Protein modulation of lipids, and vice-versa, in membranes. *Biochim Biophys Acta 1778*, 1545-75.

(54) Galdiero, S., Falanga, A., Cantisani, M., Vitiello, M., Morelli, G., and Galdiero, M. (2013) Peptide-lipid interactions: experiments and applications. *Int J Mol Sci 14*, 18758-89.

(55) Lee, A. G. (2011) Lipid-protein interactions. *Biochem Soc Trans 39*, 761-6.

(56) Teixeira, V., Feio, M. J., and Bastos, M. (2012) Role of lipids in the interaction of antimicrobial peptides with membranes. *Prog Lipid Res 51*, 149-77.

(57) Oliva, R., Del Vecchio, P., Stellato, M. I., D'Ursi, A. M., D'Errico, G., Paduano, L., and Petraccone, L. (2015) A thermodynamic signature of lipid segregation in biomembranes induced by a short peptide derived from glycoprotein gp36 of feline immunodeficiency virus. *Biochim Biophys Acta 1848*, 510-7.

(58) Plemper, R. K. (2011) Cell entry of enveloped viruses. *Curr Opin Virol 1*, 92-100.

(59) Falanga, A., Cantisani, M., Pedone, C., and Galdiero, S. (2009) Membrane fusion and fission: enveloped viruses. *Protein Pept Lett 16*, 751-9.

(60) Barbato, G., Bianchi, E., Ingallinella, P., Hurni, W. H., Miller, M. D., Ciliberto, G., Cortese, R., Bazzo, R., Shiver, J. W., and Pessi, A. (2003) Structural analysis of the epitope of the anti-HIV antibody 2F5 sheds light into its mechanism of neutralization and HIV fusion. *J Mol Biol 330*, 1101-15.

(61) Lorizate, M., Huarte, N., Saez-Cirion, A., and Nieva, J. L. (2008) Interfacial pre-transmembrane domains in viral proteins promoting membrane fusion and fission. *Biochim Biophys Acta 1778*, 1624-39.

(62) D'Errico, G., Vitiello, G., D'Ursi, A. M., and Marsh, D. (2009) Interaction of short modified peptides deriving from glycoprotein gp36 of feline immunodeficiency virus with phospholipid membranes. *Eur Biophys J 38*, 873-82.

(63) Chai, H., Allen, W. E., and Hicks, R. P. (2014) Spectroscopic investigations of the binding mechanisms between antimicrobial peptides and membrane models of Pseudomonas aeruginosa and Klebsiella pneumoniae. *Bioorg Med Chem 22*, 4210-22.

Chapter 2

Antimicrobial peptides

2.1 Antimicrobial peptides and the problem of antibiotic resistance

In the last decades the emergence of antibiotic resistance from microrganisms has become a great problem in the international community. Our knowledge about the antibiotics derives from the random discovery of the penicillin by Alexander Fleming in 1928 (*1*). Based on their mechanism of action, the antibiotics can be divided into different classes: i) those that inhibit cell wall synthesis (penicillin) (*1*); ii) those that interfere with protein synthesis (amino-glycosides); iii) folic acid metabolism (sulphonamide, trimethoprim); iv) DNA gyrase (quinolones); v) RNA synthesis (rifampicin) of the target bacteria. In turn, to assicure their survival, bacteria develop different antibiotic-resistance mechanisms: alteration of the antibiotic target site, enzymatic inactivation and/or variation of the permeability of the antibiotics in the bacterial cells (*2*). The capacity of the bacteria to evade modern chemotherapy and to evolve strategies for inactivating the most common antibiotics has prompted the medical research to the development of new alternative agents in the bacterial infection field. Antimicrobial peptides are the most promising potential candidate drugs that could resolve the antibiotic-resistance problem. The potency of these peptides is their ability to kill bacterial cells with different multi-factorial mechanisms of action, minimizing a possible collateral strategy of resistance. Different antimicrobial peptides have been studied in order to develop new selective therapeutic drugs against bacterial infections.

2.2 Diversity and physico-chemical properties of the antimicrobial peptides

Antimicrobial peptides (AMPs) are a heterogeneous class of compounds found in nature in different kingdoms of life (bacteria, fungi, insects, plants, microorganisms, amphibians, protozoa and mammals)(*3*).They are evolutionarily conserved components of the innate immune response of the multi-cellular organisms, constituting the first line of defense against pathogens (*4*). More of 2000 AMPs have been discovered until 2015 year (http://aps.unmc.edu/AP/main.php) (*5*).The biological diversity of the antimicrobial peptides is supported by their different biosynthetic pathway. In fact the most known AMPs are gene encoded, but some microorganism such as bacteria and fungi assemble these peptides by using a multiple-enzyme system, leading to post-translational modifications: halogenations, phosphorylation, incorporation of D-amino acid, amidation, glycosylation, hydroxylation(*6*) (Table 2.2.1).

Table 2.2.1 Post-translational modifications found in different AMPs

Modification	**Peptides**	**Reference**
glycosylation	diptericin drosocin pyrrhocorricin	(*7*) (*8*) (*9*)
halogenation	misgurin	(*10*)
amidation	melittin cecropin PGLa dermaseptin clavanin	(*11*) (*12*) (*13*) (*14*) (*15*)
phosphorylation	histatin	(*16*)
D-amino acid	bombinin	(*17*)
hydroxylation	cecropin B	(*18*)

Despite a large dissimilarity of AMPs primary sequence that defines a structural diversity, the evolution has conserved common physico-chemical properties indispensable for AMPs biological activity. Generally, antimicrobial peptides are small, amphipathic and cationic peptides at physiological conditions (*19, 20*). Normally, the length of the antimicrobial peptides varies between 12 and 50 amino acid residues, their positive charge due to lysine and arginine residues ranges from +1 to +9 and they often content about 50% of hydrophobic residues (*21*). In the folded conformation, these AMPs show amphipathic properties, exhibiting spatially separated charged and hydrophobic regions. These physico-chemical properties confer to AMPs a selective interaction with bacterial negatively charged membranes (*19*). It is believed that the electrostatic attraction between the positive charges of the antimicrobial peptides and the negative charges of the bacterial membranes is the first step of the interaction process. In fact, different studies have shown that the number of positively charged amino acid residues and their distribution in the peptide sequence have a relationship with the antimicrobial activity (*22*). The correlation between the positive charges of the peptide and its antimicrobial activity is not linear. In fact, a drastic enhancement of the positive charge (+7, +8, +9) of the peptide, surprisingly, causes a decrease or little changes of its antimicrobial activity and an increase of the unwanted hemolytic activity (*23, 24*). In fact the peptide (ovispirin-1), that has the highest positive charge density, is very cytotoxic (*25*) for mammalian cells. The decrease of the antimicrobial activity on the increasing of the positive charges probably is due to the reduced lifetime of the membrane permeabilization by the peptide and also to the correlation between excessive charge and the rearrangement of the secondary structure (*26*). The optimal charge for a high antimicrobial activity is found to be in the range from +4 to +6 (*26*). For a high antimicrobial activity,also, the distribution of the positively charged amino acids along the sequence of the peptide is important. Different studies have shown that a different localization of lysine and arginine residues and/or the cyclization in the linear AMPs containing these residues is linked to membrane lipid selectivity and thereby contributes to the different activity of the antimicrobial peptides (*27*). Although the cationicity is an important property of AMPs, a few anionic antimicrobial peptides have been discovered and their mechanism of action is completely different than most famous cationic antimicrobial peptides. For example, a human anionic antimicrobial peptide is the dermicidin, which is active against Gram negative and Gram positive bacteria and its mechanism of action include the presence of Zn^{2+} ions as cofactor (*28, 29*).

For AMPs an important role is also played by the hydrophobicity, which is indispensable for the partitioning of the peptides into lipid bilayer. It is known that an increase of this property is correlated to a decrease of the selectivity for the bacterial negatively charged membranes. In fact

studies in literature have shown that peptides containing a high number of hydrophobic residues have a strong toxicity towards eukaryotic cells, indicating a lost of the selective interaction with bacterial cells (*30*).

Another conserved and key element of the AMPs is their amphipathic nature, typical of the membrane active sequences. These peptides are capable to adopt amphiphilic shape with hydrophilic and hydrophobic residues situated in two distinct sides of the peptide. This property enhances the interaction and insertion of hydrophobic residues of the peptides with the apolar membrane lipid tails together with the interaction between the hydrophilic residues of the peptides and the head groups of the membranes. The amphipathicity of a peptide is quantitatively measured by hydrophobic moment (M_H) as proposed by Eisenberg (*31*), which is the vectorial sum of the hydrophobicity of all amino acids and it is referred at the α-helical conformation. There are controversial studies about the relationship between the amphipathicity and the activity of the AMPs. Different studies report that an increase of the amphipathicity of the antimicrobial peptides is correlated with an increase of the antibacterial but also hemolytic activity, suggesting a unfavorable contribution of this property to the selective interaction of the AMPs with bacterial target membranes (*32, 33*). Differently, other authors showed that arginine and tryptophan rich and cyclic hexapeptides have a selective interaction with bacterial membranes thanks to a perfect amphipathicity due to ideal positioning of positively charged arginine and hydrophobic tryptophan residues in the peptide (*34*).

In conclusion a reasonable and unique balance between the cationicity, hydrophobicity and amphipathicity of AMPs allows to obtain/design an ideal and selective drug for different bacterial strains with low toxicity against human mammalian cells.

2.3 Classification of the AMPs

A systematic classification of the AMPs is based on their secondary structure and amino acid composition. It is possible to identify four groups: a) linear cystein-free peptides with an α-helical conformation; b) β-sheet peptides stabilized by disulfide bridges; c) β-hairpin and looped peptides containing disulfide bonds; d) peptides rich in a specific amino acids such as proline, arginine, tryptophan. The most characterized AMPs that belong to the first class of linear cystein-free peptides with an α-helical secondary structure are: melittin, cecropin, magainin, dermaseptins. They adopt a random coil conformation in aqueous solution, but they form α-helical structures in membrane environment and this conformational change favors the permeabilization of these AMPs in bacterial membranes, enhancing their antimicrobial activity. These α-helical peptides have a tendency to form pore in the bacterial membranes, as it has been verified in the case of mellittin and magainin (*35*). However, the α-helical formation upon the binding with lipid bilayers is an important but not indispensable factor required for the antimicrobial activity of the AMPs (*36*).

The second class of the antimicrobial peptides includes protegrins, defensins, tachyplesins, lactoferrin. These peptides adopt a β-sheet conformation and they are conformationally more restrained than those with an α-helical secondary structure. In fact they have a cyclic structure due to the peptide backbone cyclization or by the presence of intramolecular disulfide bridges (*37*) and these peptides have moderate antimicrobial activity but also high hemolytic activity (*38*).

In the third class it is possible to find peptides such as lantibiotics, thanatin, that have looped structures containing disulfide bridges. These peptides often contain unusual structure containing thioether bridges due to the reaction between cysteine and the side chains of the serine residues. It has been shown that these peptides have a lower hemolytic activity than β-sheet peptides (*39*).

The fourth class of peptides is a heterogeneous group of AMPs, that have the common element to contain in their sequence an overrepresentation of specific amino acid residues such as glycine, proline, histidine, tryptophan and arginine. The most studied peptides that belong to this class are: indolicin (Ladokhin and White, 2001), triptrpticin (Lawyer et al., 1996), lactoferricin B (Bellamy et al., 1992), Pac-525 (Wei et al., 2006) rich in tryptophan; cathelicidin rich in proline (Anderson RC,2003); histatine rich in histidine (Frank G. Oppenheirn, 1998), clavanin rich in glycine (van Kan et al., 2002), PR-39 rich in arginine (Agerberth *et al.*, 1991).

Despite the low frequency of arginine and tryptophan residues in the most of known proteins, many AMPs contain an unusual high percentage of these two residues. Probably the nature uses the physico-chemical properties of two amino acids that confer to AMPs a potent activity against different bacterial strains. In particular the positively charged arginine has an important role in the initial electrostatic interaction with bacterial negatively charged membranes, whereas the importance of the tryptophan is due to its propensity to localize at the interface of the membranes, favoring a deeper and stronger penetration of AMPs into lipid bilayer (*40*).

2.4 Different mechanisms of action of AMPs

It is known that AMPs can interact with a plurality of target in bacterial cells. For example it has been found that the peptide PGLa interacts with negatively charged lipopolysaccharides (LPS), which are the main components of the outer membrane of Gram negative bacteria (*41*) and this interaction probably facilitates its entry in the periplasmic space of the bacterial cell. Other studies have indicated that antimicrobial peptides may target intracellular bacterial components, such as DNA, proteins and/or enzymes. For example indolicin (*42*), pleurocidin (*43*), PR-39 (*44*), HPN-1 (*45*) have been proposed to inhibit DNA and proteins synthesis; buforin II (*46*) and tachyplesin (*47*) to bind DNA and RNA; mersacidin to inhibit the cell-wall synthesis (*48*); histatin to inhibit enzymatic activity (*6*); PR-26 (*49*), microcin (*50*) to alter the cytoplasmic membrane septum formation; drosocin, pyrrhocoricin, and apidaecin (*51*) to inhibit the natural ATPase activity; GL13K (*52*) to reduce the bio-films formation in *Pseudomonas aeruginosa* bacteria. All these processes cause the death of the bacterial cells, suggesting that antimicrobial peptides are metabolic bacterial inhibitors.

Despite the heterogeneity of the possible target, the most known antimicrobial peptides principally interact with bacterial negatively charged cytoplasmic membranes causing their permeabilization and damage. This interaction process is modulated by the lipid membrane composition and depend on the physico-chemical properties of the peptides.

It is well known that both the peptides and the membranes may experience different structural changes (conformational changes, aggregation phenomena) (*53*) in this interaction process. In particular the possible effects of the peptides on the membranes are: pore formation, phase separation, clustering of particular classes of lipids, membrane thinning, promotion of non-lamellar phases, peptide-lipid aggregate formation, bilayer disruption (*54*).

In addition peptide-membrane interaction is strongly dependent on the peptide concentration or lipid/peptide ratio. In fact antimicrobial peptides exert their activity against a specific lipid membrane composition above a threshold peptide concentration, due to the peptide-peptide interaction (*55*).This peptide concentration is typically of each AMPs and depend on the targeted type of bacterial membrane.

In order to explain the AMPs mechanism of action, different models have been proposed, such as barrel-stave, toroidal and carpet-like models. The first step of these models is always the electrostatic interaction due to the positive charges of AMPs and the negative charges of the membranes. This step explains the selectivity of the antimicrobial peptides for bacterial over

mammalian cells, where instead zwitterionic lipids predominate at the cell surface. These electrostatic interactions cause an adsorption of the peptides on the membrane surface. At low peptide/lipid ratio, antimicrobial peptides adopt a parallel orientation respect to the membrane in all proposed models (*56*). At high peptide/lipid ratio and in particular above the threshold peptide concentration, there are differences between the three proposed models in the final step. In particular, in this step, the hydrophobic interaction plays an important role in the eventually insertion of the peptides into lipid bilayer. A representation of three models is reported in Fig.2.4.1.

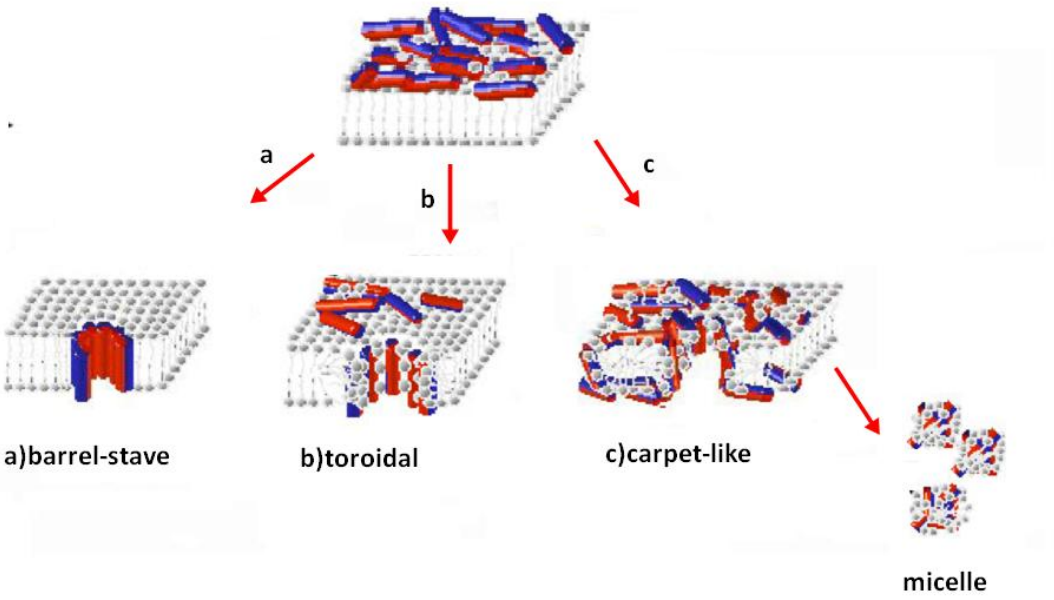

Fig.2.4.1. Representation of the most famous mechanisms of action of AMPs: a) barrel-stave; b) toroidal; c) carpet-like mechanism. Taken and modified by (Papo and Shai. Cell. Mol. Life Sci. 62:784-790, 2005)

The barrel stave mechanism was the first model described for transmembrane pore formation into lipid bilayer (*57*). After the adsorption of peptides on the membrane surface and when the threshold peptide concentration is reached, a variable number of peptides orients perpendicular to the membrane plane (*58*). In particular AMPs bind to the membrane surface as a monomer, which is followed by their oligomerization and pore formation, due to the peptide-peptide interaction. It has been demonstrated that peptides inserted into the lipid bilayer align their hydrophobic regions with those of the membrane, while the hydrophilic peptide regions form the lumen of the channel (*59*).

This mechanism is used by peptide with α-helix or β-sheet conformation, low charge density and a high content of hydrophobic residues. The most characterized case is alamethicin (*60*).

The toroidal mechanism is another model that describes the pore formation in the membranes and, also in this case above a threshold concentration, peptides align in a perpendicular orientation to lipid bilayer (*58*).Differently to the barrel-stave mechanism, in this case, the peptides perpendicularly oriented in the membrane are always associated with the lipid polar head groups, which play a pivotal role in the screening of the peptides charge (*56*). In fact, in the toroidal model, the lipids are intercalated with peptides in the transmembrane pore. In addition, in this model, the peptides induce the lipid monolayer to bend continuously though the pore. The most characterized peptides that use the toroidal mechanism are: mellittin (*61*) and magainin (*62*), which are rich in positively charged amino acid residues.

The carpet-like mechanism explains the behavior of AMPs that exert their activity when they orientate parallel to the membrane plane (*63*). These peptides accumulate on the membrane surface and when the threshold concentration is reached, AMPs disrupt the lipid bilayer in a detergent-like mode, leading to the formation of micelles (*64*). For example a peptide that interacts with bacterial membrane using this mechanism is the dermaseptin (*65*). It has been shown that some AMPs can form transient pores below the threshold peptide concentration and, above this concentration, they use the carpet-like mechanism to induce the membrane disruption (Lohner, 2009).

In conclusion, different physico-chemical properties of the AMPs, such as the size, charge, conformation, hydrophobicity, affect the mechanism of action of these peptides against negatively charged bacterial cytoplasmic membranes, but it is difficult to establish a relationship between the molecular structure of the AMPs and their mechanism of action.

2.5 AMPs in clinical phase

Antimicrobial peptides are promising drugs with a high affinity against different bacterial strains, but they often are cytotoxic for eukaryotic cells. To study the specificity of the antimicrobial peptides for bacterial cells, values of MIC (Minimum Inhibitory Concentration) and MHC(Maximum Hemolytic Concentration) are compared. MIC is the minimum inhibitory concentration of the peptide that blocks the bacterial growth, thus lower values of MIC correspond to greater antimicrobial activity. On the contrary MHC is the maximum peptide concentration need to produce no hemolysis of human erythrocytes at 37 °C and after 18 h of incubation (*66*). A perfect antimicrobial peptide with a high selectivity against bacterial cells and low toxicity for eukaryotic cells should have low values of MIC and high values of MHC.

Today a few antimicrobial peptides have entered in clinical phase and the most promising are: MSI-78 in clinical phase III trial of therapy for diabet foot ulcer infections; MBI-226 in preclinical studies that has efficacy against the skin colonization by different bacteria known to cause catheter-related infections (*67*).

It is important to note that the most known AMPs exert their antimicrobial activity (MIC) at low micromolar concentration, suggesting a high affinity between this class of peptides and bacterial cytoplasmic membranes.

2.6 Myxinidin and WMR: are they promising antibiotic peptides?

In the last years a promising antimicrobial peptide, named Myxinidin, was discovered by Subramanian in 2009 (*68*).This peptide has been identified in epidermal mucus of hagfish (*Myxine glutinosa L.*) (Fig. 2.6.1), one of the most primitive living verterbrates and a potential source of novel AMPs for human health related applications (*69*).

Fig.2.6.1 Representation of *Myxine glutinosa L.* Taken and modified by http://org.uib.no/ilab/eng_tjenester.html

Myxinidin is a 12 amino acid-long antimicrobial peptide and its sequence is: NH_2-GIHDILKYGKPS-$CONH_2$. It is a small peptide containing a high number of hydrophobic residues, only one positive charge and with an amphipathic nature, typical of an antimicrobial peptide. Different studies of biological activity conducted by Cantisani *et al.* (*70*) have shown that Myxinidin exhibits a broad spectrum of antimicrobial activity against different Gram negative and Gram positive bacteria with a low hemolytic activity for human erythrocytes. In this study various Myxinidin-analogues have been designed in order to understand the role of each amino acid residue on the antibacterial activity. A mutant, named WMR, has shown to posses higher antimicrobial activity than Myxinidin against different bacterial strains (Table 2.6.1) and low hemolytic activity for eukaryotic cells such as the native peptide (Table 2.6.2). The sequence of this mutant is:NH_2-**W**GI**RR**ILKYGK**R**S-$CONH_2$ and amino acid substitution are written in bold. In particular a histidine, aspartic acid and proline are substituted by arginine residues and, in addition, a tryptophan

residue is added at the N-terminus. In this way WMR is a 13 amino acid-long peptide, containing five positive charges and a minor number of hydrophobic residues than Myxinidin.

Table 2.6.1 Antimicrobial activity (MIC) of Myxinidin and WMR against different bacterial cells

MIC(μM)					
Peptide	***E. coli***	***P. aeriginosa***	***S. typhimurium***	***K.pneumoniae***	***S. aureus***
Myxinidin	5	30	20	10	10
WMR	2	2	1.2	3	2.2

These values have been reported in (*70*).

Table 2.6.2 Toxicity of Myxinidin and WMR determined by hemolysis at different peptides concentrations

Hemolysis (% of control) at indicated peptide concentration (μM)					
Peptide	***1***	***20***	***50***	***100***	***200***
Myxinidin	0	0	1	1	5
WMR	0	0	1	1	5

These values have been reported in (*70*).

The MIC (Minimum Inhibitory Concentration) values reported in the Table 2.6.1 indicate that WMR has a stronger antimicrobial activity (MIC) than Myxinidin against different Gram negative and Gram positive bacteria such as *P. aeruginosa, S. typhimurium, K. pneumoniae, S. aureus* and, only in the case of *E. coli* bacterium, the difference of MIC values is less significant, indicating a

similar activity of two peptides against this bacterium. In addition toxicity assays determined by hemolysis activity of two antimicrobial peptides at different concentrations (from 1 to 200 μM) against human erythrocytes have suggested that both peptides don't show hemolytic effect up to 50 μM (Table 2.6.2), a considerably high concentration for their antimicrobial activity.

Probably the difference of the antimicrobial activity exerted by the two AMPs is due to the presence of tryptophan and arginine residues in WMR peptide. In particular the presence of a tryptophan residue at the N-terminus of many antimicrobial peptides has shown to be an important factor for their antimicrobial activity, favoring the penetration of these peptides into lipid bilayer (*71*). In this case the importance of tryptophan residue has been confirmed comparing the antibacterial activity of WMR and another Myxinidin-analogue named MR. The latter differs from WMR for the absence of a tryptophan residue and in fact MR has a lower antimicrobial activity than WMR. In addition to the presence of tryptophan, probably also arginine residues contribute to improve the antimicrobial activity of WMR. In fact the replacement of arginine with lysine residues in a WMR-analogue (MK) has not shown an increase of the antimicrobial activity as demonstrated for WMR, suggesting the important role of the arginine residues. The side chain of arginine favors electrostatic interaction and hydrogen bonds formation between AMPs and bacterial negative membranes. In fact the guanidinium group of arginine side chain can form geometrically and energetically favorable bidentate hydrogen bonds with negatively charged phosphate groups of the bacterial membranes (*72*), whereas lysine residue can form only one hydrogen bond. The complementary properties of tryptophan and arginine residues could explain the better antimicrobial activity of WMR than Myxinidin.

In conclusion, both Myxinidin and its mutant WMR have low toxicity against mammalian membranes and a broad spectrum of action against Gram negative and Gram positive bacteria. These results highlight the possibility of a potential use of these two peptides as alternative candidate antibiotics against bacterial infections.

References

(1) Lewis, K. (2013) Platforms for antibiotic discovery. *Nat Rev Drug Discov 12*, 371-87.

(2) Pantosti, A., Sanchini, A., and Monaco, M. (2007) Mechanisms of antibiotic resistance in Staphylococcus aureus. *Future Microbiol 2*, 323-34.

(3) Zasloff, M. (2007) Antimicrobial peptides, innate immunity, and the normally sterile urinary tract. *J Am Soc Nephrol 18*, 2810-6.

(4) Park, I. Y., Cho, J. H., Kim, K. S., Kim, Y. B., Kim, M. S., and Kim, S. C. (2004) Helix stability confers salt resistance upon helical antimicrobial peptides. *J Biol Chem 279*, 13896-901.

(5) Wang, G., Li, X., and Wang, Z. (2009) APD2: the updated antimicrobial peptide database and its application in peptide design. *Nucleic Acids Res 37*, D933-7.

(6) Andreu, D., and Rivas, L. (1998) Animal antimicrobial peptides: an overview. *Biopolymers 47*, 415-33.

(7) Bulet, P., Hegy, G., Lambert, J., van Dorsselaer, A., Hoffmann, J. A., and Hetru, C. (1995) Insect immunity. The inducible antibacterial peptide diptericin carries two O-glycans necessary for biological activity. *Biochemistry 34*, 7394-400.

(8) Bulet, P., Dimarcq, J. L., Hetru, C., Lagueux, M., Charlet, M., Hegy, G., Van Dorsselaer, A., and Hoffmann, J. A. (1993) A novel inducible antibacterial peptide of Drosophila carries an O-glycosylated substitution. *J Biol Chem 268*, 14893-7.

(9) Mackintosh, J. A., Veal, D. A., Beattie, A. J., and Gooley, A. A. (1998) Isolation from an ant Myrmecia gulosa of two inducible O-glycosylated proline-rich antibacterial peptides. *J Biol Chem 273*, 6139-43.

(10) Park, C. B., Lee, J. H., Park, I. Y., Kim, M. S., and Kim, S. C. (1997) A novel antimicrobial peptide from the loach, Misgurnus anguillicaudatus. *FEBS Lett 411*, 173-8.

(11) Kreil, G. (1973) Biosynthesis of melittin, a toxic peptide from bee venom. Amino-acid sequence of the precursor. *Eur J Biochem 33*, 558-66.

(12) Andreu, D., Merrifield, R. B., Steiner, H., and Boman, H. G. (1983) Solid-phase synthesis of cecropin A and related peptides. *Proc Natl Acad Sci U S A 80*, 6475-9.

(13) Kuchler, K., Kreil, G., and Sures, I. (1989) The genes for the frog skin peptides GLa, xenopsin, levitide and caerulein contain a homologous export exon encoding a signal sequence and part of an amphiphilic peptide. *Eur J Biochem 179*, 281-5.

(14) Mor, A., Nguyen, V. H., Delfour, A., Migliore-Samour, D., and Nicolas, P. (1991) Isolation, amino acid sequence, and synthesis of dermaseptin, a novel antimicrobial peptide of amphibian skin. *Biochemistry 30*, 8824-30.

(15) Lee, I. H., Zhao, C., Cho, Y., Harwig, S. S., Cooper, E. L., and Lehrer, R. I. (1997) Clavanins, alpha-helical antimicrobial peptides from tunicate hemocytes. *FEBS Lett 400*, 158-62.

(16) Oppenheim, F. G., Xu, T., McMillian, F. M., Levitz, S. M., Diamond, R. D., Offner, G. D., and Troxler, R. F. (1988) Histatins, a novel family of histidine-rich proteins in human parotid secretion. Isolation, characterization, primary structure, and fungistatic effects on Candida albicans. *J Biol Chem 263*, 7472-7.

(17) Mignogna, G., Simmaco, M., Kreil, G., and Barra, D. (1993) Antibacterial and haemolytic peptides containing D-alloisoleucine from the skin of Bombina variegata. *EMBO J 12*, 4829-32.

(18) Lambert, J., Keppi, E., Dimarcq, J. L., Wicker, C., Reichhart, J. M., Dunbar, B., Lepage, P., Van Dorsselaer, A., Hoffmann, J., Fothergill, J., and et al. (1989) Insect immunity: isolation from immune blood of the dipteran Phormia terranovae of two insect antibacterial peptides with sequence homology to rabbit lung macrophage bactericidal peptides. *Proc Natl Acad Sci U S A 86*, 262-6.

(19) Fidai, S., Farmer, S. W., and Hancock, R. E. (1997) Interaction of cationic peptides with bacterial membranes. *Methods Mol Biol 78*, 187-204.

(20) Niyonsaba, F., Nagaoka, I., Ogawa, H., and Okumura, K. (2009) Multifunctional antimicrobial proteins and peptides: natural activators of immune systems. *Curr Pharm Des 15*, 2393-413.

(21) Powers, J. P., and Hancock, R. E. (2003) The relationship between peptide structure and antibacterial activity. *Peptides 24*, 1681-91.
(22) Jiang, Z., Vasil, A. I., Hale, J. D., Hancock, R. E., Vasil, M. L., and Hodges, R. S. (2008) Effects of net charge and the number of positively charged residues on the biological activity of amphipathic alpha-helical cationic antimicrobial peptides. *Biopolymers 90*, 369-83.
(23) Dathe, M., Nikolenko, H., Meyer, J., Beyermann, M., and Bienert, M. (2001) Optimization of the antimicrobial activity of magainin peptides by modification of charge. *FEBS Lett 501*, 146-50.
(24) Scott, M. G., Yan, H., and Hancock, R. E. (1999) Biological properties of structurally related alpha-helical cationic antimicrobial peptides. *Infect Immun 67*, 2005-9.
(25) Sawai, M. V., Waring, A. J., Kearney, W. R., McCray, P. B., Jr., Forsyth, W. R., Lehrer, R. I., and Tack, B. F. (2002) Impact of single-residue mutations on the structure and function of ovispirin/novispirin antimicrobial peptides. *Protein Eng 15*, 225-32.
(26) Tossi, A., Sandri, L., and Giangaspero, A. (2000) Amphipathic, alpha-helical antimicrobial peptides. *Biopolymers 55*, 4-30.
(27) Unger, T., Oren, Z., and Shai, Y. (2001) The effect of cyclization of magainin 2 and melittin analogues on structure, function, and model membrane interactions: implication to their mode of action. *Biochemistry 40*, 6388-97.
(28) Becucci, L., Valensin, D., Innocenti, M., and Guidelli, R. (2014) Dermcidin, an anionic antimicrobial peptide: influence of lipid charge, pH and Zn2+ on its interaction with a biomimetic membrane. *Soft Matter 10*, 616-26.
(29) Li, S., Hao, L., Bao, W., Zhang, P., Su, D., Cheng, Y., Nie, L., Wang, G., Hou, F., and Yang, Y. (2016) A novel short anionic antibacterial peptide isolated from the skin of Xenopus laevis with broad antibacterial activity and inhibitory activity against breast cancer cell. *Arch Microbiol*.
(30) Yin, L. M., Edwards, M. A., Li, J., Yip, C. M., and Deber, C. M. (2012) Roles of hydrophobicity and charge distribution of cationic antimicrobial peptides in peptide-membrane interactions. *J Biol Chem 287*, 7738-45.
(31) Eisenberg, D., Weiss, R. M., and Terwilliger, T. C. (1984) The hydrophobic moment detects periodicity in protein hydrophobicity. *Proc Natl Acad Sci U S A 81*, 140-4.
(32) Wieprecht, T., Dathe, M., Krause, E., Beyermann, M., Maloy, W. L., MacDonald, D. L., and Bienert, M. (1997) Modulation of membrane activity of amphipathic, antibacterial peptides by slight modifications of the hydrophobic moment. *FEBS Lett 417*, 135-40.
(33) Chen, Y., Mant, C. T., Farmer, S. W., Hancock, R. E., Vasil, M. L., and Hodges, R. S. (2005) Rational design of alpha-helical antimicrobial peptides with enhanced activities and specificity/therapeutic index. *J Biol Chem 280*, 12316-29.
(34) Wessolowski, A., Bienert, M., and Dathe, M. (2004) Antimicrobial activity of arginine- and tryptophan-rich hexapeptides: the effects of aromatic clusters, D-amino acid substitution and cyclization. *J Pept Res 64*, 159-69.
(35) Leveritt, J. M., 3rd, Pino-Angeles, A., and Lazaridis, T. (2015) The structure of a melittin-stabilized pore. *Biophys J 108*, 2424-6.
(36) Oren, Z., Hong, J., and Shai, Y. (1999) A comparative study on the structure and function of a cytolytic alpha-helical peptide and its antimicrobial beta-sheet diastereomer. *Eur J Biochem 259*, 360-9.
(37) Epand, R. M., and Vogel, H. J. (1999) Diversity of antimicrobial peptides and their mechanisms of action. *Biochim Biophys Acta 1462*, 11-28.
(38) Mai, X. T., Huang, J., Tan, J., Huang, Y., and Chen, Y. (2015) Effects and mechanisms of the secondary structure on the antimicrobial activity and specificity of antimicrobial peptides. *J Pept Sci 21*, 561-8.
(39) Fernandez-Lopez, S., Kim, H. S., Choi, E. C., Delgado, M., Granja, J. R., Khasanov, A., Kraehenbuehl, K., Long, G., Weinberger, D. A., Wilcoxen, K. M., and Ghadiri, M. R. (2001) Antibacterial agents based on the cyclic D,L-alpha-peptide architecture. *Nature 412*, 452-5.

(40) Chan, D. I., Prenner, E. J., and Vogel, H. J. (2006) Tryptophan- and arginine-rich antimicrobial peptides: structures and mechanisms of action. *Biochim Biophys Acta 1758*, 1184-202.
(41) da Silva, A., Jr., and Teschke, O. (2003) Effects of the antimicrobial peptide PGLa on live Escherichia coli. *Biochim Biophys Acta 1643*, 95-103.
(42) Subbalakshmi, C., and Sitaram, N. (1998) Mechanism of antimicrobial action of indolicidin. *FEMS Microbiol Lett 160*, 91-6.
(43) Patrzykat, A., Friedrich, C. L., Zhang, L., Mendoza, V., and Hancock, R. E. (2002) Sublethal concentrations of pleurocidin-derived antimicrobial peptides inhibit macromolecular synthesis in Escherichia coli. *Antimicrob Agents Chemother 46*, 605-14.
(44) Boman, H. G., Agerberth, B., and Boman, A. (1993) Mechanisms of action on Escherichia coli of cecropin P1 and PR-39, two antibacterial peptides from pig intestine. *Infect Immun 61*, 2978-84.
(45) Lehrer, R. I., Barton, A., Daher, K. A., Harwig, S. S., Ganz, T., and Selsted, M. E. (1989) Interaction of human defensins with Escherichia coli. Mechanism of bactericidal activity. *J Clin Invest 84*, 553-61.
(46) Park, C. B., Kim, H. S., and Kim, S. C. (1998) Mechanism of action of the antimicrobial peptide buforin II: buforin II kills microorganisms by penetrating the cell membrane and inhibiting cellular functions. *Biochem Biophys Res Commun 244*, 253-7.
(47) Yonezawa, A., Kuwahara, J., Fujii, N., and Sugiura, Y. (1992) Binding of tachyplesin I to DNA revealed by footprinting analysis: significant contribution of secondary structure to DNA binding and implication for biological action. *Biochemistry 31*, 2998-3004.
(48) Brotz, H., Bierbaum, G., Leopold, K., Reynolds, P. E., and Sahl, H. G. (1998) The lantibiotic mersacidin inhibits peptidoglycan synthesis by targeting lipid II. *Antimicrob Agents Chemother 42*, 154-60.
(49) Shi, J., Ross, C. R., Chengappa, M. M., Sylte, M. J., McVey, D. S., and Blecha, F. (1996) Antibacterial activity of a synthetic peptide (PR-26) derived from PR-39, a proline-arginine-rich neutrophil antimicrobial peptide. *Antimicrob Agents Chemother 40*, 115-21.
(50) Salomon, R. A., and Farias, R. N. (1992) Microcin 25, a novel antimicrobial peptide produced by Escherichia coli. *J Bacteriol 174*, 7428-35.
(51) Otvos, L., Jr., O, I., Rogers, M. E., Consolvo, P. J., Condie, B. A., Lovas, S., Bulet, P., and Blaszczyk-Thurin, M. (2000) Interaction between heat shock proteins and antimicrobial peptides. *Biochemistry 39*, 14150-9.
(52) Hirt, H., and Gorr, S. U. (2013) Antimicrobial peptide GL13K is effective in reducing biofilms of Pseudomonas aeruginosa. *Antimicrob Agents Chemother 57*, 4903-10.
(53) Galdiero, S., Falanga, A., Cantisani, M., Vitiello, M., Morelli, G., and Galdiero, M. (2013) Peptide-lipid interactions: experiments and applications. *Int J Mol Sci 14*, 18758-89.
(54) Lohner, K., and Prenner, E. J. (1999) Differential scanning calorimetry and X-ray diffraction studies of the specificity of the interaction of antimicrobial peptides with membrane-mimetic systems. *Biochim Biophys Acta 1462*, 141-56.
(55) Stark, M., Liu, L. P., and Deber, C. M. (2002) Cationic hydrophobic peptides with antimicrobial activity. *Antimicrob Agents Chemother 46*, 3585-90.
(56) Yang, L., Harroun, T. A., Weiss, T. M., Ding, L., and Huang, H. W. (2001) Barrel-stave model or toroidal model? A case study on melittin pores. *Biophys J 81*, 1475-85.
(57) Ehrenstein, G., and Lecar, H. (1977) Electrically gated ionic channels in lipid bilayers. *Q Rev Biophys 10*, 1-34.
(58) Lee, M. T., Chen, F. Y., and Huang, H. W. (2004) Energetics of pore formation induced by membrane active peptides. *Biochemistry 43*, 3590-9.
(59) Yeaman, M. R., and Yount, N. Y. (2003) Mechanisms of antimicrobial peptide action and resistance. *Pharmacol Rev 55*, 27-55.
(60) Rahaman, A., and Lazaridis, T. (2014) A thermodynamic approach to alamethicin pore formation. *Biochim Biophys Acta 1838*, 1439-47.
(61) Lee, M. T., Sun, T. L., Hung, W. C., and Huang, H. W. (2013) Process of inducing pores in membranes by melittin. *Proc Natl Acad Sci U S A 110*, 14243-8.

(62) Pino-Angeles, A., Leveritt, J. M., 3rd, and Lazaridis, T. (2016) Pore Structure and Synergy in Antimicrobial Peptides of the Magainin Family. *PLoS Comput Biol 12*, e1004570.
(63) Yamaguchi, S., Huster, D., Waring, A., Lehrer, R. I., Kearney, W., Tack, B. F., and Hong, M. (2001) Orientation and dynamics of an antimicrobial peptide in the lipid bilayer by solid-state NMR spectroscopy. *Biophys J 81*, 2203-14.
(64) Shai, Y. (1999) Mechanism of the binding, insertion and destabilization of phospholipid bilayer membranes by alpha-helical antimicrobial and cell non-selective membrane-lytic peptides. *Biochim Biophys Acta 1462*, 55-70.
(65) Pouny, Y., Rapaport, D., Mor, A., Nicolas, P., and Shai, Y. (1992) Interaction of antimicrobial dermaseptin and its fluorescently labeled analogues with phospholipid membranes. *Biochemistry 31*, 12416-23.
(66) Tachi, T., Epand, R. F., Epand, R. M., and Matsuzaki, K. (2002) Position-dependent hydrophobicity of the antimicrobial magainin peptide affects the mode of peptide-lipid interactions and selective toxicity. *Biochemistry 41*, 10723-31.
(67) Hancock, R. E., and Patrzykat, A. (2002) Clinical development of cationic antimicrobial peptides: from natural to novel antibiotics. *Curr Drug Targets Infect Disord 2*, 79-83.
(68) Subramanian, S., Ross, N. W., and MacKinnon, S. L. (2009) Myxinidin, a novel antimicrobial peptide from the epidermal mucus of hagfish, Myxine glutinosa L. *Mar Biotechnol (NY) 11*, 748-57.
(69) Subramanian, S., Ross, N. W., and MacKinnon, S. L. (2008) Comparison of antimicrobial activity in the epidermal mucus extracts of fish. *Comp Biochem Physiol B Biochem Mol Biol 150*, 85-92.
(70) Cantisani, M., Leone, M., Mignogna, E., Kampanaraki, K., Falanga, A., Morelli, G., Galdiero, M., and Galdiero, S. (2013) Structure-activity relations of myxinidin, an antibacterial peptide derived from the epidermal mucus of hagfish. *Antimicrob Agents Chemother 57*, 5665-73.
(71) Bi, X., Wang, C., Ma, L., Sun, Y., and Shang, D. (2013) Investigation of the role of tryptophan residues in cationic antimicrobial peptides to determine the mechanism of antimicrobial action. *J Appl Microbiol 115*, 663-72.
(72) Su, Y., Waring, A. J., Ruchala, P., and Hong, M. (2010) Membrane-bound dynamic structure of an arginine-rich cell-penetrating peptide, the protein transduction domain of HIV TAT, from solid-state NMR. *Biochemistry 49*, 6009-20.

Chapter 3

Materials and Methods

3.1 Materials

All experiments were performed using Millipore water. To mimic different model bio-membranes, zwitterionic and anionic lipids were used.

3.1.1 Lipid components

- **Zwitterionic phospholipids**

a) 1,2-dioleoyl-*sn*-glycero-3-phosphoethanolamine (DOPE) was obtained from Avanti Polar with a purity > 99%

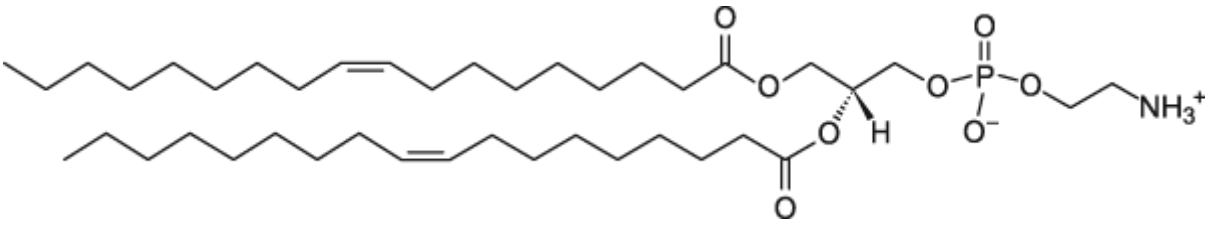

b) 1,2-dipalmitoyl-*sn*-glycero-3-phosphoethanolamine (DPPE) was obtained from Avanti Polar with a purity > 99%

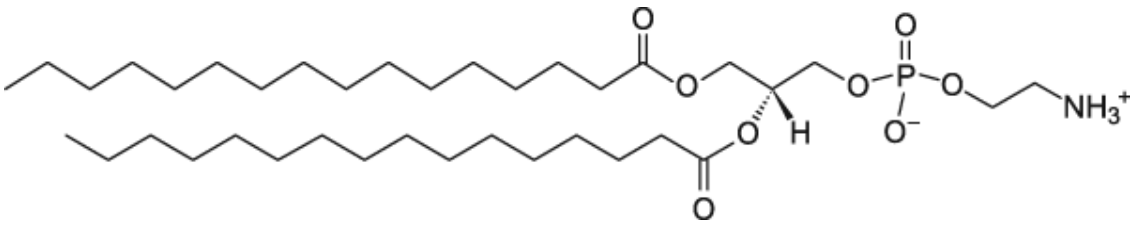

c) 1,2-dipalmitoyl-*sn*-glycero-3-phosphocholine (DPPC) was obtained from Avanti Polar with a purity > 99%

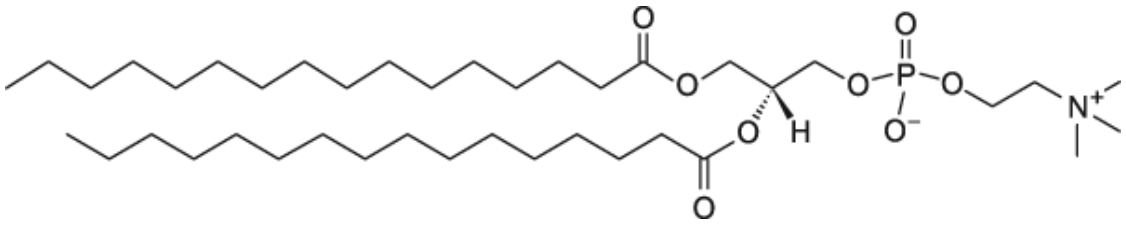

d) 1,2-diheptanoyl-*sn*-glycero-3-phosphocholine (DihepPC) was obtained from Avanti Polar with a purity >99%.

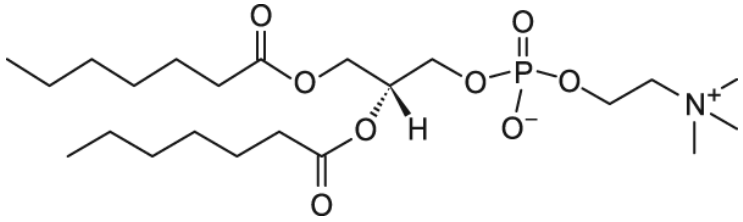

- **Anionic phospholipids**

a) 1,2-dioleoyl-*sn*-glycero-3-phospho-(1'-*rac*-glycerol) (sodium salt) (DOPG) was obtained from Avanti Polar with a purity > 99%

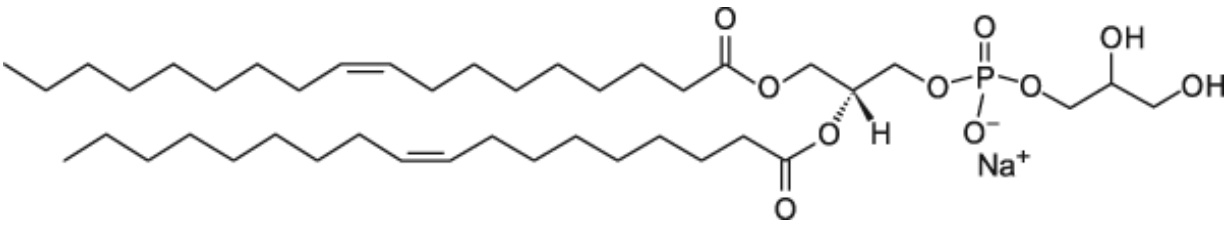

b) 1,2-dipalmitoyl-*sn*-glycero-3-phospho-(1'-*rac*-glycerol) (sodium salt)(DPPG) was obtained from Avanti Polar with a purity > 99%

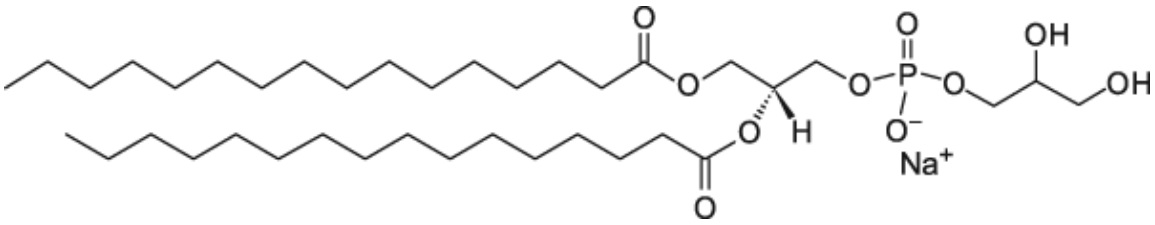

c) 1,2-dimyristoyl-*sn*-glycero-3-phospho-(1'-rac-glycerol) (sodium salt)(DMPG) was obtained from Avanti Polar with a purity > 99%

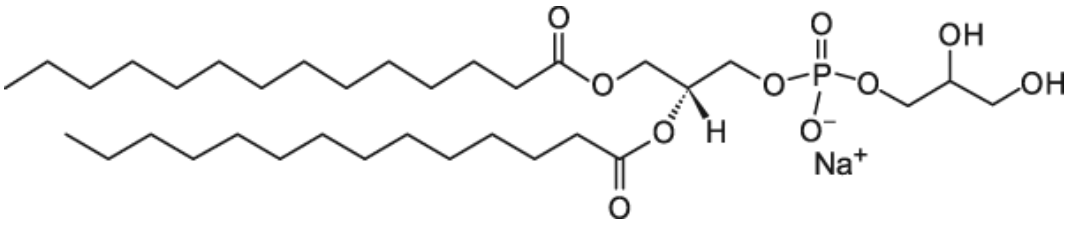

d) Cardiolipin sodium salt from bovine heart (CL) was obtained from Sigma Aldrich with a purity > 98%

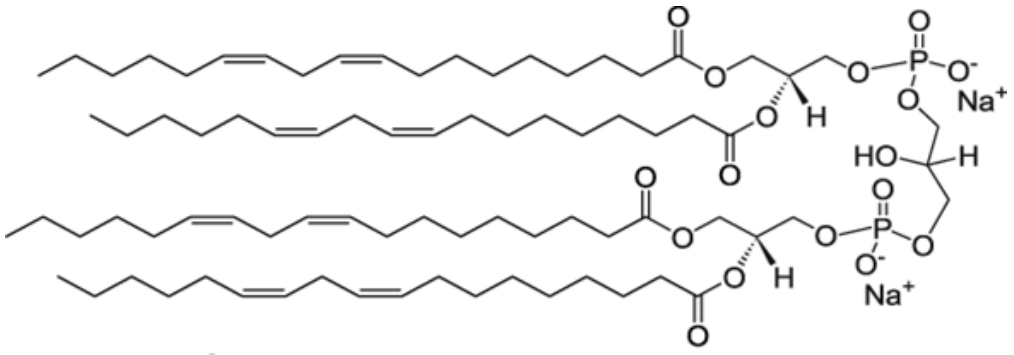

- **Deuterated phospholipids**

a) Sodium dodecyl sulfate-d_{25} -98% atom % D-(SDS-d_{25}) was obtained from Sigma Aldrich with a purity > 98%

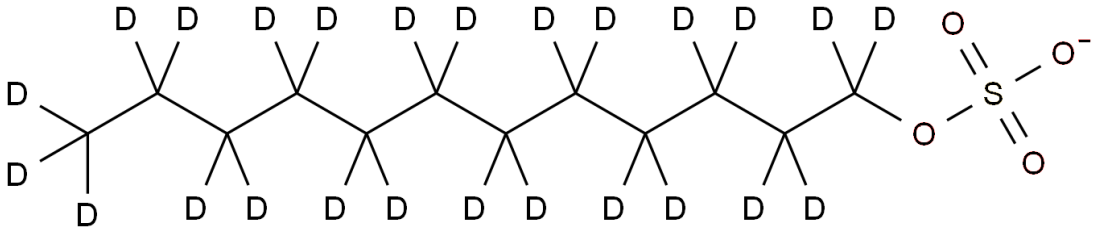

b) 1,2-dimyristoyl-d_{54}-*sn*-glycero-3-phosphocholine (DMPC-d_{54}) was obtained from Avanti Polar with a purity > 99%

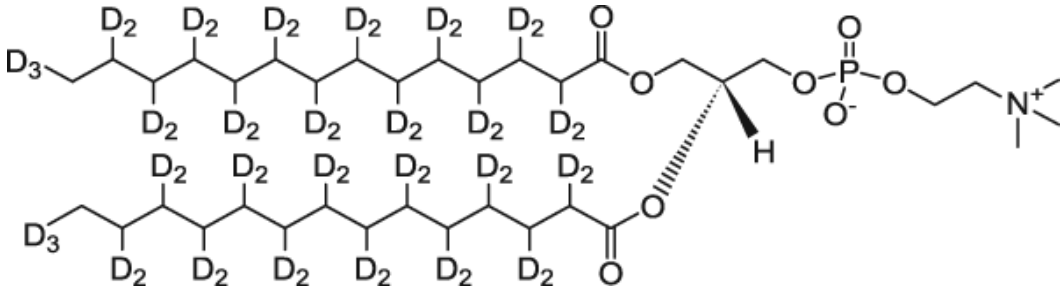

3.1.2 Peptides

Myxinidin and WMR peptides were synthesized by Prof. Galdiero S. Group, Department of Pharmacy, University "Federico II", Naples. Peptides were synthesized using the standard solid phase 9-fluorenylmethoxy carbonyl (Fmoc) method.

Myxinidin and WMR sequences are:

Peptides	**Sequences**
Myxinidin	NH_2-GIHDILKYGKPS-$CONH_2$
WMR	NH_2-WGIRRILKYGKRS-$CONH_2$

Their molar extinction coefficients were determined spectroscopically by UV-VIS and they are: $\varepsilon(275nm) = 1647 \pm 159\ M^{-1}\ cm^{-1}$ and $\varepsilon(280nm) = 4777 \pm 281\ M^{-1}\ cm^{-1}$ for Myxinidin and WMR peptides respectively.

3.1.3 Solvents

a) PBS buffer (0.010M Na_2HPO_4, 0.002M KH_2PO_4, 0.135M NaCl, 0,0027M KCl, pH=7.4) was used to prepare liposomes and peptides solutions. All salts were obtained from Sigma Aldrich with a purity > 99%.

b) Organic Solvents: $CHCl_3$, CH_3OH,C_2H_5OH were used to prepare liposomes stock solutions and were obtained from Sigma Aldrich with a purity > 99%.

3.2 Methods

3.2.1 Liposomes preparation

Liposomes with appropriate size were prepared for different experiments. In particular Multi Lamellar Vesicles (MLVs) were used to characterize the stability and physico-chemical properties of the liposomes, whereas Small and Large Unilamellar vesicles (SUVs and LUVs respectively) were used to analyze the interaction between liposomes and peptides by calorimetric and spectroscopic techniques. An appropriate amount of lipids was weighed and dissolved in $CHCl_3/CH_3OH$ (70/30 v/v) mixture to prepare liposomes at different composition. A thin film of lipids was obtained through evaporation of the organic solvent with dry nitrogen gas and vacuum desiccation. Lipid films were kept in vacuum overnight to remove all residual organic solvent, then were hydrated with a definite amount of PBS buffer pH 7.4 and finally vortexed to obtain a suspension of Multi Lamellar Vesicles (MLVs). Small Unilamellar Vesicles (SUVs) were produced from MLVs by sonication with a Sonics VCX130 (Sonics and Materials, Newtown, USA) for 30 min at room temperature. Instead Large Unilamellar Vesicles (LUVs), were obtained by extrusion using a Mini-Extruder (Avanti Polar Lipid Inc.) (Fig.3.2.1) according to the extrusion method of Hope et al(*1*). In fact, the MultiLamellar suspension was passed through a 100 nm pore size polycarbonate membrane 25 times. Dynamic light scattering measurements were used to check the size of the vesicles after the sonication or extrusion protocol.

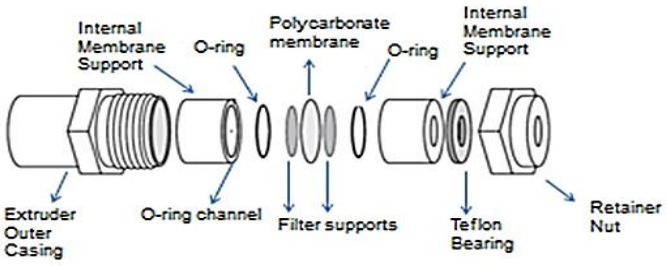

Fig.3.2.1 Schematic representation of an extruder.

Taken and modified by Avanti Polar website.

3.2.2 Differential Scanning Calorimetry measurements

Differential Scanning Calorimetry (DSC) measurements were performed using a nano-DSC from TA instruments (New Castle, DE, USA) with capillary cells of 0.3 ml sensitive volume. A total pressure of 3.0 atm was applied with nitrogen gas to both cells during the temperature scanning. A volume of 300μL of MLVs (0.5mM) in the absence or in the presence of Myxinidin and WMR peptides at different lipid/peptide ratios was placed in the calorimetry vessel. Successive heating and cooling scans were performed for each sample operating at a scan rate of 1°C/min over the temperature range of 25–80°C. A buffer-buffer scan was subtracted from the sample scan. The excess molar heat capacity function, $<\Delta C_p>$ was obtained after a baseline subtraction, assuming that the baseline is given by the linear temperature dependence of the pre-transition heat capacity. Samples were prepared immediately before the DSC experiment, by adding the appropriate amount of peptide solution to the vesicles suspension and waiting 20 min to ensure that equilibrium has been reached. The results provided here always refer to the second scan. DSC data were analyzed by means of the NanoAnalyze software supplied with the instrument and plotted using the Origin software package. For all DSC experiments, MultiLamellar Vesicles (MLVs) were warmed at 70°C for 10 min and vortexed to obtain a homogeneous dispersion. The heating at a temperature above gel to liquid crystalline phase transition melting temperature (T_m) ensures that the lipid systems are in the fluid phase. MultiLamellar Vesicles (MLVs) were chosen to investigate thermal behavior of liposomes because they provide a high resolution of lipid phase transitions and give more accurate enthalpy values (*2*).It has been demonstrated that different vesicle preparations can alter DSC profile. In fact Small Unilamellar Vesicles (SUVs) give a lower resolution peak than MLVs, a decrease of cooperative peak and a lower enthalpy value. The explanation lies in the smaller radius of SUVs than MLVs and this involves in a less ordered orientation of the small unilamellar vesicles and thus an increase of the free motion of the hydrocarbon chains (*3*). Another problem to use SUVs is their tendency to fuse to form LUVs during the heating scan. In addition also DSC profiles of LUVs present some problems, because they produce broader and highly asymmetric transition profiles than that observed for MLVs. Probably this result is due to the size inhomogeneity(*4*) (*5*) of LUVs. On the contrary the calorimetric profiles of MLVs are highly cooperative and reversible(*4*).

3.2.3 Isothermal Titration Calorimetry measurements

Isothermal Titration Calorimetry (ITC) measurements were performed using a nano-ITC III (TA instruments, New Castle, DE, USA) at 25°C. The peptide solution (50-100μM) was injected in the calorimetric vessel (1mL) containing Large Unilamellar Vesicles (LUVs) (0.2-0.5 mM concentration range). Under these conditions, during the whole titration experiment the lipid is much in excess over the peptide, and thus the injected peptide is completely bound to the membrane surface. In this way, each injection should produce the same heat denominated h_i providing the association enthalpy $\Delta_a H°$ when divided by the molarity of the peptide. The peptide solution was injected in aliquots of 10μL with 400s intervals between the individual injections. The association enthalpy was obtained by dividing the total heat of injections by the moles of the peptide in the calorimetry vessel. ITC profiles were obtained after the subtraction of dilution heat, which was determined by titration of peptides into the buffer. In all ITC experiments, LUVs were prepared by extrusion protocol as described above. In fact MLVs are not ideal membrane model for thermodynamic study of the interaction between peptides and lipids(*6*).They are never used for binding experiments, since the geometry of MLVs are undefined and many of the formed bilayers are not available to membrane-binding molecules(*6*).

3.2.4 Circular Dichroism measurements

Circular Dichroism (CD) spectra in the far UV-region (190–250 nm) were recorded on a Jasco J-715 spectropolarimeter (Jasco Corporation, Tokyo, Japan) under constant nitrogen flow, equipped with a Peltier type temperature control system (Model PTC-348WI). The spectra were recorded as an average of 3 scans with 20 nm/min scan speed, 4 s response time, and 2 nm bandwidth, using a 0.1 cm path length quartz cuvette and finally corrected for the buffer signal. Cell cuvette thickness, peptides and Small Unilamellar Vesicles (SUVs) concentrations were chosen in away that the maximum high-tension voltage of the photomultiplier was not exceeding 600 V at the lowest wavelength (200 nm). All CD spectra were recorded at 25°C. Myxinidin and WMR peptides were dissolved in PBS buffer solution pH=7.4 at 100μM concentration in the absence and in the presence of vesicles. For each sample, a background blank of either solvent or lipid vesicles without peptide was subtracted. Mean residue ellipticity (MRE), [θ] in deg cm^2dmol^{-1} values were calculated by the following relation: $[\theta] = ([\theta]_{obs}\ MRW\ ) / (10 \times l \times C)$, where θ is the measured ellipticity (millidegrees); MRW=M/(n-1) where M is molecular mass in Da and (n-1) is the number peptide

bonds; C is the peptide concentration in mg mL^{-1} and l is the path length in cm. For CD measurements SUVs were used because the small radius decreases the light scattering phenomenon at low wavelength (< 200 nm) (*7*).

3.2.5 Fluorescence measurements

Fluorescence spectra were recorded at 25°C on a Fluoromax-4 fluorescence spectrophotometer (Horiba, Edison, NJ, USA), equipped with a thermostatically controlled cuvette holder, using quartz cells of 1 cm path length. In order to monitor changes of triptophan and tyrosine residues fluorescence emission spectra upon the binding with Small Unilamellar Vesicles (SUVs), fluorescence spectra were performed. For WMR the excitation wavelength was 295 nm and the emission spectra were collected from 300 nm to 500 nm to selectively excite the tryptophan (Trp) residue of the peptide. For Myxinidin, the excitation wavelength was 280 nm and the emission spectra were collected from 285 to 500 nm to monitor the changes of the tyrosine (Tyr) residue fluorescence. The slit widths for both excitation and emission wavelengths were 5 nm. The titrations were performed by recording the spectra at fixed peptide concentration (20μM and 10μM for Myxinidin and WMR respectively) and increasing lipid concentration. Different samples containing the same concentration of peptide but at various L/P ratios were prepared. For each sample, a background blank of lipid vesicles without peptide was subtracted. For fluorescence measurements, SUVs were used to minimize the light scattering phenomenon.

3.2.6 Dynamic Light Scattering measurements

DLS measurements were performed with a set up composed by a SMD 6000 Laser Quantum 50 mW light source operating at 5325 Å, a Photocor compact goniometer, a photomultiplier (PMT-120-OP/B) and a correlator (Flex02-01D) from *Correlator.com*. The experiments were carried on at 25°C, by using a thermostatic bath and at the scattering angle of 90° (θ=90°).The value of scattering vector $q = 4\pi n/\lambda \sin(\theta / 2)$ was calculated assuming the refractive index of solution n=1.33 for water suspensions. Considering liposomes as spheres diffusing in a continuum medium at infinite dilution, their hydrodynamic radius (R_h) is correlated to the diffusion coefficient (D) through the Stokes-Einstein equation:

$$R_h = (kT) / (6\pi\eta D)$$

where k is the Boltzmann constant, T is the absolute temperature and η is the medium viscosity. This equation was used to evaluate the hydrodynamic radius (R_h) of the liposomes from their translational diffusion coefficient(D).Large Unilamellar Vesicles (LUVs) obtained by extrusion

method were analyzed at the concentration of 0.2 mM in the absence and presence of peptides at L/P=10.

3.2.7 Lipid mixing assay

This assay was performed by Prof. Galdiero S. Group, Department of Pharmacy, University ”Federico II”, Naples. Membrane lipid mixing was monitored using the fluorescence resonance energy transfer (FRET) assay reported by Struck *et al.* (*8*).This assay exploits the dilution of the fluorescent probes N-(7-nitro-benz-2-oxa-1,3-diazol-4-yl) phosphatidylethanolamine (NBD-PE) (donor) and N-(Lissaminerhodamine-Bsulfonyl) phosphatidylethanolamine (Rho-PE) (acceptor). Vesicles containing 0.6 mol% of each probe were mixed with unlabelled vesicles at a 1:4 ratio in buffer 5mM HEPES plus 100 mM NaCl pH 7.4 (final lipid concentration in the cuvette 0.1 mM). It has been monitored the change in donor emission as aliquots of peptides were added to vesicles at different peptide/lipid molar ratios. Dilution due to membrane mixing promoted by peptides results in an increase in NBD-PE fluorescence. The NBD emission at 530 nm was followed with the excitation wavelength set at 465 nm. A cut off filter at 515 nm was used between the sample and the emission monochromator to avoid scattering interferences. The fluorescence scale was calibrated such that the zero level corresponded to the initial residual fluorescence of the labeled vesicles and the 100% value corresponding to complete mixing of all lipids in the system was set by the fluorescence intensity of vesicles upon the addition of Triton X-100 (0.05% v/v) at the same total lipid concentrations of the fusion assay

3.2.8 Inner-monolayer phospholipid mixing assay

This assay was performed by Prof. Galdiero S. Group, Department of Pharmacy, University ”Federico II”, Naples. Inner-monolayer phospholipid mixing assay was measured by a modification of the lipid mixing assay reported before. The unlabelled vesicles were prepared as done for lipid mixing assays. The labelled vesicles were prepared in a different buffer (10mM TRIS, 100mM NaCl, 1mM EDTA) and were treated with sodium dithionite 100 mM (from a stock solution of 200 mM dithionite in 200 mM TRIS, pH 10.0) to reduce completely the NBD-labelled phospholipid located at the outer monolayer of the membrane, for approximately 30 min on ice in the dark. Sodium dithionite was then removed by size exclusion chromatography through a Sephadex G-75 50 DNA Grade filtration column (GE Healthcare) eluted with a buffer containing 5mM HEPES plus 100 mM NaCl pH 7.4.

3.2.9 ANTS/DPX leakage assay

This assay was performed by Prof. Galdiero S. Group, Department of Pharmacy, University ”Federico II”, Naples. ANTS (8-aminonaphtalene-1,3,6-trisulfonic acid, disodium salt) and DPX (p-xylene-bis-pyridinium bromide) were incapsulated in liposomes. ANTS/DPX assay was used to measure the ability of the peptides to induce leakage of ANTS/DPX pre-encapsulated in liposomes. Details of this assay are reported by Parente et al. *(9)*. The peptides, in a stock solution containing 5 mM HEPES and 100 mM NaCl pH 7.4, were added to vesicle suspensions (0.1 mM lipid) at different peptide/lipid molar ratios.

References

(1) Hope, M. J., Bally, M. B., Webb, G., and Cullis, P. R. (1985) Production of large unilamellar vesicles by a rapid extrusion procedure: characterization of size distribution, trapped volume and ability to maintain a membrane potential. *Biochim Biophys Acta 812*, 55-65.

(2) Chiu, M. H., and Prenner, E. J. (2011) Differential scanning calorimetry: An invaluable tool for a detailed thermodynamic characterization of macromolecules and their interactions. *J Pharm Bioallied Sci 3*, 39-59.

(3) McElhaney, R. N. (1982) The use of differential scanning calorimetry and differential thermal analysis in studies of model and biological membranes. *Chem Phys Lipids 30*, 229-59.

(4) Rodney L. Biltonen, D. L. (1993) The use of differential scanning calorimetry as a tool to characterize liposome preparations. . *Chem Phys Lipids 64*, 129–42.

(5) Mason, J. T., Huang, C., and Biltonen, R. L. (1983) Effect of liposomal size on the calorimetric behavior of mixed-chain phosphatidylcholine bilayer dispersions. *Biochemistry 22*, 2013-8.

(6) Samad, A., Sultana, Y., and Aqil, M. (2007) Liposomal drug delivery systems: an update review. *Curr Drug Deliv 4*, 297-305.

(7) Ladokhin, A. S., Fernandez-Vidal, M., and White, S. H. (2010) CD spectroscopy of peptides and proteins bound to large unilamellar vesicles. *J Membr Biol 236*, 247-53.

(8) Struck, D. K., Hoekstra, D., and Pagano, R. E. (1981) Use of resonance energy transfer to monitor membrane fusion. *Biochemistry 20*, 4093-9.

(9) Parente, R. A., Nir, S., and Szoka, F. C., Jr. (1990) Mechanism of leakage of phospholipid vesicle contents induced by the peptide GALA. *Biochemistry 29*, 8720-8.

Chapter 4

Results and discussion

Physico-chemical characterization of the interaction of the antimicrobial peptide Myxinidin and its mutant WMR with liposomes mimicking *P. aeruginosa* and *E. coli* cell membranes

4.1 Introduction

In this Chapter, a physico-chemical characterization of the interaction of the antimicrobial peptide Myxinidin and its mutant WMR with liposomes mimicking *P. aeruginosa* and *E. coli* cell cytoplasmic membranes is reported. A combined approach, including calorimetric (DSC and ITC) and spectroscopic (Fluorescence, CD, DLS) techniques has been adopted with the aim to investigate the membrane perturbing properties of two peptides from different perspectives. Differential Scanning Calorimetry (DSC) was used to monitor changes in the cooperative thermal transitions of the lipid bilayers, whereas Isothermal Titration Calorimetry (ITC) to get information on thermodynamics of interaction between AMPs and liposomes. Intrinsic fluorescence was used to estimate the microenvironment of peptides upon binding with the membranes, Circular Dichroism (CD) to study the conformational changes of peptides in the presence of liposomes and Dynamic Light Scattering (DLS) provided the dimensions of the liposomes in the absence and presence of peptides. The liposomes studied were made by using the following phospholipid mixtures:

- DOPE, DOPG and Cardiolipin
- DOPE and DOPG

in order to mimic the cytoplasmic membrane of the Gram negative bacteria such as *Pseudomonas aeruginosa* and *Escherichia coli*.

The aim of the study is to investigate the role of lipid composition on the antimicrobial activity of Myxinidin and WMR, in fact the liposomes studied differ in their total negative charge and the presence of Cardiolipin, that is anionic at physiological pH.

Further, the role of the peptide charge, sequence and conformation on the interaction with the model bio-membranes is elucidated.

4.2 Characterization of Myxinidin and WMR peptides

The two peptides were first characterized in solution by CD measurements in the far-UV region (190-250 nm).

To mimic the physiological environment of the cells the PBS buffer (0.010M Na_2HPO_4, 0.002M KH_2PO_4, 0.135M NaCl, 0,0027M KCl, pH=7.4) was used. CD spectra of both peptides (Fig.4.2.1) show a negative band around 200 nm, indicating a random coil like structure, but only for WMR peptide it is possible to observe a weak positive band around 225 nm, typical of peptides containing tryptophan residues (*1*). In fact, between 220-230 nm the aromatic side chains have an important contribute in CD spectra.

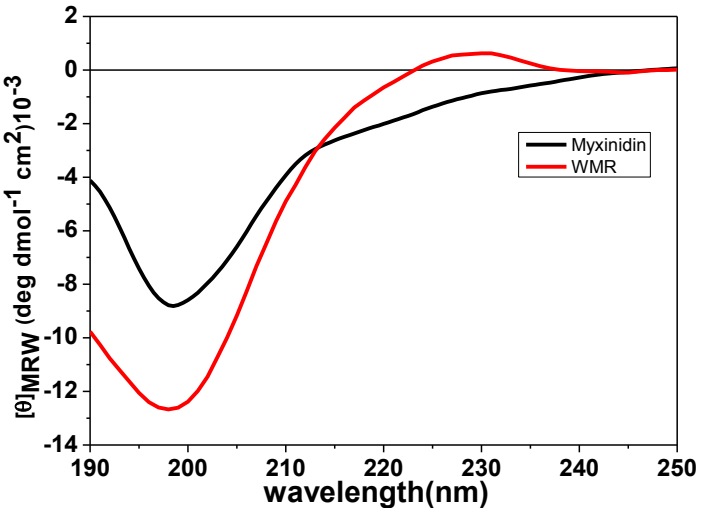

Fig.4.2.1 Far-UV CD spectra of Myxinidin (black line) and WMR (red line) peptides in PBS buffer pH=7.4 recorded at 25°C

To study the secondary structure adopted by peptides in different environments, CD spectra in the TFE/H_2O mixtures were recorded. TFE (2, 2, 2- trifluoroethanol) is a solvent that mimics dielectric constant of the membranes and represents a good model to monitor the ability of peptides to adopt a helical structure (*2*, *3*).

Inspection of CD spectra (Fig.4.2.2) reveals that Myxinidin adopts a more structured conformation in a solution at 50% v/v of TFE. In this latter solvent, the CD spectrum shows a positive band around 195 nm (amide transition π-π*, perpendicular coupling) and two negative bands around 208 nm (amide transition π-π*) and 222 nm (amide transition n-π), which are all typical features of a helical conformation of the peptides (*4*).

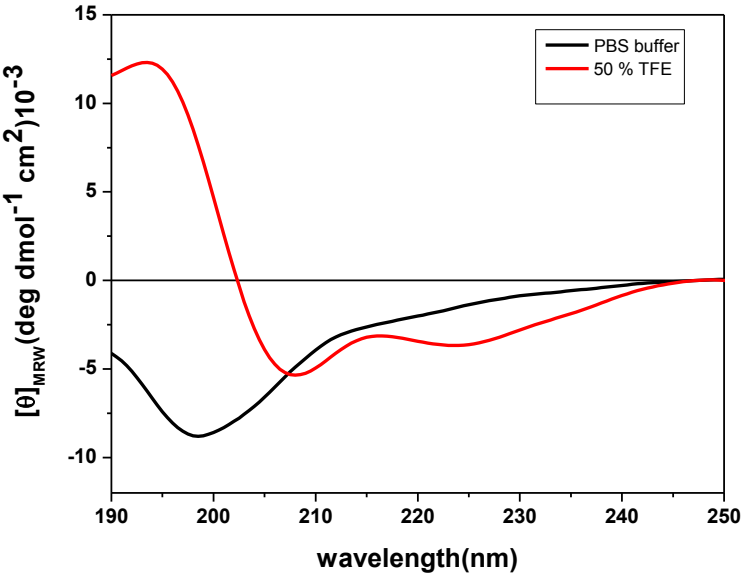

Fig.4.2.2. Far-UV CD spectra of Myxinidin in PBS buffer (black line) and 50% v/v TFE (red line) recorded at 25°C

The effect of TFE on the mutant peptide WMR (Fig. 4.2.3) is similar to that observed for Myxinidin (Fig. 4.2.2). In fact, also in this case, in the presence of 50% v/v TFE, the CD spectrum shows the helical conformation typical bands.

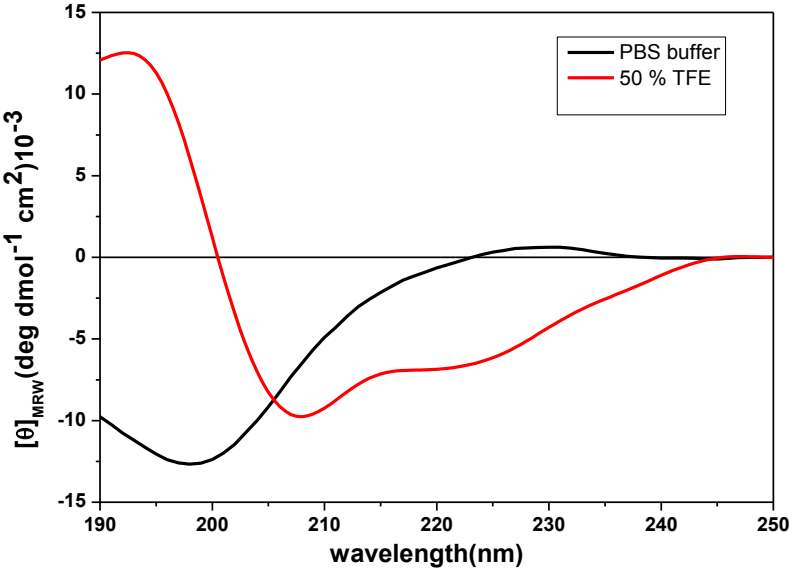

Fig.4.2.3. Far-UV CD spectra of WMR in PBS buffer (black line) and 50% v/v TFE (red line) recorded at 25°C

CD spectra of two peptides recorded in TFE/H_2O mixture demonstrated that both Myxinidin and WMR can adopt a helical conformation. CD spectra of Myxinidin and WMR were also recorded in the presence of liposomes at L/P=10, by adding opportune volumes of a peptide solution in a suspension of vesicles made as follow: DOPE/DOPG/Cardiolipin (65:23:12 % mol) and DOPE/DOPG (80:20 % mol) (Fig. 4.2.4) to mimic *P.aeruginosa* and *E. coli* cytoplasmic membranes, respectively.

CD spectra of both peptides show that the random coil conformation adopted in the buffer changes towards a more ordered secondary structure as indicated by the decrease and shift at higher wavelength of the negative band at 200 nm. This could indicate an interaction between peptides and vesicles.

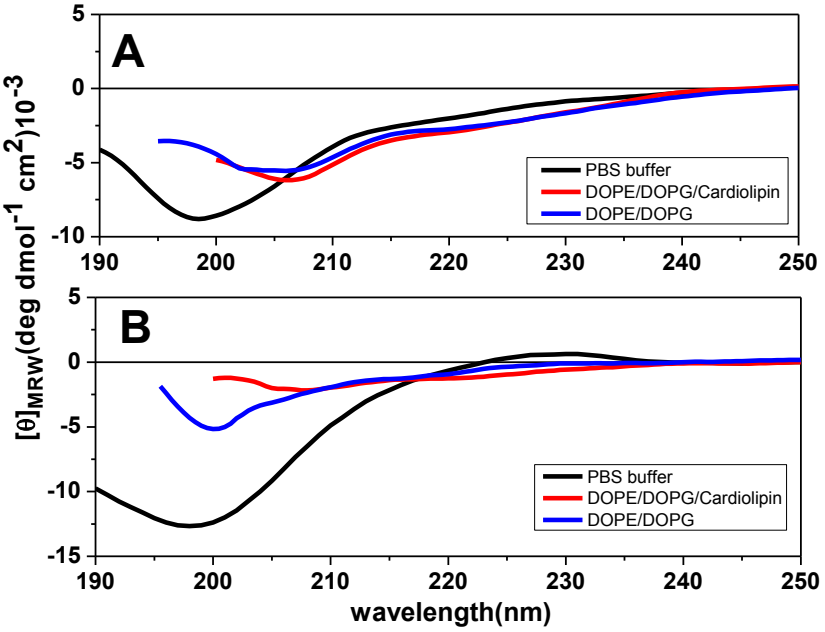

Fig.4.2.4. Far-UV CD spectra of Myxinidin (A) and WMR (B) in PBS buffer (black line) and in the presence of DOPE/DOPG/Cardiolipin (red line) and DOPE/DOPG (blue line) liposomes at L/P=10. All CD spectra were recorded at 25°C

CD spectra showed that Myxinidin and WMR assume a random coil structure in buffer solution and a helical structure in the TFE/H_2O mixtures. Further, both peptides adopt a more ordered secondary structure in the presence of the negatively charged DOPE/DOPG/Cardiolipin and DOPE/DOPG liposomes. In the presence of zwitterionic liposomes as DPPC and DOPE, the CD spectra of peptides still displayed a unordered structure (data not shown), suggesting a role of

liposomes charge. This result is consistent with a specificity of AMPs for the negatively charged membranes typical of the bacteria.

4.3 Myxinidin and WMR microenvironment in the presence of two different model bacterial membranes

In order to obtain information about the microenvironment of Myxinidin and WMR peptides upon the interaction with DOPE/DOPG/Cardiolipin and DOPE/DOPG vesicles (SUVs), intrinsic fluorescence experiments were performed. WMR contains two aromatic residues: a tryptophan (Trp 1) at N-terminal position and a tyrosine (Tyr 9), whereas Myxinidin contains only a residue of tyrosine (Tyr 8). The changes of Tyr and Trp fluorescence emission spectra have been monitored for Myxinidin and WMR in the presence of liposomes. Fig. 4.3.1 shows the fluorescence spectra of the Myxinidin in buffer and in the presence of vesicles at different lipid/peptide (L/P) ratios.

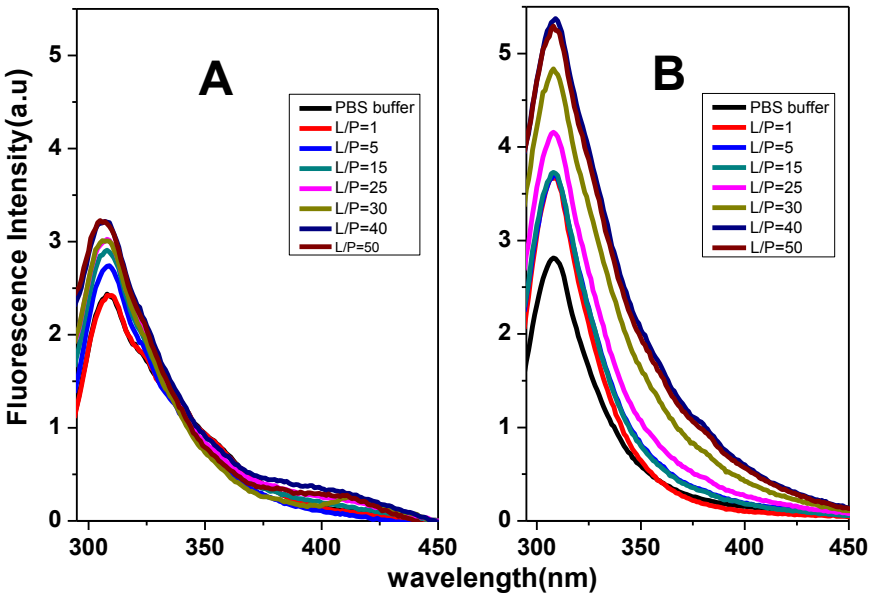

Fig.4.3.1 Fluorescence spectra of Myxinidin in the absence and in the presence of DOPE/DOPG/Cardiolipin (A) and DOPE/DOPG (B) liposomes at different lipid/peptide ratios recorded at 25°C.

Inspection of Fig.4.3.1 reveals that fluorescence spectrum of Myxinidin in buffer solution has a maximum around 310 nm, typical of peptides containing a tyrosine residue exposed to the aqueous medium. At increasing of lipid/peptide (L/P) ratio, an increase of fluorescence intensity is recorded, suggesting that the peptide does not deeply penetrate in the lipid bilayer. This could indicated that tyrosine residue is more sterically confined in the presence of model membranes (*5*). The two liposomes used have a slight different effect on the Myxinidin. In particular it is possible to note that in the presence of DOPE/DOPG the increase of fluorescence intensity is greater than DOPE/DOPG/Cardiolipin liposome, suggesting a trivial preference in the interaction of Myxinidin for DOPE/DOPG.

The behavior of the WMR in the presence of two model bacterial membrane is completely different as shown in Fig. 4.3.2.

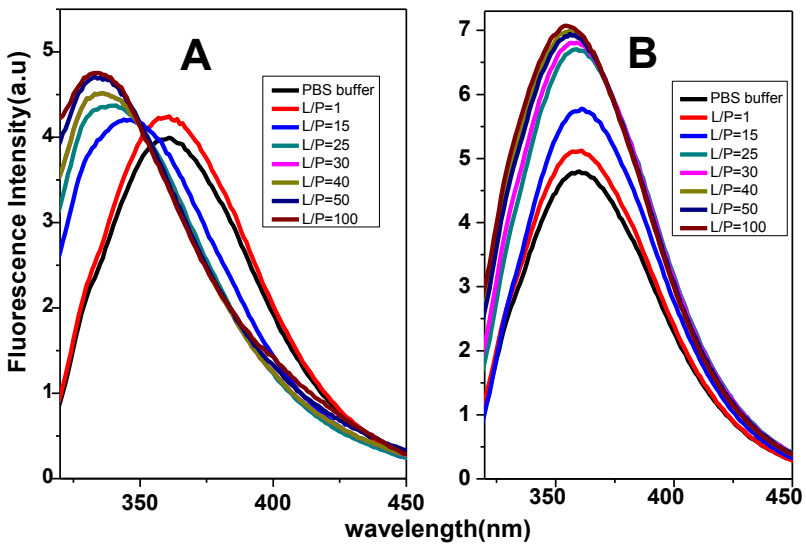

Fig.4.3.2 Fluorescence spectra of WMR in the absence and in the presence of DOPE/DOPG/Cardiolipin (A) and DOPE/DOPG (B) liposomes at different lipid/peptide ratios recorded at 25°C.

The fluorescence spectrum of WMR in buffer solution has a maximum at 361 nm, characteristic of a triptophan residue fully exposed to the aqueous medium. At increasing of DOPE/DOPG/Cardiolipin vesicles up to L/P=100, the emission intensity is enhanced and the maxima shifted to lower wavelengths with a blue shift of 28 nm (from 361 nm to 333 nm). Blue shifts of this magnitude are consistent with a significant change in the peptide microenvironment

polarity suggesting that the tryptophan indole moiety is partially immersed in the membrane. This result suggests that the peptide could be capable of penetrating the lipid bilayer. Indeed, it is widely accepted that the fluorescence emission of tryptophan residues increases when the amino acid penetrates a more hydrophobic environment and the maximal spectral position may be shifted toward shorter wavelengths (*6*). A smaller blue shift ($\Delta\lambda$ = 7 nm) of the tryptophan fluorescence is observed in the presence of DOPE/DOPG vesicles, suggesting that a weaker interaction occurs in this case.

The overall fluorescence results suggest that both Myxinidin and WMR interact with studied liposomes. Myxinidin has a slight preference for DOPE/DOPG liposomes, whereas WMR preferentially interacts with DOPE/DOPG/Cardioliopin liposomes, probably because these vesicles have a major percentage of anionic lipids than DOPE/DOPG.

The different penetration capability in the liposomes between two peptides can be attributed to the presence of an additional tryptophan (Trp) residue at N-terminal position in WMR peptide. In fact the characteristic of tryptophan residues to prefer the interfacial region of the membranes has been well documented (*6, 7*) and this behavior favors a deeply penetration of tryptophan rich AMPs into lipid bilayer (*8, 9*). In addition it is known that tryptophan residues contain an extensive π–electron system of the indole that contribute to a quadrupole moment of the side chain (*10*). This π–electron system can also contribute in cation-π interactions with side chains of positively charged amino acids. In fact WMR contains three arginine residues that can form these interaction with π–electron system of tryptophan and these cation-π interactions make energetically favorable the entry of antimicrobial peptides containing arginine and tryptophan residues in the bilayers because some residues of arginine can be shielded from the more hydrophobic Trp. In addition, the presence of cation-π interactions between arginine and tryptophan residues has been confirmed by the NMR structure of WMR in negatively charged bicelles containing Cardiolipin, as will be shown in the Chapter 5.

4.4 Heats of the interaction between peptides and liposomes by ITC

The interaction between the peptides and the model membranes was further studied by means of Isothermal Titration Calorimetry (ITC).

ITC is a potent versatile technique used to study the energetic of the association process between peptides and lipids. The enthalpy of association for the studied systems was directly measured by injecting a dilute peptide solution into the cell containing a concentrated vesicles suspension (peptide-into-lipid titration). Under these conditions, the lipid is much in excess over the peptide during the whole titration experiment, and the injected peptide is completely bound to the membrane surface. As a consequence the same heat effect is recorded during each injection. Fig. 4.4.1 shows the ITC traces obtained by the titration of the Myxinidin and WMR into the liposomes (LUVs) up to about a lipid/peptide ratio of 50 (L/P = 50).

.

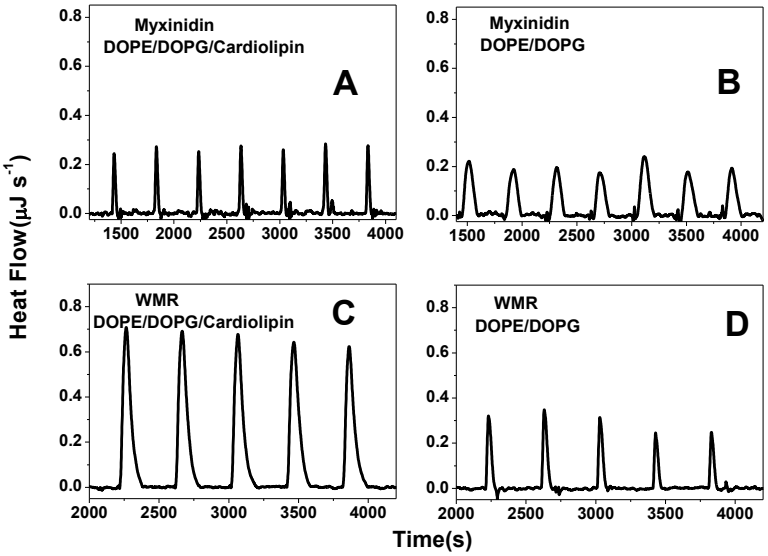

Fig.4.4.1 ITC traces obtained from the titration of DOPE/DOPG/Cardiolipin (A and C) and DOPE/DOPG (B and D) liposomes with Myxinidin (A and B) and WMR (C and D) peptides at 25 °C

As expected, in conditions of high L/P ratio, each injection produces the same heat. Analysis of the ITC trace obtained by the titration of Myxinidin into DOPE/DOPG/Cardiolipin (Fig. 4.4.1, panel A) and DOPE/DOPG (Fig. 4.4.1, panel B) liposomes provides negative values of association enthalpy of -5.9 ± 1.1 kJ/mol and -11.9 ± 1.3 kJ/mol respectively, revealing a favorable enthalpy contribution in the peptide-lipid interaction. The titration of WMR into DOPE/DOPG/Cardiolipin (Fig. 4.4.1, panel C) and DOPE/DOPG (Fig. 4.4.1, panel D) liposomes gives negative values of association enthalpy of -38.6 ± 2.0 kJ/mol and -13.7 ± 0.7 kJ/mol respectively.

At high lipid/peptide ratio, the ITC results suggest that, the binding of WMR with DOPE/DOPG/Cardiolipin liposomes is driven by an higher number of favorable interactions ($\Delta_a H°$= -38.6 ± 2.0 kJ/mol) in comparison with Mixinidin ($\Delta_a H°$= -5.9 ± 1.1 kJ/mol). This observation can be explained by the different aminoacidic sequence of the two peptides. In fact, differently from Myxinidin, WMR contains three arginine (Arg) and a tryptophan (Trp) residues that can establish a variety of additional interactions (electrostatic, hydrogen bond) with the more negatively charged liposomes. On the contrary the analysis of the titration of Myxinidin (Fig. 4.4.1, panel B) and WMR (Fig. 4.4.1, panel D) into DOPE/DOPG liposomes reveal a similar enthalpy contribution in the peptide-lipid interaction. This result suggests a similar behavior of Myxinidin and WMR with the less negatively charged liposomes in this condition of high L/P ratio. It is worth note that the enthalpy of interaction recorded in the titration contains contributions from both the lipid and peptide rearrangements and solvation upon interaction.

Since many AMPs exert their antimicrobial activity above a threshold concentration *L/P**(*11*) due to the occurrence of peptide-peptide interaction, additional ITC experiments were performed at high peptide concentration up to L/P = 7. (Fig.4.4.2).

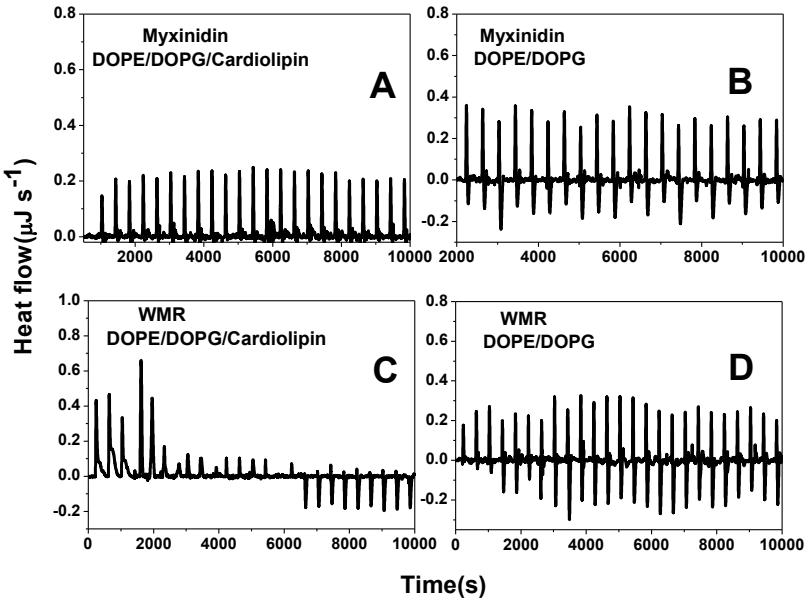

Fig.4.4.2 ITC traces obtained from the titration of DOPE/DOPG/Cardiolipin (A and C) and DOPE/DOPG (B and D) liposomes with Myxinidin (A and B) and WMR (C and D) peptides at 25 °C

In this condition of high peptide concentration (low L/P ratio), other phenomena (such as peptide aggregation processes, lipids reorganization, liposome disruption, pore formation) can occur. All these different phenomena concur to the global interaction process between peptides and lipids giving exothermic and endothermic contributions and the measured enthalpy change is the balance of all these processes (*12*-*15*).

Inspection of the ITC traces reveals that at high peptide concentration the association enthalpy of Myxinidin with the DOPE/DOPG/Cardiolipin liposomes (Fig. 4.4.2, panel A) is very similar to the one recorded at low peptide concentration (Fig. 4.4.1, panel A) suggesting no peptide-peptide interaction. On the contrary, the ITC trace of WMR titration into the DOPE/DOPG/Cardiolipin liposomes at low L/P ratio was completely different (Fig. 4.4.2, panel C) from the one obtained at high L/P ratio (Fig. 4.4.1,panel C), suggesting the presence of strong peptide-peptide interaction above a threshold concentration. Particularly, at L/P = 10, the ITC profile changes from exothermic to endothermic. Similar ITC profiles have been attributed previously to the pore formation in the membrane (*16*). On the contrary, the inspection of the ITC traces of the titration of Myxinidin and WMR in the DOPE/DOPG liposomes at low L/P ratio (Fig.4.4.2, panel B and D) are very similar

and more complex with respect to the ITC traces observed at high L/P ratio (Fig. 4.4.1, panel B and D). These results suggest the presence of secondary processes that depend on peptide concentration (such as peptide aggregation and lipids reorganization).

These ITC results show that Myxinidin and WMR differently interact with two studied liposomes. In particular, the enthalpy of interaction between WMR and DOPE/DOPG/Cardiolipin is greater that Myxinidin. Differently from Myxinidin, WMR contains three arginine and a tryptophan residues that are able to establish a variety of additional interactions (electrostatic, hydrogen bond) with negatively charged membranes. In fact, arginine residues contain a guanidinium mojety that can form two hydrogen bonds with negative phosphate groups of the liposomes, whereas Myxinidin has not arginine but two lysines residues that can form only a hydrogen bond. The formation of hydrogen bonds between arginine side chains and phosphate groups of the phospholipids could contribute to stabilize the negatively charged liposomes. Surprisingly, the enthalpy contribution to the interaction of Myxinidin ($\Delta_a H° = -11.9 \pm 1.3$ kJ/mol) and WMR ($\Delta_a H° = -13.7 \pm 0.7$ kJ/mol) with DOPE/DOPG liposome is similar, suggesting a preferential interaction of Myxinidin with this liposome containing a minor percentage of anionic lipids.

4.5 Effects of peptide interactions on the liposome size

In order to estimate the size distribution of DOPE/DOPG/Cardiolipin and DOPE/DOPG liposomes in the absence and presence of Myxinidin and WMR peptides, Dynamic Light Scattering (DLS) experiments were performed. They were achieved in collaboration with Prof. Paduano L. Group, Department of Chemical Sciences, University "Federico II", Naples.

DLS is a potent technique to study the effect of the peptides on the size and shape of liposomes (*17, 18*). Extruded DOPE/DOPG/Cardiolipin and DOPE/DOPG liposomes were prepared as described in the Material and Methods Chapter.

To study the potential effect of peptide-peptide interaction on the liposomes integrity, DLS experiments were recorded at high peptide concentration (L/P=10). Fig.4.5.1 shows DLS data of both liposomes before and after the addition of the peptides.

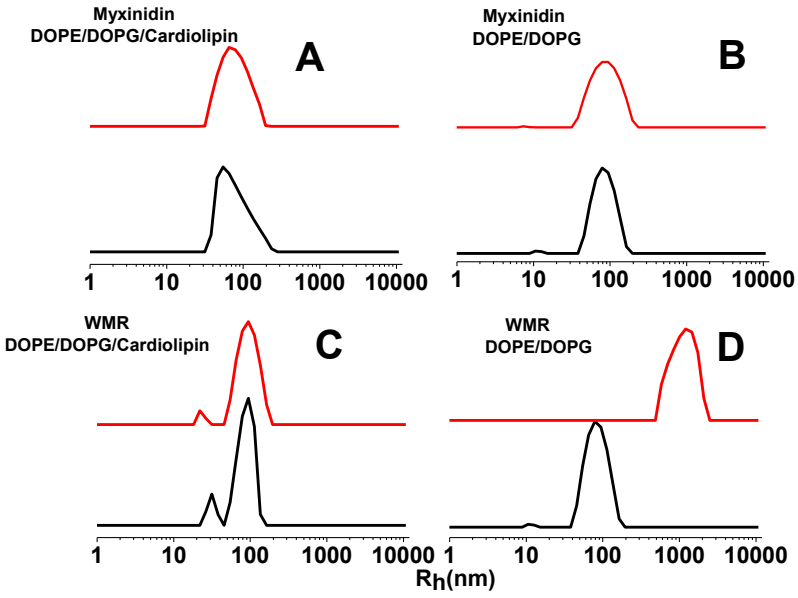

Fig.4.5.1 DLS measurements of DOPE/DOPG/Cardiolipin (A and C) and DOPE/DOPG (B and D) liposomes in the absence (black line) and presence (red line) of Myxinidin (A and B) and WMR (C and D) at L/P=10.

Analysis of DLS measurements provides the hydrodynamic radius of the scattered liposome (Table 4.5.1).

Table 4.5.1 Hydrodynamic radius values obtained from DLS measurements of DOPE/DOPG/Cardiolipin and DOPE/DOPG liposomes in the absence and presence of Myxinidin and WMR at L/P=10

Sample	**Hydrodynamic radius (nm)**
DOPE/DOPG/Cardiolipin	74 ± 5
Myxinidin-(DOPE/DOPG/Cardiolipin)	70 ± 1
WMR-(DOPE/DOPG/Cardiolipin)	94 ± 12
DOPE/DOPG	77 ± 1
Myxinidin-(DOPE/DOPG)	75 ± 3
WMR-(DOPE/DOPG)	1022 ± 35

Fig. 4.5.1 (panel A and B) shows that the hydrodynamic radius of two liposomes does not change in the presence of Myxinidin at L/P =10 (Table 4.5.1). These results suggest that the liposomes are still the dominant structure in the presence of Myxinidin at this lipid/peptide ratio. The same result is observed in the case of DOPE/DOPG/Cardiolipin in the presence of WMR at high peptide concentration. In fact the hydrodynamic radius of DOPE/DOPG/Cardiolipin remains still constant upon the addition of WMR at L/P = 10 ratio. (Fig. 4.5.1, panel C) suggesting that the liposome is the dominant structure also in this case. This result, together with ITC results at high peptide concentration (L/P =10), supports the assumption of a pore formation in this membrane. On the contrary, the effect of WMR on the DOPE/DOPG liposomes is different at high peptide concentration. In this case, the hydrodynamic radius of the liposomes strongly increases (from R_h=

77 ± 1 nm to R_h= 1022 ± 35 nm) in the presence of WMR. Interestingly, a significant increase of the intensity of the light scattered was observed immediately upon the addition of WMR. This result is consistent with liposomes aggregation or fusion in the presence of WMR. The formation of large aggregates can be explained by the self-association of liposomes, which can be driven by peptides that bridge between two or more liposomes or by peptide-peptide interactions between peptides bound to liposomes, as reported in literature (*19*). This result is according to ITC results at high peptide concentration (L/P=10).

Further DSL data of all studied systems have shown that the micellization/solubilization of the membranes in the presence of Myxinidin and WMR does not occur at the explored peptide concentrations, excluding the carpet like mechanism observed for many antimicrobial peptides and supporting other possible mechanisms such as pore and aggregate formation.

4.6 Effect of the Myxinidin and WMR on the liposome phase transition

Differential Scanning Calorimetry (DSC) is a varsatile technique that gives information on the thermal behavior of the liposomes and the effects of the peptides on their phase transitions. Fluorescence, ITC, CD, DLS experiments were performed using DOPE/DOPG/Cardiolipin (65:23:12) and DOPE/DOPG(80:20) vesicles. These liposomes were in a liquid crystalline phase in the experimental conditions (25°C). For DSC experiments it was impossible to use these liposomes because they have a temperature of melting below 0°C (our DSC instrument is not capable to arrive at these low temperatures). The low melting temperatures of DOPE, DOPG and Cardiolipin are due to their high unsaturated fatty acid content.

For this reason, DPPE and DPPG were chosen to replace DOPE and DOPG as they have the same zwitterionic heads and at the same time, they show a main phase transition in a temperature range suitable for DSC study. Thus, DSC experiments were performed with DPPE/DPPG/Cardiolipin (65:23.12) and DPPE/DPPG(80:20) vesicles. These liposomes are in gel phase at 25°C .

DPPE and DPPG structures are:

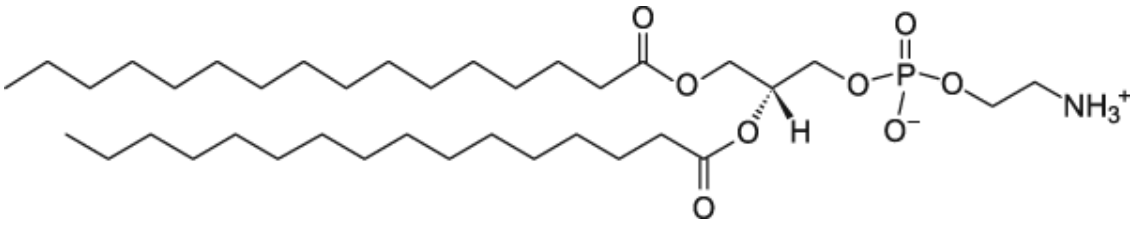

DPPE

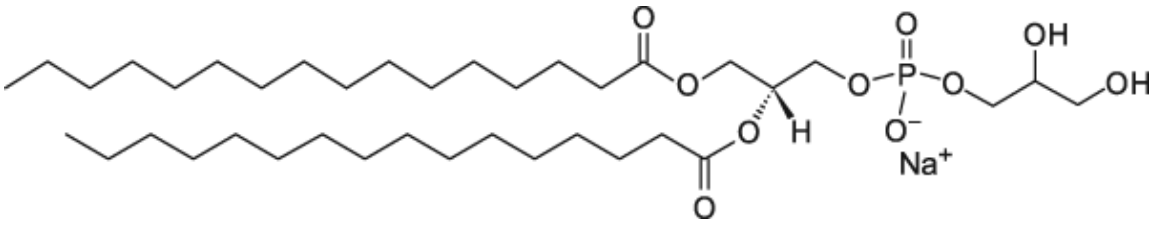

DPPG

DPPE and DPPG have saturated acyl chains and for this reason their melting temperatures from gel phase (L_β) to liquid crystalline phase (L_α) are, respectively, 63°C and 41°C.

DSC profile of the mixture DPPE/DPPG/cardiolipin (65:23:12) is not published in the literature. On the contrary the mixture DPPE/DPPG (80:20) has been characterized in literature. DPPE and DPPG shows non-ideal miscibility in the liquid-crystalline phase, whereas in the lamellar-gel phase a region of immiscibility exists in the mole fraction range *x(*DPPE)=0.05–0.4 (*20*). The non-ideal miscibility of the PE and PG lipids is due to their different chemical properties. In fact the molecular shape of PG can be described as a cylinder, while PE exhibits a smaller head group area as compared to the cross sectional area required by the acyl chains, which can be described by a truncated cone. The liposome compositions used in this thesis are in the range of miscibility of the binary mixture PE/PG lipids in the gel phase. The thermodynamic parameters measured by DSC profiles are: melting temperature (T_m), the enthalpy change ($\Delta_m H$), and width half-height ($\Delta T_{1/2}$) of the main transition of the liposomes. The $\Delta T_{1/2}$ is inversely correlated to the cooperativity of the transition (low $\Delta T_{1/2}$ values correspond to high cooperativity, whereas high $\Delta T_{1/2}$ values indicate low cooperativity).These parameters allow to understand the potential tendency of the peptides to interact with lipid head groups or to perturb the packing of the lipid acyl chains (*21-23*).

In order to study the perturbation effect of two peptides on the phase transition of both liposomes, DSC experiments were performed at high peptide concentration (L/P=10). Fig.4.6.1 shows DSC cooling profiles of two liposomes in the presence of Myxinidin and WMR at L/P=10. The more pronounced effect of the peptides are observed in DSC cooling profiles than heating and for this reason DSC cooling profiles are reported. This observation suggests that two peptides could start to interact with two liposomes in the liquid crystalline phase, as verified for other antimicrobial peptides (*24*). This phenomenon could indicate a preference of the peptides to bind vesicles in liquid crystalline phase. This result has a great biological importance because bacterial membranes are in a fluid phase at their normal conditions (*25*).

The effects of the peptides on the phase transition of two liposomes are shown in Fig.4.6.1 and the thermodynamic parameters are collected in Table 4.6.1.

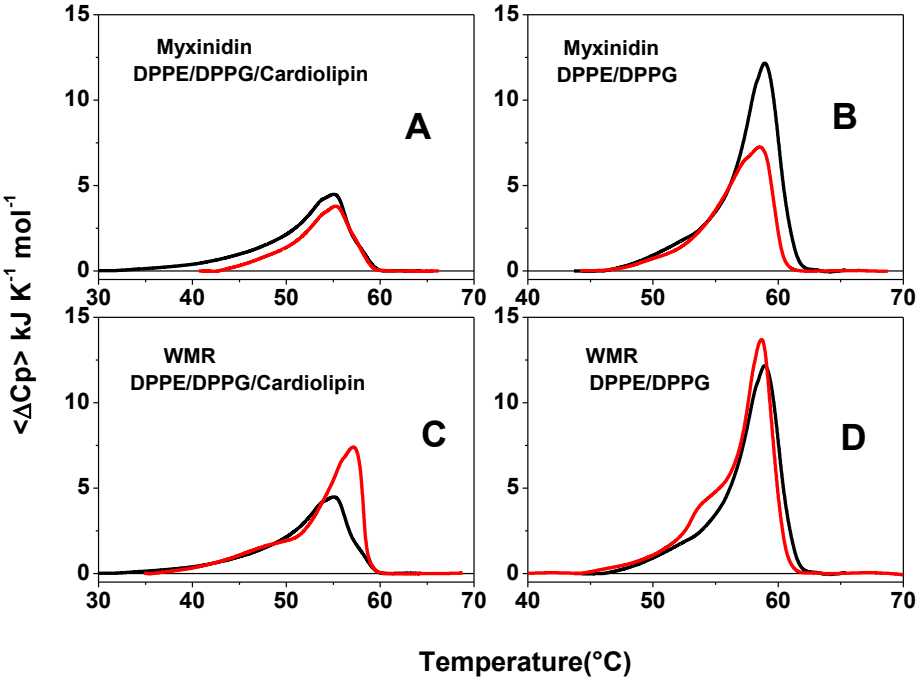

Fig. 4.6.1 DSC cooling profiles of DPPE/DPPG/Cardiolipin (A and C) and DPPE/DPPG (B and D) liposomes in the absence (black lines) and in the presence of Myxinidin (A and B) (red line) and WMR (C and D) (red line) at L/P=10 ratio

Table 4.6.1 Thermodynamic parameters of DSC cooling profiles of DPPE/DPPG/Cardiolipin and DPPE/DPPG liposomes in the absence and presence of Myxinidin and WMR at L/P=10

Systems	$\Delta_m H$ (kJ/mol)	T_m (°C)	$\Delta T_{1/2}$ (°C)
Myxinidin (DPPE/DPPG/Cardiolipin)			
Liposome	-31.1 ± 3.1	55.1 ± 0.5	6.3 ± 0.5
L/P=10	-26.0 ± 2.6	55.2 ± 0.5	6.0 ± 0.5
Myxinidin (DPPE/DPPG)			
Liposome	-57.4 ± 5.7	59.0 ± 0.5	3.6 ± 0.5
L/P=10	-39.1 ± 3.9	58.5 ± 0.5	4.7 ± 0.5
WMR (DPPE/DPPG/Cardiolipin)			
Liposome	-31.1 ± 3.1	55.1 ± 0.5	6.3 ± 0.5
L/P=10	-50.3 ± 5.0	57.1 ± 0.5	4.9 ± 0.5
WMR (DPPE/DPPG)			
Liposome	-57.4 ± 2.8	59.0 ± 0.5	3.6 ± 0.5
L/P=10	-61.6 ± 3.1	58.7 ± 0.5	3.0 ± 0.5

DSC profile of DPPE/DPPG/Cardiolipin shows a single, asymmetric and broad transition centered at 55.1 ± 0.5°C (Fig.4.6.1, panel A and C) due to the complexity of the ternary mixture. On the contrary the DSC profile of DPPE/DPPG liposome (Fig.4.6.1, panel B and D) shows a single and

more cooperative transition centered at 59.0 ± 0.5 °C, according to previous studies in literature(*20*). Both studied lipid mixtures show a larger DSC profile than that of DPPE or DPPG alone as expected as the DSC profiles of the pure lipids are sharp and highly cooperative.

Fig.4.6.1 shows that Myxinidin marginally changes the thermodynamic parameters of the DPPE/DPPG/Cardiolipin transition (Fig.4.6.1, panel A and Table 4.6.1), whereas has a major effect on the DPPE/DPPG transition (Fig.4.6.1, panel B and Table 4.6.1). In the latter case, Myxinidin decreases the melting enthalpy and the cooperativity (Table 4.6.1) of the DPPE/DPPG transition without changing the overall shape of the DSC profile, indicating a lower packing of acyl chain lipids in the presence of the peptide (*21*). This result confirms the preference of Myxinidin to interact with the vesicles containing a minor percentage of anionic lipids, according to Fluorescence and ITC results. On the contrary, WMR has a major effect on the more negatively charged liposomes containing Cardiolipin. In particular, after the addition of WMR, the enthalpy change increases and the main phase transition appears sharper and shifted at higher temperature (Fig.4.6.1, panel C). This behavior is consistent with a preferential interaction of WMR with anionic DPPG and Cardiolipin lipids, leading to the clustering of these lipids and to the formation of DPPE-enriched domain that melts more cooperatively and at higher temperatures (*26*). Interestingly, the DSC profile of the DPPE/DPPG/Cardiolipin, in the presence of WMR, closely resembles the DSC profile of the DPPE/DPPG liposome (Fig.4.6.1, panel B), suggesting that WMR preferentially segregates more Cardiolipin than DPPG, leaving the remaining liposome domains enriched with DPPE/DPPG. Further, in absence of Cardiolipin, WMR marginally changes the thermodynamic parameters of the DPPE/DPPG transition (Fig.4.6.1, panel D and Table 4.6.1), confirming that the presence of the Cardiolipin with its negative head group is a key element to determine the membrane-WMR interaction. In addition, WMR increase the enthalpy of DPPE/DPPG liposome and a small shoulder in DSC profile is observed. This result could indicate the presence of aggregation phenomena of the membrane upon binding with WMR, according to DLS experiments (*27*).

To better investigate the drastic effects of WMR on both liposomes, additional DSC experiments were performed at low peptide concentration (high L/P ratio), to check its potent activity in these conditions. DSC profiles are reported in Fig.4.6.2 and thermodynamic parameters are collected in Table 4.6.2.

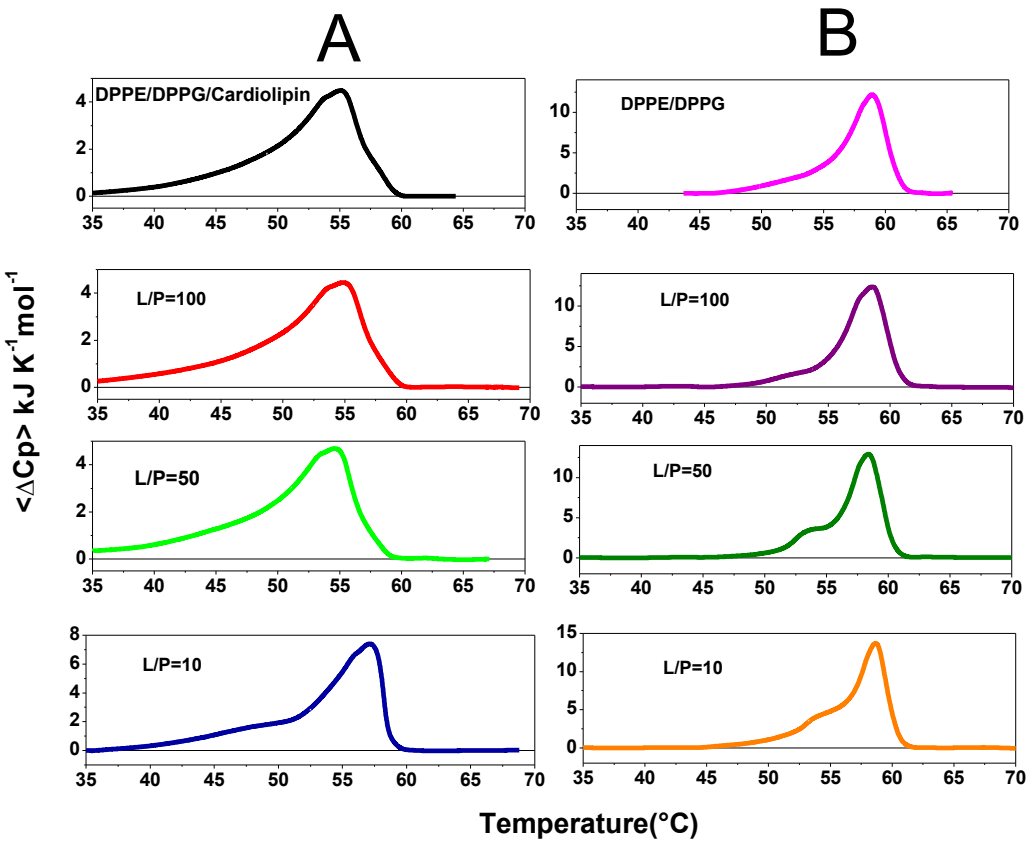

Fig.4.6.2. DSC cooling profiles of DPPE/DPPG/Cardiolipin (A)and DPPE/DPPG (B) liposomes in the absence and presence of WMR at different L/P ratios as indicated

Table 4.6.2 Thermodynamic parameters of DSC cooling profiles of DPPE/DPPG/Cardiolipin and DPPE/DPPG liposomes in the absence and presence of the WMR peptide at different L/P ratios

Systems	**$\Delta_m H$ (kJ/mol)**	**T_m (°C)**	**$\Delta T_{1/2}$ (°C)**
WMR (DPPE/DPPG/Cardiolipin)			
Liposome	- 31,1 ± 3.1	55.1 ± 0.5	6.3 ± 0.5
L/P=100	- 43.0 ± 4.3	54. 9 ± 0.5	7.2 ± 0.5
L/P=50	- 44.3 ± 4.4	54.6 ± 0.5	6.8 ± 0.5
L/P=10	- 50.3 ± 5.0	57.1 ± 0.5	4.9 ± 0.5
WMR (DPPE/DPPG)			
Liposome	-57.4 ± 5.7	59.0 ± 0.5	3.6 ± 0.5
L/P=100	-57.2 ± 5.2	58.6 ± 0.5	3.7 ± 0.5
L/P=50	-57.7 ± 5.7	58.4 ± 0.5	3.1 ± 0.5
L/P=10	-61.6 ± 6.1	58.7 ± 0.5	3.0 ± 0.5

DSC results at low peptide concentration reveal that WMR marginally affects the thermodynamic parameters and the shape of DSC profile of DPPE/DPPG/Cardiolipin at high lipid/peptide ratio (L/P=100 and L/P=50), but it drastically changes the thermodynamic parameter and the shape of DSC profile of DPPE/DPPG/Cardiolipin at L/P=10 as described above. This results confirms that

the threshold L/P* ratio for the antimicrobial activity of WMR on this lipid composition is L/P=10. On the contrary, in the case of DPPE/DPPG liposome, small differences in the thermodynamic parameters and the shape of DSC profiles are observed. In particular, a small shoulder in the DSC profile at L/P=50 and L/P=10 appears and a weak increase of enthalpy change occurs only at L/P=10.Probably this result is due to liposome aggregation phenomenon, occurring at high peptide concentration, according to DSL results.

In conclusion, DSC results show that Myxinidin has a stronger interaction with the liposomes containing a minor percentage of anionic lipids, causing a lower packing between the acyl chain lipids. This result is according to Fluorescence and ITC experiments. On the contrary WMR has a preference for the liposome with a higher content of anionic lipids. In particular, WMR induces the segregation of the anionic Cardiolipin and DPPG lipids from zwitterionic DPPE, and this segregation could favour the pore formation in the membrane. A drastic membrane perturbation upon WMR binding is also consistent with our ITC measurements performed at high peptide concentration (low L/P ratio), suggesting pore formation in the DPPE/DPPG/Cardiolipin liposome. We suppose that WMR preferentially segregate Cardiolipin than DPPG and this hypothesis is supported by the absence of segregation phenomena in the membrane without Cardiolipin. In fact, in DPPE/DPPG liposome, no segregation of anionic DPPG is observed, supporting that the Cardiolipin is a key element to induce the segregation of anionic and zwitterionic lipids in the membranes. These results confirm the potency of DSC technique, capable to individue micro-domains in the membranes and gives information about the different effect of membrane perturbation by Myxinidin and WMR .

4.7 Lipid mixing, inner monolayer fusion and leakage assays

To further show the potential membrane permeabilization by Myxinidin and WMR, different experiments such as lipid mixing, inner monolayer fusion and leakage were performed by Prof. Galdiero S. Group, Department of Pharmacy, University "Federico II", Naples. Fig.4.7.1 shows the effects of two peptides on DOPE/DOPG/Cardiolipin and DOPE/DOPG liposomes.

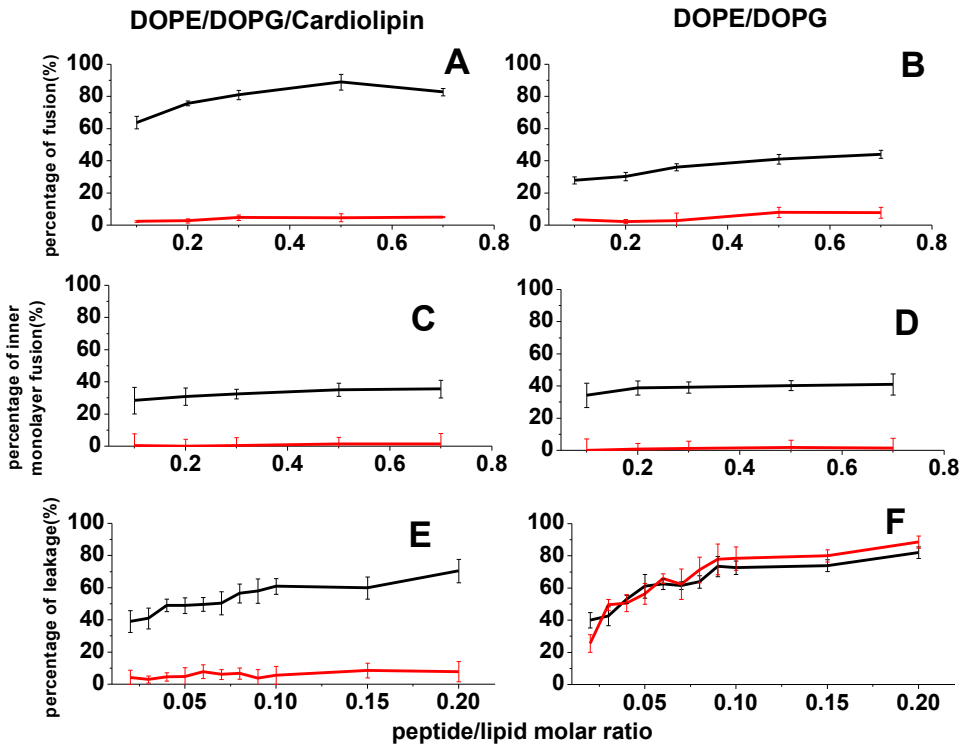

Fig.4.7.1 Lipid mixing promoted by WMR (red) and Myxinidin (black) in DOPE/DOPG/CL (A) and DOPE/DOPG (B) vesicles; inner monolayer fusion promoted by WMR (red) and Myxinidin (black) in DOPE/DOPG/CL (C) and DOPE/DOPG (D) vesicles; leakage promoted by WMR (red) and Myxinidin (black) in DOPE/DOPG/CL (E) and DOPE/DOPG (F) vesicles

Fig.4.7.1 (panel A and B) shows the results of lipid mixing assays in two studied liposomes for Myxinidin and WMR at 37 °C. Unlike Myxinidin, the peptide WMR induces significant levels of fusion in both types of liposomes, suggesting that it is able to interact with the bilayers. In

particular, the fusion activity obtained for WMR is higher in presence of Cardiolipin. In fact, it is evident from the results obtained that the negatively charged phospholipids are preferred by WMR containing arginine residues as we expected. The less charged nature of Myxinidin promotes a lower fusion in vesicles without Cardiolipin.

Fig.4.7.1 (panel C and D) shows a significant fusion of the inner monolayer for WMR in both studied lipid compositions. This is slightly lower than the fusion level obtained in the lipid mixing experiment, since the latter measures both hemi-fusion and complete fusion. Therefore, this assay clearly indicates that WMR is able to induce fusion of both the inner and the outer monolayers. For Myxinidin no inner monolayer fusion was observed.

Fig.4.7.1 (panel E and F) shows the effect of Myxinidin and WMR on the release of encapsulated fluorophores in model membranes made of DOPE/DOPG/CL and DOPE/DOPG liposomes. Release of ANTS and DPX from vesicle is commonly used as a measure of bilayer perturbation and interpreted as ‘‘transient pore formation”. When ANTS (fluorophore) and DPX (quencher) are both in the internal watery part of liposomes, the increase of ANTS fluorescence isn’t observed but, when pore formation occurs, the two molecules escape from vesicles and get far from each other resulting in an increase of ANTS fluorescence intensity. The leakage experiment (fig. 4.7.1 panel E and F) shows that WMR exhibits a greater leakage than Myxinidin with *P. aeruginosa* lipids, according to ITC and DLS experiments and supporting the pore formation in the membrane containing Cardiolipin. Differently the leakage promoted by the two peptides in *E. coli* membranes is almost the same.

In conclusion, these results show that WMR has a greater effect on DOPE/DOPG/Cardiolipin liposome than Myxinidin, whereas the difference of the effects of Myxinidin and WMR on DOPE/DOPG liposome is smaller than that observed in Cardiolipin containing liposome. These results are according to ITC, Fluorescence and DSC results.

4.8 Conclusion

In conclusion, the effects of Myxinidin and WMR peptides on two model membrane mimicking *P. aeruginosa* and *E. coli* are completely different. The findings of this work have elucidated the importance of the peptide and membrane composition in the interaction process between antimicrobial peptides and membranes. In particular, the role of the amino acid sequence, conformation and charge density of peptides on antimicrobial activity against DOPE/DOPG/Cardiolipin and DOPE/DOPG liposomes has been understood. All the results obtained by different experimental techniques have coherently shown that Myxinidin with a high hydrophobicity, has a slight preference to interact with membranes containing a low amount of anionic lipids. On the contrary, WMR with a high positively charge density, strongly interacts with membranes containing a high percentage of anionic lipids. In particular, our results suggest the functional role of the specific amino acid residues (Arg and Trp) in the mutant WMR, due to additional cation-π interactions, that probably contribute to increase the antimicrobial activity of this peptide respect to Myxinidin. Surprisingly, the different behaviour of Myxinidin and WMR on the membranes doesn't depend on the peptide conformation. In fact, CD results have shown that both AMPs have a tendency to adopt a similar more ordered conformation in the studied liposomes, despite the difference of lipid composition of two membrane mimetic environments.

On the other hand, this Ph.D. thesis has allowed to understand also the role of lipid composition on the antimicrobial activity of Myxinidin and WMR. The presence of the anionic Cardiolipin has been demonstrated to be a key element in the peptide-lipid interaction. In fact, WMR induces the segregation of Cardiolipin away from zwitterionic lipids in the membrane containing this anionic lipid and probably this segregation favors the pore formation in the membrane at L/P=10. As support of the segregation of Cardiolipin, WMR is not capable to induce the domains and pore formation in the membrane without this anionic lipid, but it causes vesicles aggregation phenomena. On the contrary, because of the high hydrophobicity, Myxinidin has a weak effect on the membrane containing anionic Cardiolipin, suggesting an interaction on the membrane surface. Unlike WMR, the peptide Myxinidin prefers to interact with the membrane containing a minor percentage of negatively charged lipids, causing a lower acyl chain packing in the membrane in the presence of the peptide.

Looking all the results obtained by different experimental techniques, the membrane perturbation effects of two peptides have been observed in the following order:

WMR-DOPE/DOPG/Cardiolipin>WMR-DOPE/DOPG≥Myxinidin-DOPE/DOPG>Myxinidin-DOPE/DOPG/Cardiolipin.

The results of this study support the higher antimicrobial activity of WMR than Myxinidin against *P. aeruginosa* and *E. coli* strains. In particular, they are consistent with a greater difference of the antimicrobial activity between the two peptides against *P. aeruginosa* and a slight difference against *E. coli*.

All the results provide additional information about the structure-activity relationship of short AMPs, which will pave the way for future *de novo* design of potent selective AMPs for therapeutic and biomedical applications.

References

(1) Nichols, M., Kuljanin, M., Nategholeslam, M., Hoang, T., Vafaei, S., Tomberli, B., Gray, C. G., DeBruin, L., and Jelokhani-Niaraki, M. (2013) Dynamic turn conformation of a short tryptophan-rich cationic antimicrobial peptide and its interaction with phospholipid membranes. *J Phys Chem B 117*, 14697-708.

(2) Dathe, M., Schumann, M., Wieprecht, T., Winkler, A., Beyermann, M., Krause, E., Matsuzaki, K., Murase, O., and Bienert, M. (1996) Peptide helicity and membrane surface charge modulate the balance of electrostatic and hydrophobic interactions with lipid bilayers and biological membranes. *Biochemistry 35*, 12612-22.

(3) Lehrman, S. R., Tuls, J. L., and Lund, M. (1990) Peptide alpha-helicity in aqueous trifluoroethanol: correlations with predicted alpha-helicity and the secondary structure of the corresponding regions of bovine growth hormone. *Biochemistry 29*, 5590-6.

(4) Greenfield, N., and Fasman, G. D. (1969) Computed circular dichroism spectra for the evaluation of protein conformation. *Biochemistry 8*, 4108-16.

(5) Christiaens, B., Symoens, S., Verheyden, S., Engelborghs, Y., Joliot, A., Prochiantz, A., Vandekerckhove, J., Rosseneu, M., and Vanloo, B. (2002) Tryptophan fluorescence study of the interaction of penetratin peptides with model membranes. *Eur J Biochem 269*, 2918-26.

(6) Yau, W. M., Wimley, W. C., Gawrisch, K., and White, S. H. (1998) The preference of tryptophan for membrane interfaces. *Biochemistry 37*, 14713-8.

(7) Persson, S., Killian, J. A., and Lindblom, G. (1998) Molecular ordering of interfacially localized tryptophan analogs in ester- and ether-lipid bilayers studied by 2H-NMR. *Biophys J 75*, 1365-71.

(8) Schibli, D. J., Hwang, P. M., and Vogel, H. J. (1999) Structure of the antimicrobial peptide tritrpticin bound to micelles: a distinct membrane-bound peptide fold. *Biochemistry 38*, 16749-55.

(9) Rozek, A., Friedrich, C. L., and Hancock, R. E. (2000) Structure of the bovine antimicrobial peptide indolicidin bound to dodecylphosphocholine and sodium dodecyl sulfate micelles. *Biochemistry 39*, 15765-74.

(10) Dougherty, D. A. (1996) Cation-pi interactions in chemistry and biology: a new view of benzene, Phe, Tyr, and Trp. *Science 271*, 163-8.

(11) Stark, M., Liu, L. P., and Deber, C. M. (2002) Cationic hydrophobic peptides with antimicrobial activity. *Antimicrob Agents Chemother 46*, 3585-90.

(12) Garidel, P., Hildebrand, A., Knauf, K., and Blume, A. (2007) Membranolytic activity of bile salts: influence of biological membrane properties and composition. *Molecules 12*, 2292-326.

(13) Zehender, F., Ziegler, A., Schonfeld, H. J., and Seelig, J. (2012) Thermodynamics of protein self-association and unfolding. The case of apolipoprotein A-I. *Biochemistry 51*, 1269-80.

(14) Heerklotz, H., and Seelig, J. (2007) Leakage and lysis of lipid membranes induced by the lipopeptide surfactin. *Eur Biophys J 36*, 305-14.

(15) McKeown, A. N., Naro, J. L., Huskins, L. J., and Almeida, P. F. (2011) A thermodynamic approach to the mechanism of cell-penetrating peptides in model membranes. *Biochemistry 50*, 654-62.

(16) Henriksen, J. R., and Andresen, T. L. (2011) Thermodynamic profiling of peptide membrane interactions by isothermal titration calorimetry: a search for pores and micelles. *Biophys J 101*, 100-9.

(17) Arouri, A., and Mouritsen, O. G. (2011) Anticancer double lipid prodrugs: liposomal preparation and characterization. *J Liposome Res 21*, 296-305.

(18) Domingues, M. M., Santiago, P. S., Castanho, M. A., and Santos, N. C. (2008) What can light scattering spectroscopy do for membrane-active peptide studies? *J Pept Sci 14*, 394-400.

(19) Arouri, A., Dathe, M., and Blume, A. (2013) The helical propensity of KLA amphipathic peptides enhances their binding to gel-state lipid membranes. *Biophys Chem 180-181*, 10-21.

(20) Lohner, K., Latal, A., Degovics, G., and Garidel, P. (2001) Packing characteristics of a model system mimicking cytoplasmic bacterial membranes. *Chem Phys Lipids 111*, 177-92.

(21) Henzler-Wildman, K. A., Martinez, G. V., Brown, M. F., and Ramamoorthy, A. (2004) Perturbation of the hydrophobic core of lipid bilayers by the human antimicrobial peptide LL-37. *Biochemistry 43*, 8459-69.
(22) Lohner, K., and Prenner, E. J. (1999) Differential scanning calorimetry and X-ray diffraction studies of the specificity of the interaction of antimicrobial peptides with membrane-mimetic systems. *Biochim Biophys Acta 1462*, 141-56.
(23) McElhaney, R. N. (1986) Differential scanning calorimetric studies of lipid-protein interactions in model membrane systems. *Biochim Biophys Acta 864*, 361-421.
(24) Seto, G. W., Marwaha, S., Kobewka, D. M., Lewis, R. N., Separovic, F., and McElhaney, R. N. (2007) Interactions of the Australian tree frog antimicrobial peptides aurein 1.2, citropin 1.1 and maculatin 1.1 with lipid model membranes: differential scanning calorimetric and Fourier transform infrared spectroscopic studies. *Biochim Biophys Acta 1768*, 2787-800.
(25) Cullis, P. R., and de Kruijff, B. (1979) Lipid polymorphism and the functional roles of lipids in biological membranes. *Biochim Biophys Acta 559*, 399-420.
(26) Epand, R. M., Epand, R. F., Arnusch, C. J., Papahadjopoulos-Sternberg, B., Wang, G., and Shai, Y. (2010) Lipid clustering by three homologous arginine-rich antimicrobial peptides is insensitive to amino acid arrangement and induced secondary structure. *Biochim Biophys Acta 1798*, 1272-80.
(27) Drazenovic, J., Wang, H., Roth, K., Zhang, J., Ahmed, S., Chen, Y., Bothun, G., and Wunder, S. L. (2015) Effect of lamellarity and size on calorimetric phase transitions in single component phosphatidylcholine vesicles. *Biochim Biophys Acta 1848*, 532-43.

Chapter 5

Structural characterization of Myxinidin and WMR in micelles and bicelles

5.1 Introduction

Within my Ph.D. project a structural characterization of Myxinidin and WMR in sodium dodecyl sulfate (SDS) micelles and DMPC/DMPG/Cardiolipin (65:23:12 % mol) bicelles has been performed in the Dr. Dames Group, at the Chair of Biomolecular NMR spectroscopy, *Technische Universität München* (TUM). Micelles can be formed by detergents and lipids with short acyl chain and they are used as membrane mimetic for solution-state Nuclear Magnetic Resonance (NMR) measurements. Because of their rahter small and rather spherical shape, they reorient rather rapidly and isotropically (*1*). For this reason, a good spectral resolution is obtained in NMR spectra of peptides in micelles. SDS micelles are often used to mimic negative bacterial membranes (*2*) and they are more mimetic of TFE solution (*3*) due to the separation between hydrophilic head groups and hydrophobic acyl chains. The NMR structures of different antimicrobial peptides have already been determined in SDS micelles (*4, 5*). A disadvantage of the micelles is their high curvature. In recent years, new model bio-membranes such as bicelles (bilayered-micelles) have been used in order to better mimic the natural bilayer. Overall bicelles mimic the properties of the natural membrane surface, such as charge, curvature, and acyl chain packing density, better than micelles (*6*). They can be thought such as a bridge between the small micelles and bigger lipid vesicles (liposomes) and are formed by lipids and detergents. In particular they are composed of long-chain and short-chain lipids (detergent) to form a disk shape in aqueous medium with a central, planar lipid bilayer that is surrounded by detergents. The size and shape of a bicelle depend on the q value, where q is the ratio between long and short chain lipids. Bicelles with high q values (> about 3) align in magnetic field and thus can be used to record residual dipolar couplings (*7*). Small bicelles with rather low q values (around 0.1-0.3) are an attractive membrane mimetic for structural studies since they still tumble relatively fast in solution, thus providing still a rather good spectral resolution in solution and solid state NMR spectra (*8, 9*). In addition, bicelles have been used in bacteriorhodopsin crystallization work (*10*). Based on the available literature, also the NMR structures of different peptides in bicelle environments have been determined (*11-13*).

During my practical work at the *Technische Universität München* (TUM) in Dr. Dames Group, a series of homonuclear 2D ^{1}H-^{1}H NMR spectra, including 2D ^{1}H-^{1}H COSY(Correlated Spectroscopy), TOCSY (Total Correlation Spectroscopy), and NOESY(Nuclear Overhauser Effect Spectroscopy), had been recorded to assign the proton chemical shifts of the backbone and side chains of the two unlabelled peptides and to obtain intermolecular distance restraints. 2D NMR COSY and TOCSY spectra are important for the assignment and provide correlations between protons connected by chemical bonds based scalar (through-bond) couplings. Whereas COSY

spectra provide only correlations between protons bound to carbons connected by 1 bond, 2D NMR TOCSY spectra correlate all protons of the same spin system, in this case amino acid side chain. 2D NMR NOESY spectra correlate protons close in space (< about 5 Å) due to dipolar couplings (through-space).

Structure determination using homonuclear 2D NMR spectra of small and unlabelled peptides can be divided in different steps (Wüthrich, 1986):

- Assignments of ^{1}H resonances and chemical shift by 2D COSY, TOCSY, NOESY.
- Integration of cross peaks to obtain information about ^{1}H-^{1}H distances
- Structure calculation

The aim of the NMR experiments of Myxinidin and WMR in negative SDS micelles and DMPC/DMPG/Cardiolipin bicelles by solution-state NMR was to investigate the peptide conformation in membrane mimetic environments. In addition preliminar CD spectra of the two peptides in SDS micelles and in DMPC/DMPG/Cardiolipin(65:23:12) bicelles were performed to complete the structural characterization.

5.2 Material and Methods

5.2.1 Micelles and bicelles preparation

Deuterated Sodium Dodecyl Sulfate (SDS- d_{25} 98% atom D) and Cardiolipin from heart bovine were purchased from Sigma Aldrich.

Deuterated 1,2-dimyristoyl-d54-*sn*-glycero-3-phosphocholine (DMPC-d_{54}); 1,2-dimyristoyl-*sn*-glycero-3-phospho-(1'-rac-glycerol) (sodium salt)(DMPG) and 1,2-diheptanoyl-*sn*-glycero-3-phosphocholine (DihepPC) were purchased from Avanti Polar.

For NMR experiments, SDS-d_{25} micelles were prepared as follow. A stock solution of SDS-d_{25} was prepared dissolving a precise amount of this lipid in $CHCl_3/C_2H_5OH/H_2O$ (65:35:8 % v/v) mixture. Then an appropriate volume of this stock solution was placed in a glass vial and dried under a stream of nitrogen gas to remove organic solvent up to obtain a thin lipid film. Finally the dried film was dissolved in PBS buffer pH=7.4 up to reach a final concentration of 150 mM.

For the preparation of bicelles, stock solutions of DMPC-d_{54}, DMPG and Cardiolipin dissolved in $CHCl_3$ were prepared. Appropriate volumes of these stock solutions were mixed and later dried under a stream of nitrogen gas in a glass vial up to remove all organic solvent. Bicelles were formed by the stepwise addition of the appropriate amount of a DihepPC stock solution dissolved in PBS buffer and thorough mixing by vortexing. In this way bicelles composed of [DMPC-d_{54}] = 0.034M, [DMPG] = 0.012M, [Cardiolipin] = 0.0065M, [DihepPC] = 0.208M with a total lipid concentration 0.26M (cL=11%) and q=0.2 (q value=(([DMPC-d_{54}]+[DMPG]+[Cardiolipin])/[DihepPC])) were obtained.

5.2.2 Preparation NMR and CD samples

For the structural characterization and NMR resonance assignment in the presence of micelles and bicelles, appropriate volumes of Mxinidin or WMR stock solutions dissolved in PBS buffer pH=7.4 were added to a lipid film containing SDS-d_{25} micelles or DMPC-d_{54}/DMPG/Cardiolipin bicelles and vortexing for 15 minutes to obtain a clear solution. This solution was later placed in a NMR tube of 250 μL containing 0.2 % v/v NaN_3 (90% H_2O 10% D_2O) and the pH was checked. The final concentration of peptides in different prepared samples was in the range 1.5-1.8 mM.

For CD experiments, Myxindin or WMR stock solutions dissolved in PBS buffer pH=7.4 were mixed with appropriate volumes of concentrated SDS micelles and DMPC/DMPG/Cardiolipin (65:23:12) bicelles dissolved in the same buffer. These last membrane mimetics were obtained as

described above. The final concentration of the peptides in different prepared samples was in the range 30-100 μM.

5.2.3 CD spectroscopy

CD spectra in the far UV-region (190–250 nm) were recorded on a Jasco J-715 spectropolarimeter under constant nitrogen flow, equipped with a Peltier type temperature control system. CD spectra were recorded at fixed 25°C, using a cuvette with a path length of 0.1 cm. The acquisition parameters were: 50 nm/min scan rate (8 s response time), 0.5 nm data pich, 2 nm bandwidth, averaged over five scans. CD spectra of the samples were finally corrected for the blank signal. Mean residue ellipticity (MRE), [θ] in deg cm^2dmol^{-1} values were calculated by the following relation: $[\theta] = ([\theta]_{obs}$ MRW) / (10 × l × C), where θ is the measured ellipticity (millidegrees); MRW=M / (n-1), where M is molecular mass in Da and (n-1) is the number peptide bonds; C is the peptide concentration in mg mL^{-1} and l is the path length in cm.

5.2.4 NMR spectroscopy

NMR spectra were acquired on a Bruker Avance 500 MHz spectrometer equipped with a cryogenic probe. 1D and 2D NMR spectra were acquired at 25 °C. NMR data were processed with NMRPipe (*14*) and analyzed with NMRView (*15*) on a Linux station. Homonuclear 2D COSY (Correlation Spectroscopy), 2D TOCSY (Total Correlation Spectroscopy), 2D NOESY (Nuclear Overhauser Spectroscopy) were recorded. NOESY spectra were recorded with mixing times of 100 an 200 ms and TOCSY spectra mostly with a mixing times of a 30 ms. The number of scans ranged from 32 to 64.

5.2.5 Structure Calculation

NMR structure calculations were performed with XPLOR-NIH(*16*) using a restrained simulated annealing and a combination of torsion and cartesian angle dynamics. NMRView software has been used to assign and integrate NOE cross peaks. NOE distance restraints were categorized in four bins with upper distance limits of 2.8, 3.5, 4.5 and 5.5 Å. The lower distance limit was always 1.8 Å, which corresponds to the van der Waals distance. For the calculation of $^1H^{\alpha}$ secondary shift, the random coil values from the literature (*17*) were subtracted from the measure chemical shifts. The respective chemical shift indices (csi) provided information about the secondary structure content.

Hydrogen bond restraints were defined based on the csi and helix typical NOEs (Wüthrich book: NMR of Proteins and Nucleic Acids) for helical regions. For the final refinement, they were however only used for the structure calculations of Myxinidin in bicelles and WMR in micelles and bicelles. The 20 lowest energy structures of in total 200 calculated ones were analyzed for the structural statistics and used to make structure pictures.

5.3 Results and Discussion

Preliminary information about the secondary structures of the Myxinidin and WMR were obtained by Circular Dichroism (CD) data. Fig.5.3.1 shows CD spectra of Myxinidin in buffer and in the presence of negatively charged SDS micelles and DMPC/DMPG/Cardiolipin bicelles.

The spectrum of Myxinidin in PBS buffer is dominated by the presence of the negative band at 200 nm, typical of a random coil conformation. On the contrary, CD spectra of the peptide in the studied micelles and bicelles indicate a more ordered conformation of Myxinidin in the presence of two membrane mimetic environments. In particular, in the presence of SDS 150 mM micelles, the absolute signal intensity increases and the minimum shifts from 200 to 208 nm. Additionally, a positive band at 190 nm and a weak second negative band at 222 nm become visible. The presence of these maxima and minima in the CD spectrum are typical of peptides with a helical like conformation. The deeper minimum at 208 compared with that at 222 nm may be explained by the presence of a remaining short unstructured stretch in the peptide.

In the presence of DMPC/DMPG/Cardiolipin q=0.2 cL=11% bicelles, Myxinidin adopts a similar helical like conformation shown in the presence of micelles. In fact, CD spectrum of the peptide in the bicelles presents two minima at 209 and 220 nm. Unfortunately, CD spectra of peptides in the presence of bicelles are usually of significantly less quality since bicelles themselves produce already a huge signal and produce a light scattering at low wavelength (< 200 nm).

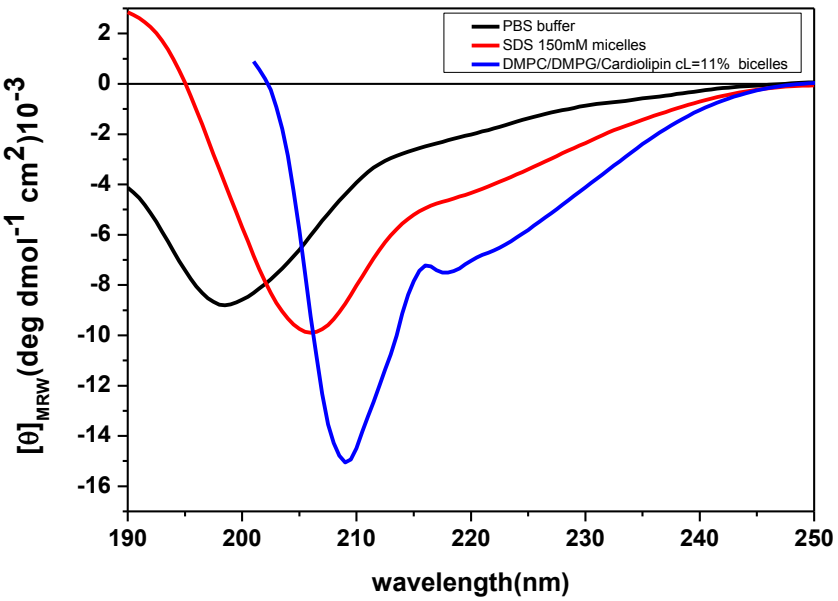

Fig.5.3.1. Far UV CD spectra of Myxinidin in PBS buffer (black line), in the presence of SDS micelles (red line) and DMPC/DMPG/Cardiolipin bicelles (blue line)

A similar behavior was obtained for WMR peptide in these two membrane mimetic environments (Fig.5.3.2). In fact WMR undergoes similar conformational changes passing from buffer to micelles and bicelles.

Fig.5.3.2 shows that WMR assumes a random coil like conformation in PBS buffer pH=7.4 (black line) as indicated by the presence of a negative band at 200 nm and a positive band at 225 nm, typical of peptides containing tryptophan residues in disordered conformation (*18*). In the presence of SDS micelles, the shift of the negative band from 200 nm to 208 nm, the appearance of a positive band at 190 nm and a negative shoulder at 222 nm, the disappearance of the weak positive band at 225 nm indicate the tendency of this peptide to adopt a helical like conformation in this environment (red line). In the presence of DMPC/DMPG/Cardiolipin bicelles, CD spectrum of WMR has two negative minima at 212 and 220 nm (blue line), indicating the propensity of this peptides to adopt a helical like conformation. Also in this case CD spectrum in bicelles is stopped at around 205 nm bacause a significantly light scattering is observed below this wavelength.

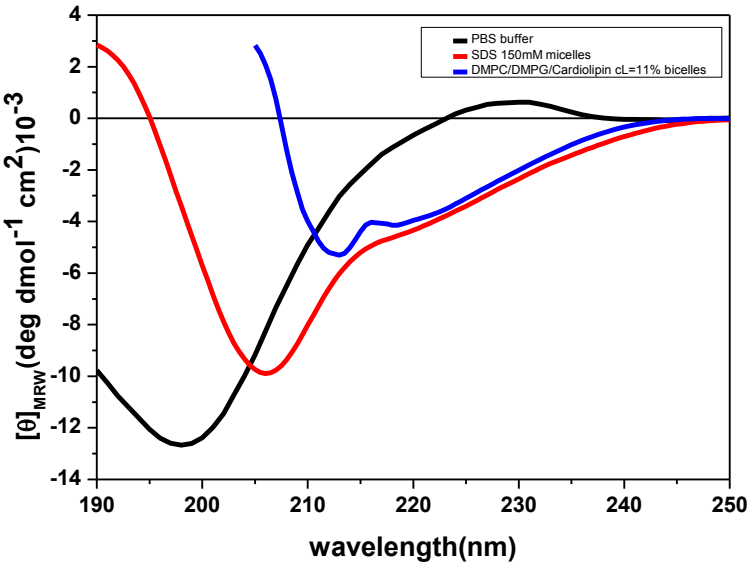

Fig.5.3.2. Far UV CD spectra of WMR in PBS buffer (black line), in the presence of SDS micelles (red line) and DMPC/DMPG/Cardiolipin bicelles (blue line)

These preliminar CD results indicate that the presence of membrane mimetic SDS micelles and DMPC/DMPG/Cardiolipin bicelles changes the secondary structure of Myxinidin and WMR. In particular, in these environments, both peptides adopt a helical like conformation.

To further investigate the peptide conformation in membrane mimetic environments, NMR spectra of Myxinidin and WMR in SDS-d_{25} 150 mM micelles and in DMPC-d_{54}/DMPG/Cardiolipin q=0.2 cL=11% bicelles had been recorded. The high concentration of micelles and bicelles has been chosen to study the conformation of two peptides in their membrane-bound state (peptide concentration 1.5-1.8 mM). Thus, NMR structures of two peptides in micelles and bicelles were determined at these high L/P ratios. Myxinidin and WMR are unlabeled peptides and for this reason only ^{1}H NMR spectra were recorded, including 2D COSY, TOCSY and NOESY to assign the proton chemical shifts and to obtain a structural information.

The calculated $^{1}H^{\alpha}$ secondary shifts of Myxinidin and WMR in SDS micelles and DMPC/DMPG/Cardiolipin bicelles, already indicate a helical conformation in agreement with the respective CD data (Fig 5.3.1 and Fig.5.3.2). Using mainly the distance restraints derived from the

NOESY data, NMR structures were calculated using a restrained simualted annealing protocol and a combination of torsion and Cartesian angle dynamics. The lowest 20 energy structures of each calculation are shown as in Figure 5.3.3. These results show that Myxinidin and WMR have the propensity to change their conformation in micelles and bicelles and that negatively charged membrane mimetic induce the formation of a helical structure. Both peptides are rather unstructured in PBS buffer as shown by CD data (Fig. 5.3.1 and Fig.5.3.2) and NMR data of the peptides in this buffer, (data not shown).

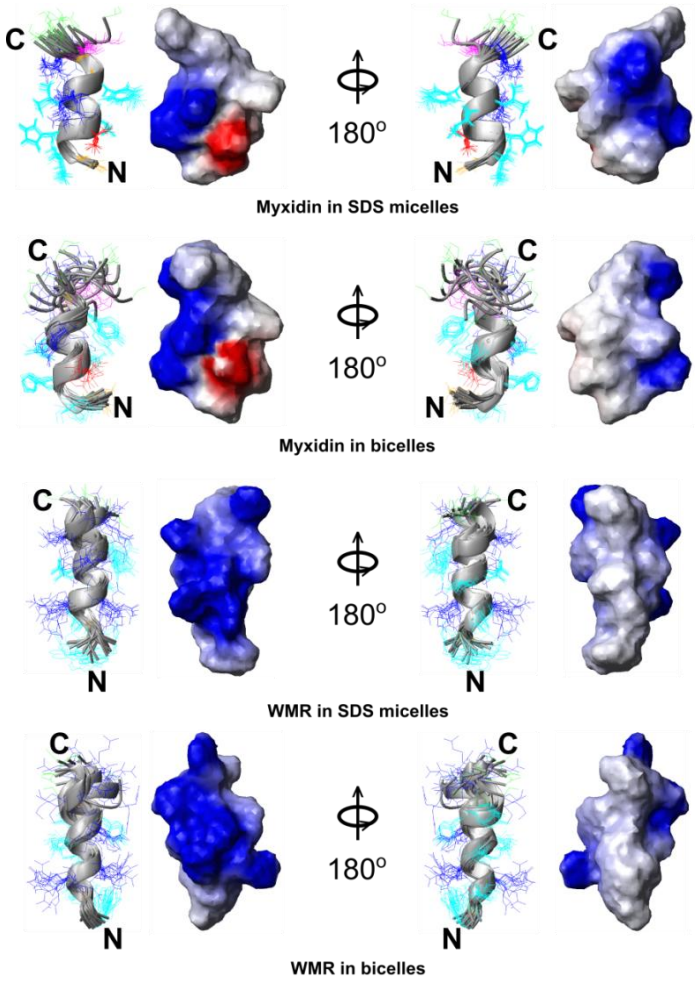

Fig. 5.3.3. Ribbon and surface charge representation of the 20 lowest energy structures of Myxinidin and WMR in SDS-d_{25} 150 mM micelles and in DMPC-d_{54}/DMPG/Cardiolipin q=0.2 cL=11% bicelles. Color code: negatively charged amino acids - red, positively charged amino acids - blue, aliphatic and aromatic amino acids - cyan, gly - orange, pro - magenta, ser – green

The shown NMR structures were determined by Dr. Sonja Alexandra Dames from the *Technische Universitat München* (TUM), Chair of Biomolecular NMR Spectroscopy. The surface charge was calculated considering that the C-terminus in uncharged due to amidation, but not including the charge from N-terminal NH_3^+. The Myxinidin structure in SDS micelles is the best resolved and was calculated using only NOE distance restraints. Due to the more variable sequence composition of Myxinidin compared to WMR, the NMR signals were overall better resolved and thus less overlapped. WMR contains three arginine (Arg) and two lysine (Lys) residues, which results in signal overlap in the 2D ^{1}H-^{1}H NMR spectra. For both peptides, more NOE distance restraints could be obtained using deuterated SDS micelles, since they resulted in less background signals than the only partially deuterated bicelles that had further been used at a higher total lipid concentration. The NMR structures of Myxinidin and WMR in bicelles and WMR in micelles were calculated based on NOE distance and hydrogen bond restraints for helical (alpha and 3^{10} helix as options because the available NOE information did not allow to discriminate between the two secondary structures) regions as well as helical typical backbone phi/psi dihedral angle restraints for residues in helical regions except glycine and proline residues. The content of secondary structures in the 20 lowest energy structures is reported in Tables 5.3.1-5.3.4 for the two peptides in SDS micelles and DMPC/DMPG/Cardiolipin bicelles. Myxinidin and WMR adopt a helical conformation from about the 3rd to the 9th residue and from 4th to 12th residues, respectively, in SDS micelles and DMPC/DMPG/Cardiolipin bicelles. Overall, the calculated structures of Myxinidin and WMR in micelles and bicelles are very similar, despite the differences in the size as well as surface charge and curvature of the two membrane mimetics.

Table 5.3.1 The secondary structure content of the 20 lowest energy structures of Myxinidin in SDS-d_{25}150mM micelles.

Structure	1Gly	2Ile	3Hys+	4Asp	5Ile	6Leu	7Lys+	8Tyr	9Gly	10Lys+	11Pro	12Ser
1st	coil	turn	helix	helix	helix	helix	helix	helix	helix	bend	coil	coil
2nd	coil	turn	helix	helix	helix	helix	helix	helix	helix	bend	coil	coil
3rd	coil	turn	helix	helix	helix	helix	helix	helix	helix	bend	coil	coil
4th	coil	turn	helix	helix	helix	helix	helix	helix	helix	coil	coil	coil
5th	coil	turn	helix	helix	helix	helix	helix	helix	helix	bend	coil	coil
6th	coil	turn	helix	helix	helix	helix	helix	helix	helix	bend	coil	coil
7th	coil	turn	helix	helix	helix	helix	helix	helix	helix	coil	coil	coil
8th	coil	turn	helix	helix	helix	helix	helix	helix	helix	coil	coil	coil
9th	coil	turn	helix	helix	helix	helix	helix	helix	helix	bend	coil	coil
10th	coil	turn	helix	helix	helix	helix	helix	helix	helix	bend	coil	coil
11th	coil	turn	helix	helix	helix	helix	helix	helix	helix	coil	coil	coil
12th	coil	turn	helix	helix	helix	helix	helix	helix	helix	bend	coil	coil
13th	coil	coil	turn	helix	helix	helix	helix	helix	helix	bend	coil	coil
14th	turn	helix	helix	helix	helix	helix	helix	helix	helix	bend	coil	coil
15th	coil	turn	helix	helix	helix	helix	helix	helix	helix	coil	coil	coil
16th	coil	turn	helix	helix	helix	helix	helix	helix	helix	coil	coil	coil
17th	coil	turn	helix	helix	helix	helix	helix	helix	helix	coil	coil	coil
18th	coil	turn	helix	helix	helix	helix	helix	helix	helix	bend	coil	coil
19th	coil	turn	helix	helix	helix	helix	helix	helix	helix	bend	coil	coil
20th	coil	turn	helix	helix	helix	helix	helix	helix	helix	bend	coil	coil

Table 5.3.2 The secondary structure content of the 20 lowest energy structures of Myxinidin in DMPC-d_{54}/DMPG/Cardiolipin (65:23:12) q=0.2 and cL=11% bicelles

Structure	1Gly	2Ile	3Hys+	4Asp	5Ile	6Leu	7Lys+	8Tyr	9Gly	10Lys+	11Pro	12Ser
1st	coil	turn	turn	helix	helix	helix	helix	helix	bend	coil	coil	coil
2nd	coil	turn	helix	helix	helix	helix	helix	bend	coil	coil	coil	coil
3rd	coil	turn	helix	helix	helix	helix	helix	helix	helix	bend	coil	coil
4th	coil	turn	turn	turn	helix	helix	helix	coil	bend	bend	coil	coil
5th	coil	turn	helix	helix	helix	helix	helix	bend	coil	coil	coil	coil
6th	coil	turn	helix	helix	helix	bend	turn	coil	bend	bend	coil	coil
7th	turn	helix	helix	helix	helix	helix	helix	bend	bend	bend	coil	coil
8th	coil	turn	helix	helix	helix	helix	helix	helix	bend	coil	coil	coil
9th	coil	turn	turn	helix	helix	helix	helix	helix	coil	coil	coil	coil
10th	turn	turn	helix	helix	helix	helix	helix	helix	bend	coil	coil	coil
11th	coil	turn	helix	helix	helix	helix	bend	bend	bend	coil	coil	coil
12th	coil	turn	helix	helix	helix	helix	turn	coil	bend	bend	coil	coil
13th	coil	turn	helix	helix	helix	helix	helix	bend	bend	bend	coil	coil
14th	coil	turn	helix	helix	helix	helix	turn	coil	bend	bend	coil	coil
15th	coil	turn	helix	helix	helix	helix	bend	bend	bend	coil	coil	coil
16th	coil	turn	helix	helix	helix	helix	helix	coil	bend	coil	coil	coil
17th	coil	turn	helix	helix	helix	helix	helix	helix	coil	coil	coil	coil
18th	coil	turn	helix	helix	helix	helix	bend	bend	coil	coil	coil	coil
19th	turn	helix	helix	helix	helix	helix	helix	helix	coil	coil	coil	coil
20th	coil	turn	helix	helix	helix	bend	turn	coil	bend	bend	coil	coil

Table 5.3.3 The secondary structure content of the 20 lowest energy structures of WMR in SDS-d_{25} 150 mM micelles.

Structure	1Trp	2Gly	3Ile	4Arg+	5Arg+	6Ile	7Leu	8Lys+	9Tyr	10Gly	11Lys+	12Arg+	13Ser
1st	coil	coil	turn	turn	helix	helix	helix	helix	helix	helix	helix	helix	coil
2nd	coil	turn	turn	turn	helix	helix	helix	helix	helix	helix	helix	helix	coil
3rd	coil	turn	helix	helix	helix	helix	helix	helix	helix	helix	helix	helix	coil
4th	coil	turn	helix	helix	helix	helix	helix	helix	helix	helix	helix	helix	coil
5th	coil	turn	turn	turn	helix	helix	helix	helix	helix	helix	helix	helix	coil
6th	coil	turn	turn	helix	helix	helix	helix	helix	helix	helix	helix	helix	turn
7th	coil	coil	turn	helix	helix	helix	helix	helix	helix	helix	bend	coil	coil
8th	turn	turn	helix	helix	helix	helix	helix	helix	helix	helix	helix	helix	coil
9th	coil	turn	helix	helix	helix	helix	helix	helix	helix	helix	bend	coil	coil
10th	coil	coil	turn	turn	helix	helix	helix	helix	helix	helix	helix	helix	coil
11th	coil	turn	helix	helix	helix	helix	helix	helix	helix	helix	helix	helix	coil
12th	coil	turn	turn	turn	helix	helix	helix	helix	helix	helix	helix	coil	coil
13th	coil	turn	helix	helix	helix	helix	helix	helix	helix	helix	helix	helix	coil
14th	coil	turn	turn	turn	helix	helix	helix	helix	helix	helix	helix	helix	coil
15th	coil	coil	turn	helix	helix	helix	helix	helix	helix	helix	helix	helix	coil
16th	coil	turn	helix	helix	helix	helix	helix	helix	helix	helix	turn	coil	coil
17th	coil	turn	turn	turn	helix	helix	helix	helix	helix	helix	helix	helix	coil
18th	turn	coil	turn	helix	helix	helix	helix	helix	helix	helix	helix	helix	coil
19th	coil	turn	helix	helix	helix	helix	helix	helix	helix	helix	helix	helix	coil
20th	coil	coil	turn	helix	helix	helix	helix	helix	helix	helix	helix	helix	coil

Table 5.3.4 The secondary structure content of the 20 lowest energy structures of WMR in DMPC-d_{54}/DMPG/Cardiolipin(65:23:12) q=0.2 and cL=11% bicelles

Structure	1Trp	2Gly	3Ile	4Arg+	5Arg+	6Ile	7Leu	8Lys+	9Tyr	10Gly	11Lys+	12Arg+	13Ser
1st	coil	turn	turn	helix	helix	helix	helix	helix	helix	helix	helix	helix	coil
2nd	coil	turn	helix	helix	helix	helix	helix	helix	helix	helix	helix	helix	coil
3rd	coil	turn	helix	helix	helix	helix	helix	helix	helix	helix	helix	helix	coil
4th	coil	turn	turn	helix	helix	helix	helix	helix	helix	helix	turn	coil	coil
5th	coil	turn	helix	helix	helix	helix	helix	helix	helix	helix	helix	helix	coil
6th	coil	turn	helix	helix	helix	helix	helix	helix	helix	helix	helix	helix	coil
7th	coil	turn	turn	helix	helix	helix	helix	helix	helix	helix	helix	coil	coil
8th	coil	turn	helix	helix	helix	helix	helix	helix	helix	helix	bend	coil	coil
9th	coil	turn	turn	turn	helix	helix	helix	helix	helix	helix	helix	helix	coil
10th	coil	turn	helix	helix	helix	helix	helix	helix	helix	helix	helix	coil	coil
11th	coil	turn	helix	helix	helix	helix	helix	helix	helix	turn	turn	coil	coil
12th	coil	turn	helix	helix	helix	helix	helix	helix	helix	helix	helix	helix	coil
13th	coil	turn	helix	helix	helix	helix	helix	helix	helix	helix	helix	helix	coil
14th	coil	turn	helix	helix	helix	helix	helix	helix	helix	helix	helix	helix	coil
15th	coil	turn	helix	helix	helix	helix	helix	helix	helix	helix	helix	coil	coil
16th	coil	turn	helix	helix	helix	helix	helix	helix	helix	helix	helix	helix	coil
17th	coil	turn	helix	helix	helix	helix	helix	helix	helix	helix	helix	coil	coil
18th	coil	turn	helix	helix	helix	turn	helix	helix	helix	turn	bend	coil	coil
19th	coil	turn	helix	helix	helix	helix	helix	helix	helix	helix	helix	helix	coil
20th	coil	turn	helix	helix	helix	helix	helix	turn	helix	helix	helix	coil	coil

Based on the 20 lowest energy structures of WMR in bicelles, cation-π interactions between the positively charged guanidinium group of the arginine 5 (Arg5) and the electron π system of the aromatic ring of the tryptophan 1 (Trp1) (Figure 5.3.4) occur, as suggesting by the average distance < 6.0 Angstrom between the guanidinium carbon (CZ) of the arginine and the center of the aromatic ring of the triptophan(*19*).

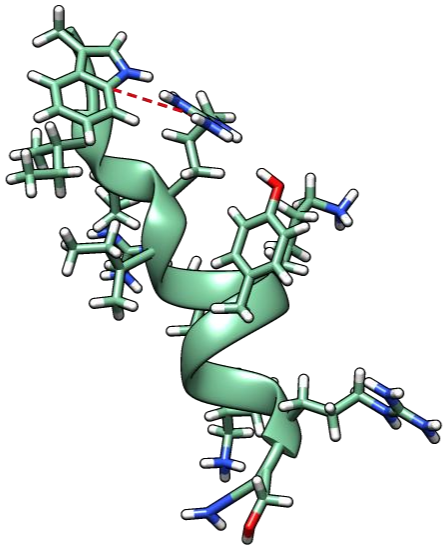

Fig.5.3.4. Ribbon representation of WMR in bicelles. This figure was created by USCF Chimera. The PDB of this NMR structure was provide by Dr. Sonja Alexandra Dames.

The cation-π interaction could justify the major degree of penetration of WMR than Myxinidin in membrane environment containing Cardiolipin, supporting our results shown in the previous Chapter. In fact cation-π interactions make energetically favorable the penetration of peptides containing arginine and tryptophan residues in the bilayers because some residues of the arginine can be shielded from the more hydrophobic Trp, favoring the entry of WMR into lipid bilayer(*20*).

5.4 Conclusions

In conclusion, NMR and CD data have allowed a complete structural characterization of Myxinidin and WMR in negatively charged SDS micelles and DMPC/DMPG/Cardiolipin bicelles. Preliminary CD results have shown the tendency of two peptides to adopt a helical like conformation in these two membrane mimetic environments. In particular, complementary NMR results have confirmed the tendency of Myxinidin and WMR to adopt a similar helical conformation in the presence of the studied micelles and bicelles, despite the difference of the size and lipid composition of two membrane mimetic environments. According to CD spectra of two peptides in TFE solvent and in liposomes shown in the Chapter 4, these results confirm that Myxinidin and WMR undergo a similar conformational change in the presence of different membrane mimetics. This observation suggests that the different behavior of WMR and Myxinidin on the studied model bio-membranes doesn't depend on the secondary structure of two peptides upon the binding with lipids. In addition, NMR structure of WMR in DMPC/DMPG/Cardiolipin bicelles has demonstrated the presence of cation-π interactions between Trp1 and Arg5 residues, as supposed in the Chapter 4, in order to further justife the different behavior between WMR and Myxinidin against liposomes containing Cardiolipin.

References

(1) McDonnell, P. A., Shon, K., Kim, Y., and Opella, S. J. (1993) fd coat protein structure in membrane environments. *J Mol Biol 233*, 447-63.

(2) Warschawski, D. E., Arnold, A. A., Beaugrand, M., Gravel, A., Chartrand, E., and Marcotte, I. (2011) Choosing membrane mimetics for NMR structural studies of transmembrane proteins. *Biochim Biophys Acta 1808*, 1957-74.

(3) Vymetal, J., Bednarova, L., and Vondrasek, J. (2016) Effect of TFE on the Helical Content of AK17 and HAL-1 Peptides: Theoretical Insights into the Mechanism of Helix Stabilization. *J Phys Chem B 120*, 1048-59.

(4) Haney, E. F., Lau, F., and Vogel, H. J. (2007) Solution structures and model membrane interactions of lactoferrampin, an antimicrobial peptide derived from bovine lactoferrin. *Biochim Biophys Acta 1768*, 2355-64.

(5) Schibli, D. J., Nguyen, L. T., Kernaghan, S. D., Rekdal, O., and Vogel, H. J. (2006) Structure-function analysis of tritrpticin analogs: potential relationships between antimicrobial activities, model membrane interactions, and their micelle-bound NMR structures. *Biophys J 91*, 4413-26.

(6) Marcotte, I., Belanger, A., and Auger, M. (2006) The orientation effect of gramicidin A on bicelles and Eu3+ -doped bicelles as studied by solid-state NMR and FT-IR spectroscopy. *Chem Phys Lipids 139*, 137-49.

(7) Triba, M. N., Zoonens, M., Popot, J. L., Devaux, P. F., and Warschawski, D. E. (2006) Reconstitution and alignment by a magnetic field of a beta-barrel membrane protein in bicelles. *Eur Biophys J 35*, 268-75.

(8) Sanders, C. R., 2nd, and Landis, G. C. (1995) Reconstitution of membrane proteins into lipid-rich bilayered mixed micelles for NMR studies. *Biochemistry 34*, 4030-40.

(9) Sanders, C. R., and Prosser, R. S. (1998) Bicelles: a model membrane system for all seasons? *Structure 6*, 1227-34.

(10) Faham, S., Boulting, G. L., Massey, E. A., Yohannan, S., Yang, D., and Bowie, J. U. (2005) Crystallization of bacteriorhodopsin from bicelle formulations at room temperature. *Protein Sci 14*, 836-40.

(11) Andersson, A., and Maler, L. (2002) NMR solution structure and dynamics of motilin in isotropic phospholipid bicellar solution. *J Biomol NMR 24*, 103-12.

(12) Wang, T., and Hong, M. (2015) Investigation of the curvature induction and membrane localization of the influenza virus M2 protein using static and off-magic-angle spinning solid-state nuclear magnetic resonance of oriented bicelles. *Biochemistry 54*, 2214-26.

(13) Lindberg, M., Biverstahl, H., Graslund, A., and Maler, L. (2003) Structure and positioning comparison of two variants of penetratin in two different membrane mimicking systems by NMR. *Eur J Biochem 270*, 3055-63.

(14) Delaglio, F., Grzesiek, S., Vuister, G. W., Zhu, G., Pfeifer, J., and Bax, A. (1995) NMRPipe: a multidimensional spectral processing system based on UNIX pipes. *J Biomol NMR 6*, 277-93.

(15) Johnson, B. A. (2004) Using NMRView to visualize and analyze the NMR spectra of macromolecules. *Methods Mol Biol 278*, 313-52.

(16) Schwieters, C. D., Kuszewski, J. J., Tjandra, N., and Clore, G. M. (2003) The Xplor-NIH NMR molecular structure determination package. *J Magn Reson 160*, 65-73.

(17) Wishart, D. S., Bigam, C. G., Holm, A., Hodges, R. S., and Sykes, B. D. (1995) 1H, 13C and 15N random coil NMR chemical shifts of the common amino acids. I. Investigations of nearest-neighbor effects. *J Biomol NMR 5*, 67-81.

(18) Nichols, M., Kuljanin, M., Nategholeslam, M., Hoang, T., Vafaei, S., Tomberli, B., Gray, C. G., DeBruin, L., and Jelokhani-Niaraki, M. (2013) Dynamic turn conformation of a short tryptophan-rich cationic antimicrobial peptide and its interaction with phospholipid membranes. *J Phys Chem B 117*, 14697-708.

(19) Gallivan, J. P., and Dougherty, D. A. (1999) Cation-pi interactions in structural biology. *Proc Natl Acad Sci U S A 96*, 9459-64.
(20) Chan, D. I., Prenner, E. J., and Vogel, H. J. (2006) Tryptophan- and arginine-rich antimicrobial peptides: structures and mechanisms of action. *Biochim Biophys Acta 1758*, 1184-202.

Chapter 6

Effect of an unusual lipid A covalently linked to a hopanoid moiety on the stability of model bio-membranes

6.1 Introduction

In order to study the importance of lipid composition in biological processes, another important part of this thesis has been focused on the physico-chemical characterization of a particular model bacterial membrane, mimicking *Bradyrhizobium BTAi1* strain. The importance of this study is due to the recent discovery of an unusual covalently linked hopanoid-lipid A in the lipopolysaccharide (LPS) of *Bradyrhizobium BTAi1* Gram negative bacterium (Fig.6.1.1) by Prof. Silipo A. Group, University "Federico II", Naples (*1*). The aim of this work is to understand the role of hopanoid and its compounds on the biophysical properties of the studied model membrane. A reasonable question about this discovery is: Why does the nature use this unusual LPS architecture in *Bradyrhizobium BTAi1*strain?

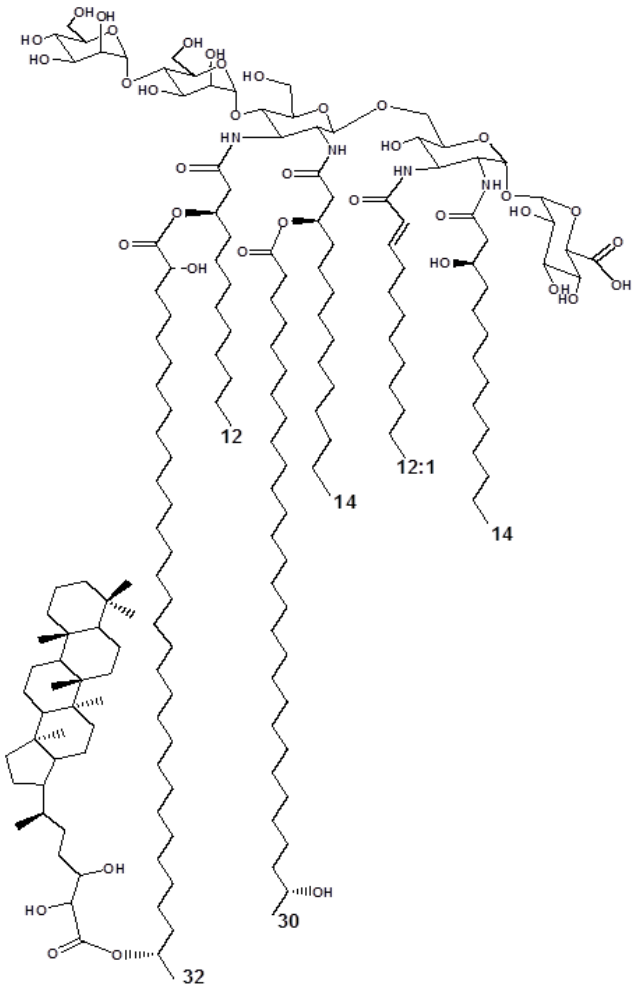

Fig.6.1.1 Structure of the covalently linked hopanoid-lipid A(HoLA) found in *Bradyrhizobium BTAi1*strain

Bradyrhizobium species are Gram negative, photosynthetic, nitrogen-fixing bacteria able to establish a mutualistic symbiotic relationship with plants of Leguminosae genus *(2, 3).* The symbiosis process involves a bacterial invasion of the plants and a consequent adaptation of the bacterium to the plant host environment (*4*).The plant-bacteria association starts with an exchange of chemical compounds between the eukaryotic host and prokaryotic symbiont. These bacteria have received significant attention and they are also used in agriculture system for their important feature to fix nitrogen and to potentially reduce the use of chemical N-fertilizer to enhance the natural nitrogen sources (*3, 5*). It has shown that a correct LPS structure contained in the outer membrane of Gram negative bacteria is a key element in the symbiosis process (*6*).

Lipolysaccharides (LPS) are the major component of Gram negative outer membrane and they are vital cell wall glycol-conjugate with a central role in the mechanisms of bacterial invasion and adaptation to the host environment (*7*).The lipopolysaccharides (LPS) cover about 75% of the outer membrane surface and they consist an hydrophilic portion composed by polysaccharide (O-antigen), a proximal oligosaccharide named core which is linked to a glycolipid moiety named lipid A. The structural diversity in the O-antigen region of LPS is believed to modulate or suppress plant defence response (*8*) and also the lipid A plays an important role in the adaptation of bacteria in the host environment (*9*). Furthermore it has been recently shown that LPS of *Bradyrhizobium BTAi1* bacterium has a peculiar sugar and lipid composition and, in particular, it contains very long-chain fatty acids (VLCFA), important in adaptation bacteria process (Fig. 6.1.1)(*1*).

The length of these VLCFA is double than that of the other acyl chains, and is reasonable to speculate that they have been purposely engineered by nature to span the entire lipid membrane profile. In particular it has been found that the *Bradyrhizobium* BTAi1 strain builds an unique lipid A in which the VLCFA terminus is covalently linked to a hopanoid structure (HoLA) (*1*). Hopanoids are pentacyclic triterpenoids, widely distributed in different bacteria and they have a broad range of structural variation in the side chain structures (*10-13*) (Figure 6.1.2).

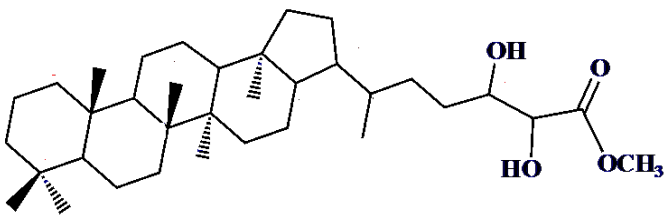

Fig.6.1.2 Hopanoid moiety present in the lipid A from *Bradyrhizobium BTAi1*strain

The biosynthesis of hopanoids depends on squalene-hopene cyclase (shc), which forms pentacyclic triterpenoid hopene from linear precursor squalene (*14*).They are structurally similar to sterols of eukaryotic membranes and act as controllers and reinforces of the fluidity and permeability of bacterial cell envelope (*13*). Hopanoids protect bacteria against different stresses, such as high temperature, acid or alkaline pH, high osmolarity, antibiotics (*13, 15, 16*).In this work the attention is focused on the role of hopanoid-containing lipid A (HoLA) and its mutant on the *Bradyrhizobium BTAi1* model membrane.

To test the role of HoLA in regulating the structure and dynamics of the lipid bilayer, different POPE/POPG (70:30 %mol) liposomes containing a determined fraction of alternatively i.) HoLA (Figure 6.1.1), ii.) BTAi1Δshc lipid A(figure 6.1.3) (the HoLA mutant deprived of the hopanoid moiety) iii.) BTAi1Δshc lipid A plus the "free hopanoid" have been used. Comparison between case i. and ii. shows the relevance of the hopanoid presence in the bilayer, while comparison between case i. and iii. highlights the effects of its covalent bond with the lipid A.

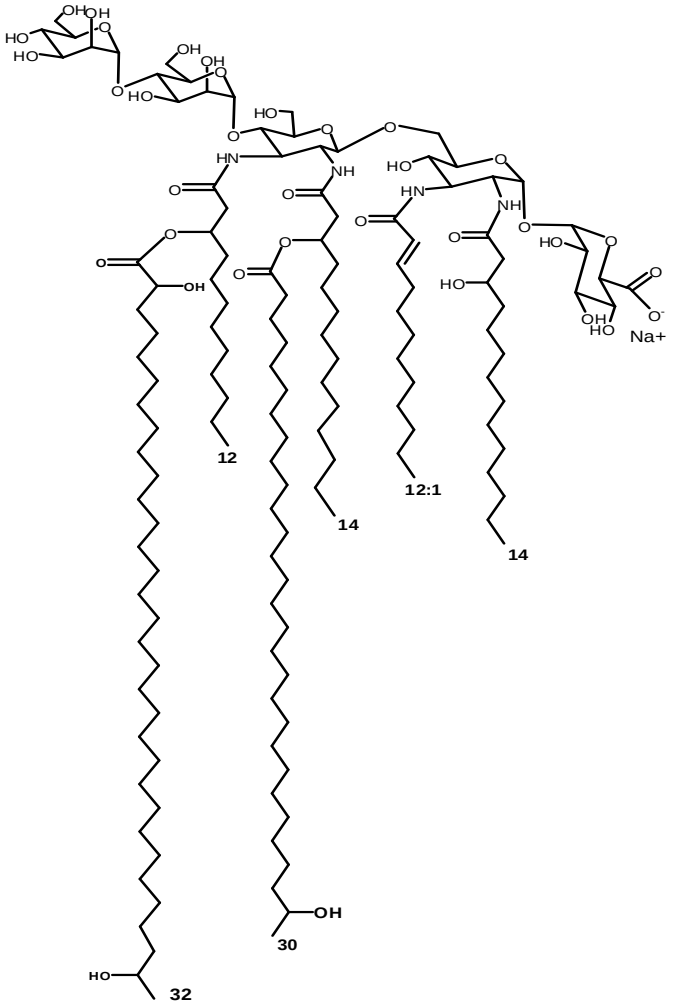

Fig.6.1.3 Structure of BTAi1Δshc lipid A in *Bradyrhizobium BTAi1*strain

To study these systems, a combined experimental strategy has been adopted, including Electron Paramagnetic Resonance (EPR) and Differential Scanning Calorimetry (DSC). The experimental techniques employed in this work allow to characterize the considered systems at different observation scales, from the thermotropic behaviour of the liposomes to the structural arrangement of lipids in the bilayer. Particularly EPR measurements allow to investigate the dynamics of the lipid hydrophobic tails in the bilayer, giving information on the local microstructure; whereas DSC measurements give information about the effect of HoLA, BTAi1Δshc lipid A and hopanoid on the membrane thermotropic properties. Changes in the thermotropic properties mainly reflect variations in the lipids distribution within the membranes and provide information on the domain formation/composition.

6.2 Material and methods

6.2.1 Liposomes preparation

HoLA, BTAi1Δshc lipid A and the "free hopanoid" have been extracted and purified by Prof. Silipo A. Group as largely reported in literature (*17*).To prepare stock solutions, HoLA and BTAi1Δshc lipid A and hopanoid have been solubilized in a chloroform/methanol 4:2 % v/v mixture. Phospholipids, 1-palmitoyl-2-oleoyl-*sn*-glycero-3-phosphoethanolamine (POPE) and 1-palmitoyl-2-oleoyl-*sn*-glycero-3-phospho-(1'-*rac*-glycerol) (POPG), have been purchased from Avanti Polar Lipids (Birmingham, AL, USA) and their stock solutions have been prepared at POPE/POPG 70/30 molar ratio in chloroform. Samples have been obtained by mixing suitable volumes of POPE/POPG (70:30)% mol solution with appropriate volumes of stock solutions of HoLA or BTAi1Δshc lipid A or the "free hopanoid" or BTAi1Δshc lipid A plus the free hopanoid to get a final molar ratio phospholipids/ (HoLA or BTAi1Δshc lipid A or "free hopanoid") 90/10 % mol. A thin film of these lipids has been formed through evaporation of organic solvent with dry nitrogen gas and vacuum desiccation. Then a PBS buffer solution, pH 7.4 containing 1 mM $CaCl_2$ has been added to the dry lipid film to yield a final total lipid final concentration of 1mg/ml. The use of Ca^{2+} ions is due to the mimic the important physiological role of these cations in the stability of LPS and outer membrane Gram negative. Samples have been then heated at 50°C for 30 min and repeatedly vortexed to obtain MLVs suspensions and used for DSC measurements.

For EPR measurements spin-labeled phosphatidylcholine have been incorporated in the studied liposomes. These spin- labelled phosphatidylcholine (1-palmitoyl-2-[*n*-(4,4 dimethyloxazolidine-*N*-oxyl)]stearoyl-*sn*-glycero-3-phosphocholine, *n*-PCSL, *n* = 5 and 14) have been purchased from Avanti Polar Lipids and stored at −20 °C in ethanol solution. Samples investigated by EPR spectroscopy have been prepared by adding proper volumes of a spin-label stock solution in ethanol (1 mg mL^{-1}) to the lipid organic mixtures before solvent evaporation to reach a final total lipid concentration of 1 mg/mL.Then the thin film of lipids has been evaporated and MLVs have been obtained as described above.

6.2.2 DSC measurements

DSC measurements were performed using a nano-DSC from TA instruments (NewCastle, DE,USA). For all DSC experiments, Multi Lamellar vesicles (MLVs) were used. The excess molar heat capacity function, $<\Delta Cp>$, was obtained after a baseline subtraction, assuming that the baseline is given by the linear temperature dependence of the pretransition heat capacity. A buffer-buffer scan was subtracted from the sample scan. A volume of 300 μL of multilamellar vesicles of lipids mixtures samples was placed in the calorimetry vessel, and successive heating and cooling scans were performed at a scan rate of 0.5°C/min over the temperature range of 0 – 50 °C. DSC data were analyzed by means of the NanoAnalyze software supplied with the instrument to determine the melting temperature (T_m) and enthalpy ($\Delta_m H$) and plotted using the Origin software package.

6.2.3 EPR measurements

ESR spectra of 5-PCSL and 14-PCSL in the considered samples were recorded on a Elexys E-500 ESR spectrometer from Bruker (Rheinstetten, Germany) operating in the X band. The temperature of the sample was regulated at 25°C and maintained constant during the measurement by blowing thermostated nitrogen gas through a quartz Dewar. The instrumental settings were as follows: sweep width, 120 G; resolution, 1,024 points; modulation frequency, 100 kHz; modulation amplitude, 1.0 G; time constant, 20.5 ms; sweep time, 42 s; incident power, 5.0mW. Several scans, typically 32, were performed and averaged to improve the signal-to-noise ratio**.** Capillaries containing the samples were placed in a standard 4-mm quartz sample tube.

6.3 Results and discussion

To further investigate how the peculiarities of the BTAi1 Lipid A reflect in the functional behaviour of the membranes in which they are included, DSC and EPR experiments have been performed to explore the effect of the HoLA, the BTAi1Δshc lipid A (the HoLA mutant deprived of the hopanoid moiety), and free hopanoid on the thermotropic properties and dynamic of acyl chain lipids of POPE/POPG liposomes respectively. Phosphatidylethanolamines (POPE) are the most abundant zwittterionic phospholipids in the membranes of Gram-negative bacteria (*18*), whereas phosphatidylglycerols (POPG) are largely used to reproduce the negative charge found in the outer membranes of Gram negative bacteria (*19*). Their structures are:

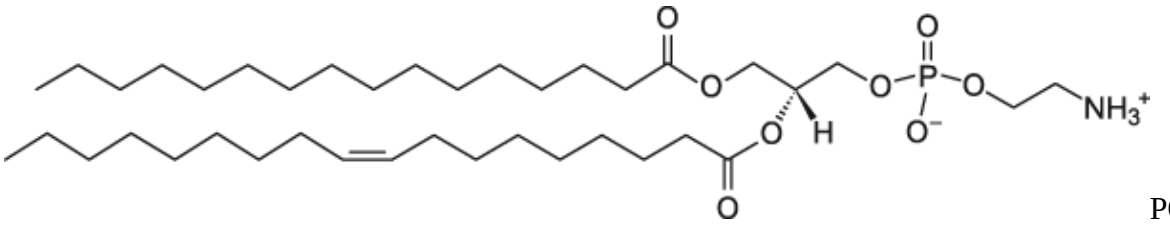

POPE

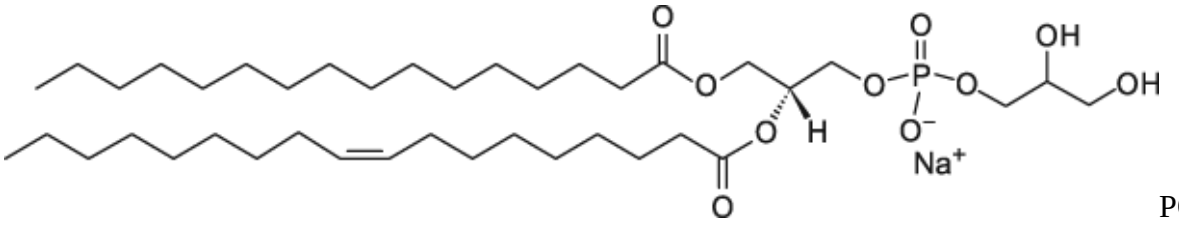

POPG

Hence liposomes containing POPE and POPG (70/30 % mol) have been studied as model bio-membranes (*1*). Fig.6.3.1 shows the DSC heating profiles of the investigated systems and the corresponding thermodynamic parameters are reported in Table 6.3.1.

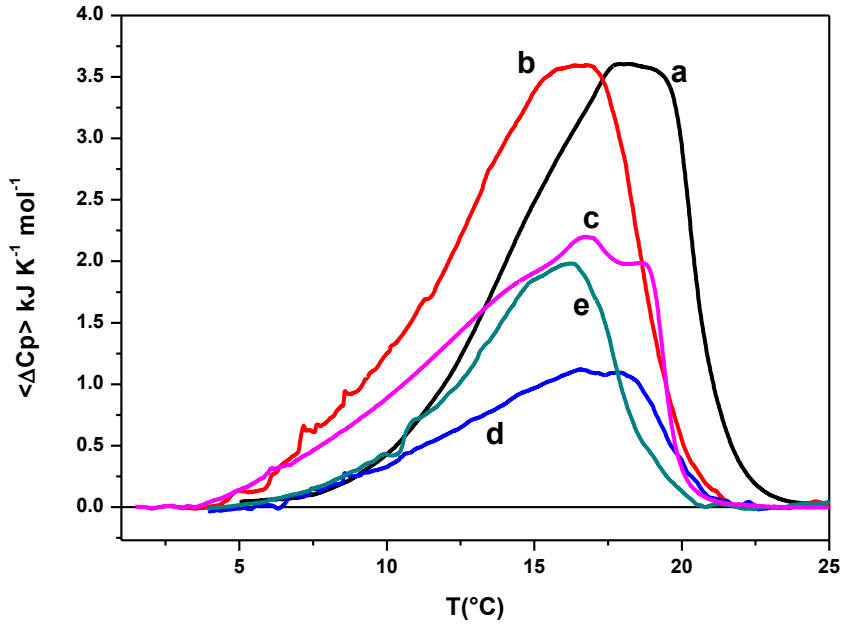

Fig 6.3.1 DSC heating profiles of a) POPE/POPG liposome in the absence (black line) and in the presence of :b) BTAi1Δshc (red line), c) free hopanoid (violet line), d) HoLA (blue line) and e) BTAi1Δshc plus free hopanoid (green line).

Table 6.3.1 Thermodynamic parameters of POPE/POPG phase transition in the absence and in presence of BTAi1Δshc, free hopanoid, HoLA and BTAi1Δshc plus free hopanoid

Liposome	**$\Delta_m H$ (kJ/mol lipid)**	**T_m (°C)**
POPE/POPG	26.4 ± 1.2	18.2 ± 0.5
POPE/POPG/BtAi1Δshc	28.0 ± 1.2	16.8 ± 0.5
POPE/POPG /hopanoid	19.0 ± 1.5	16.7 ± 0.5 18.7 ± 0,5
POPE/POPG/ HoLA	3.0 ± 1.5	16.5 ± 0.5 18.0 ± 0.5
POPE/POPG/ BtAi1Δshc/hopanoid	12.7 ± 1.5	16.3 ± 0.5

All samples showed overlapping consecutive scans confirming the reversibility of gel-liquid crystalline phase transition (data not shown). The comparison between the POPE/POPG thermal profile (Fig. 6.3.1, curve a) with that containing BTAi1Δshc lipid A (Fig. 6.3.1, curve b) shows that the presence of the HoLA mutant deprived of the hopanoid moiety marginally affects the gel-liquid membrane transition (Table 6.3.1). Most importantly, the presence of BTAi1Δshc lipid A does not change the overall shape of the DSC profile suggesting that BTAi1Δshc lipid A is distributed randomly in the POPE/POPG phase and does not induce specific lipids distributions (domains formation). On the contrary, the presence of the free hopanoid drastically changes the shape and the thermodynamic parameters of the gel-liquid phase transition (Fig.6.3.1,curve c and Table 6.3.1). Particularly, the total enthalpy change is significantly decreased and the main gel-liquid transition peak is turned into a multi-component DSC profile consisting of several overlapping transitions, thus suggesting the presence of domains of different lipid compositions. This behavior has been previously described for structural similar eukaryotic sterols and attributed to a non homogeneous distribution of the sterols inside the lipid bilayers (*20*). The presence of the HoLA in POPE/POPG vesicles results in a multi-component DSC profile (Fig.6.3.1,curve d) similar to the one observed for the free hopanoid, suggesting that it also induces formation of domains at different composition inside the lipid bilayers. Further, the system containing HoLA in the liposome shows the lower value for the transition enthalpy (Table 6.3.1). Finally, the POPE/POPG bilayer containing the same amount of BTAi1Δshc lipid A mutant and free hopanoid, has a DSC profile (Fig. 6.3.1, curve e) less complex than the one observed for the free hopanoid (Fig. 6.3.1, curve c) and with a shape similar to the DSC profile of the vesicles containing the BTAi1Δshc mutant alone (although different in <ΔCp> magnitude). This result suggests that the hopanoid is more homogeneously distributed inside the bilayer in the presence of the BTAi1Δshc mutant, although not linked covalently to it. A reasonable hypothesis to explain this result is that the BTAi1Δshc mutant is still randomly distributed in the POPG/POPE bilayer as it does in absence of the hopanoid (Fig. 6.3.1, curve b),whereas the hopanoid tends to "follow" the BTAi1Δshc mutant and its random distribution differently from what it does in absence of the BTAi1Δshc mutant (Fig. 6.3.1, curve c). In other words, these results reveals that the BTAi1Δshc mutant and the free hopanoid, although not covalently linked, do not behave independently but rather show a preferential interaction.

These results are according to those obtained by EPR experiments, in which phosphatidylcholine spin-labeled 5 and 14 PCSL have been incorporated in the studied liposomes to give information on the acyl chains structuring in the lipid bilayers. EPR experiments have been recorded in

collaboration with Prof. D'Errico G. Group, University "Federico II", Naples. The temperature chosen in these experiments was 25°C, where all analyzed systems were in liquid crystalline disordered (L_α) phase. The comparative use of 5 and 14-PCSL spin-labels has allowed a detailed analysis of perturbations in the dynamics of the different segments of the lipid hydrophobic tails. In particular 5-PCSL has a radical label nitroxide group close to the lipid hydrophilic head group, giving information on the behaviour of the acyl chain region just underneath the polar external layers, whereas 14-PCSL has a radical label nitroxide group close to the terminal methyl group of the acyl chain, allowing to monitor the behaviour of the more internal region of the membrane. Fig. 6.3.2 and Fig.6.3.3 show EPR spectra of 5- PCSL and 14-PCSL, respectively, in all studied systems.

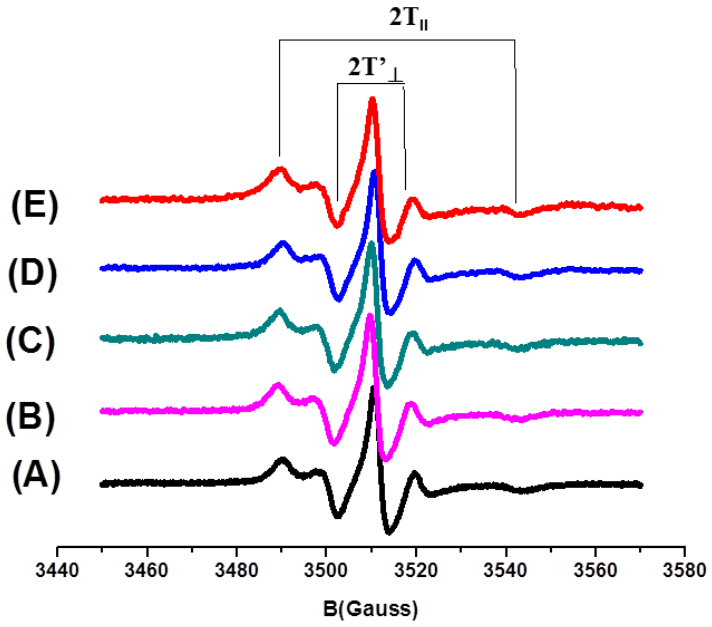

Fig.6.3.2 EPR spectra of 5-PCSL in lipid bilayers of **(A)** POPE/POPG (70:30)%mol (black line), **(B)** POPE/POPG/ BtAi1Δshc/hopanoid (violet line), **(C)** POPE/POPG/ BtAi1Δshc (green line) , **(D)** POPE/POPG/ hopanoid(blue line), **(E)** POPE/POPG/HoLA(red line).All studied systems contain a molar ratio phospholipid/(HoLA or BtAi1Δshc or free hopanoid or BtAi1Δshc plus hopanoid) of 90/10 % mol.

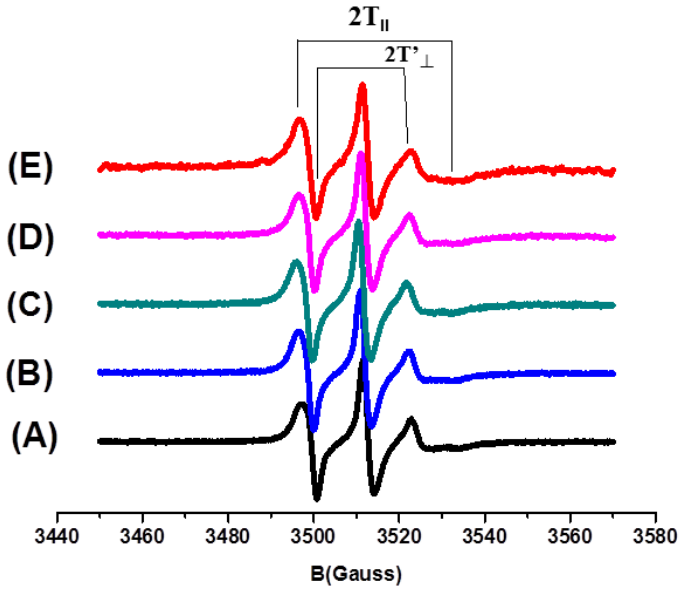

Fig.6.3.3 EPR spectra of 14-PCSL in lipid bilayers of **(A)** POPE/POPG (70:30)%mol (black line), **(B)** POPE/POPG/hopanoid (blue line), **(C)** POPE/POPG/BtAi1Δshc (green line), **(D)** POPE/POPG/ BtAi1Δshc/hopanoid (violet line), **(E)** POPE/POPG/HoLA (red line). All studied systems contain a molar ratio phospholipid/(HoLA or BtAi1Δshc or free hopanoid or BtAi1Δshc plus hopanoid) of 90/10 % mol.

In all analyzed systems, EPR spectra of 5-PCSL present a clearly defined axial anisotropy (Fig.6.3.2), indicating that the mobility of the label in the region of the bilayer just below the hydrophilic external surface is strongly reduced. Inspection of these EPR spectra show that anisotropy increases in order POPE/POPG/BTAi1Δshc < POPE/POPG = POPE/POPG/hopanoide < POPE/POPG/HoLA < POPE/POPG/ BTAi1Δshc/ hopanoide.

On the contrary EPR spectra of 14-PCSL show an almost isotropic three-line line shape (Fig.6.3.3), suggesting a relatively less restricted motion of the radical label and for this label a broadening of signals is evident in the same order reported above. The major broadening in the EPR spectra

lineshape is observed in the HoLA containing liposomes, indicating that the presence of this unusual covalently linked hopanoid-lipid A causes a lower fluidity of the membrane. A quantitative analysis of EPR spectra has been determined by order parameter (S value), that is related to the angular amplitudes of motion of the label and then it reflects the motion of the acyl chain segment to which the label is bound (*21*).S value is calculated according to the relation:

$$S = \frac{(T_{\parallel} - T_{\perp})a_N}{(T_{zz} - T_{xx})a'_N} \qquad \text{(E1)}$$

where $T_{\parallel}$ and $T_{\perp}$ are two hyperfine splitting parameters determined experimentally from each EPR spectrum as shown in Fig.6.3.2 and Fig.6.3.3 (note that $2T'_{\perp} = 2T_{\perp}$-1.6 , ref. (*22*)); T_{xx} and T_{zz} are principal elements of the real hyperfine splitting tensor in the spin Hamiltonian of the spin-label and their values are T_{xx}= 6.1 G and T_{zz} 32.4 G; whereas a_N and a'_N are isotropic hyperfine coupling constant for the spin label in crystal and membrane state respectively and they are calculated by:

$$a_N = \frac{1}{3}(T_{zz} + 2T_{xx}) \qquad \text{(E2)}$$

$$a'_N = \frac{1}{3}(T_{\parallel} + 2T_{\perp}) \qquad \text{(E3)}$$

The order parameters (S values) of all analyzed systems are collected in Table 6.3.2 and Table 6.3.3 for 5 and 14-PCSL respectively.

Table 6.3.2 Values of the order parameter (S value) of 5-PCSL in POPE/POPG liposome in the absence and in the presence of hopanoid, BTAi1Δshc, HoLA and BTAi1Δshc plus hopanoid

Systems	S value
POPE/POPG(70:30)	0.64 ± 0.01
POPE/POPG/hopanoid	0.64± 0.01
POPE/POPG/BTAi1Δshc	0.64± 0.01
POPE/POPG/HoLA	0.67 ± 0.01
POPE/POPG/BTAi1Δshc/hopanoid	0.68 ± 0.01

Table 6.3.3 Values of the order parameter (S value) of 14-PCSL in POPE/POPG liposome in the absence and in the presence of hopanoid, BTAi1Δshc, HoLA and BTAi1Δshc plus hopanoid

Systems	S value
POPE/POPG(70:30)	0.27 ± 0.01
POPE/POPG/hopanoid	0.27± 0.01
POPE/POPG/BTAi1Δshc	0.25± 0.01
POPE/POPG/HoLA	0.32 ± 0.01
POPE/POPG/BTAi1Δshc/hopanoid	0.26 ± 0.01

Inspection of the Table 6.3.2 and Table 6.3.3 show that the presence of BTAi1Δshc causes a weak decrease of the dynamic of acyl chain lipids in the more interior region of the bilayer; free hopanoid doesn't change the microstructure of membrane, whereas HoLA induces an increase of S value in EPR spectra of both 5 and 14-PCSL spin labels. In addition the presence of the hopanoid moiety not covalently linked to BTAi1Δshc lipid A causes an increase of rigidity of hydrophilic region of the membranes.

6.4 Conclusions

In conclusion, DSC and EPR results are perfectly consistent and provide a clear interpretation on the effect of hopanoid and different lipid A in POPE/POPG membrane. Looking at the enthalpy changes for the different bilayer composition (Table 6.3.1), the following trend was observed : BTAi1Δshc mutant > POPE/POPG > Hopanoid > BTAi1Δshc mutant plus hopanoid > HoLA. Interestingly, EPR measurements show that the vesicles corresponding to the lower transition enthalpies have the more ordered liquid phase (i.e HoLA and BTAi1Δshc mutant plus free hopanoid), whereas the vesicles having the highest transition enthalpies correspond to the vesicles having the more disordered liquid phase (i.e. BTAi1Δshc mutant). This observation can be rationalized by noting that the liquid state is the final state of the gel-liquid transition measured by DSC. Keeping this in mind, it is reasonable that more ordered final states (thus liquid states retaining a major fraction of the intermolecular interactions characterizing the gel state) results in minor gel-liquid transition enthalpies. In other words, lower enthalpies of gel-liquid disordered transitions should correspond to more ordered and rigid liquid states (higher S values). In this frame, the results show that hopanoid and BTAi1Δshc in the lipid bilayer don't behave indipendently, but they show a preferential interaction and probably their affinity has prompted the nature to form a covalent in the unusual moiety named HoLA. In fact our results show that this particular covalently linked hopanoid-lipid A induces a more rigid and with lower fluidity liquid phase among the studied lipid components. These characteristics are evocative of an improved resistance and adaptation of *Bradyrhizobium BTAi1* strain in host environments.

References

(1) Silipo, A., Vitiello, G., Gully, D., Sturiale, L., Chaintreuil, C., Fardoux, J., Gargani, D., Lee, H. I., Kulkarni, G., Busset, N., Marchetti, R., Palmigiano, A., Moll, H., Engel, R., Lanzetta, R., Paduano, L., Parrilli, M., Chang, W. S., Holst, O., Newman, D. K., Garozzo, D., D'Errico, G., Giraud, E., and Molinaro, A. (2014) Covalently linked hopanoid-lipid A improves outer-membrane resistance of a Bradyrhizobium symbiont of legumes. *Nat Commun 5*, 5106.

(2) Murray, J. D. (2011) Invasion by invitation: rhizobial infection in legumes. *Mol Plant Microbe Interact 24*, 631-9.

(3) Zahran, H. H. (2001) Rhizobia from wild legumes: diversity, taxonomy, ecology, nitrogen fixation and biotechnology. *J Biotechnol 91*, 143-53.

(4) Delamuta, J. R., Ribeiro, R. A., Ormeno-Orrillo, E., Melo, I. S., Martinez-Romero, E., and Hungria, M. (2013) Polyphasic evidence supporting the reclassification of Bradyrhizobium japonicum group Ia strains as Bradyrhizobium diazoefficiens sp. nov. *Int J Syst Evol Microbiol 63*, 3342-51.

(5) Masson-Boivin, C., Giraud, E., Perret, X., and Batut, J. (2009) Establishing nitrogen-fixing symbiosis with legumes: how many rhizobium recipes? *Trends Microbiol 17*, 458-66.

(6) Lerouge, I., and Vanderleyden, J. (2002) O-antigen structural variation: mechanisms and possible roles in animal/plant-microbe interactions. *FEMS Microbiol Rev 26*, 17-47.

(7) Fraysse, N., Couderc, F., and Poinsot, V. (2003) Surface polysaccharide involvement in establishing the rhizobium-legume symbiosis. *Eur J Biochem 270*, 1365-80.

(8) Kannenberg, E. L., and Carlson, R. W. (2001) Lipid A and O-chain modifications cause Rhizobium lipopolysaccharides to become hydrophobic during bacteroid development. *Mol Microbiol 39*, 379-91.

(9) Ferguson, G. P., Datta, A., Baumgartner, J., Roop, R. M., 2nd, Carlson, R. W., and Walker, G. C. (2004) Similarity to peroxisomal-membrane protein family reveals that Sinorhizobium and Brucella BacA affect lipid-A fatty acids. *Proc Natl Acad Sci U S A 101*, 5012-7.

(10) Jahnke, L. L., Stan-Lotter, H., Kato, K., and Hochstein, L. I. (1992) Presence of methyl sterol and bacteriohopanepolyol in an outer-membrane preparation from Methylococcus capsulatus (Bath). *J Gen Microbiol 138*, 1759-66.

(11) Jurgens, U. J., Simonin, P., and Rohmer, M. (1992) Localization and distribution of hopanoids in membrane systems of the cyanobacterium Synechocystis PCC 6714. *FEMS Microbiol Lett 71*, 285-8.

(12) Simonin, P., Jurgens, U. J., and Rohmer, M. (1996) Bacterial triterpenoids of the hopane series from the prochlorophyte Prochlorothrix hollandica and their intracellular localization. *Eur J Biochem 241*, 865-71.

(13) Welander, P. V., Hunter, R. C., Zhang, L., Sessions, A. L., Summons, R. E., and Newman, D. K. (2009) Hopanoids play a role in membrane integrity and pH homeostasis in Rhodopseudomonas palustris TIE-1. *J Bacteriol 191*, 6145-56.

(14) Kleemann, G., Kellner, R., and Poralla, K. (1994) Purification and properties of the squalene-hopene cyclase from Rhodopseudomonas palustris, a purple non-sulfur bacterium producing hopanoids and tetrahymanol. *Biochim Biophys Acta 1210*, 317-20.

(15) Kulkarni, G., Wu, C. H., and Newman, D. K. (2013) The general stress response factor EcfG regulates expression of the C-2 hopanoid methylase HpnP in Rhodopseudomonas palustris TIE-1. *J Bacteriol 195*, 2490-8.

(16) Schmerk, C. L., Welander, P. V., Hamad, M. A., Bain, K. L., Bernards, M. A., Summons, R. E., and Valvano, M. A. (2015) Elucidation of the Burkholderia cenocepacia hopanoid biosynthesis pathway uncovers functions for conserved proteins in hopanoid-producing bacteria. *Environ Microbiol 17*, 735-50.

(17) Rezania, S., Amirmozaffari, N., Tabarraei, B., Jeddi-Tehrani, M., Zarei, O., Alizadeh, R., Masjedian, F., and Zarnani, A. H. (2011) Extraction, Purification and Characterization of Lipopolysaccharide from Escherichia coli and Salmonella typhi. *Avicenna J Med Biotechnol 3*, 3-9.

(18) White, D. A., Lennarz, W. J., and Schnaitman, C. A. (1972) Distribution of lipids in the wall and cytoplasmic membrane subfractions of the cell envelope of Escherichia coli. *J Bacteriol 109*, 686-90.
(19) Ruiz, N., Kahne, D., and Silhavy, T. J. (2006) Advances in understanding bacterial outer-membrane biogenesis. *Nat Rev Microbiol 4*, 57-66.
(20) Xu, X., and London, E. (2000) The effect of sterol structure on membrane lipid domains reveals how cholesterol can induce lipid domain formation. *Biochemistry 39*, 843-9.
(21) Hubbell, W. L., and McConnell, H. M. (1971) Molecular motion in spin-labeled phospholipids and membranes. *J Am Chem Soc 93*, 314-26.
(22) Gordon, L. M., and Sauerheber, R. D. (1977) Studies on spin-labelled egg lecithin dispersions. *Biochim Biophys Acta 466*, 34-43.

Pubblications

1) Amato J*, **Stellato MI***, Pizzo E, Petraccone L,Oliviero G, Borbone N, Piccialli G,Orecchia A, Bellei B, Castiglia D and Giancola C.

* These authors contributed equally as first authors.

PNA as a potential modulator of COL7A1 gene expression in dominant dystrophic epidermolysis bullosa: a physico-chemical study

Mol Biosyst. 2013;9(12):3166-74.

Abstract

Dominant diseases are single gene disorders occurring in the heterozygous state. The mutated allele exerts a dominant effect because it produces an abnormal polypeptide that interferes with the function of the normal allele product. Peptide Nucleic Acids (PNAs) offer a route for a potential therapy for dominant diseases by selectively silencing the allele carrying the dominant mutation. Here, we have synthesized and studied the properties of a 15-mer PNA fully complementary to the site of the c.5272-38T>A sequence variation, which identifies a recurrent mutant COL7A1 allele causing dominant dystrophic epidermolysis bullosa (DDEB), a mendelian disease characterized by skin blistering. The PNA was conjugated with four lysine residues at the C-terminus and a fluorescent probe at the N-terminus. Physico-chemical results proved the formation of a stable, selective PNA/mutant-DNA heteroduplex in vitro. Intriguingly, when transfected into normal human fibroblasts, the PNA correctly localized in the cell nucleus. Our results open new therapeutic possibilities for patients with DDEB.

2) Oliva R, Del Vecchio P, **Stellato MI**, D'Ursi AM, D'Errico G, Paduano L, Petraccone L.

A thermodynamic signature of lipid segregation in biomembranes induced by a short peptide derived from glycoprotein gp36 of feline immunodeficiency virus.

Biochim Biophys Acta. 2015 Feb;1848(2):510-7.

Abstract

The interactions between proteins/peptides and lipid bilayers are fundamental in a variety of key biological processes, and among these, the membrane fusion process operated by viral glycoproteins is one of the most important, being a fundamental step of the infectious event. In the case of the feline immunodeficiency virus (FIV), a small region of the membrane proximal external region (MPER) of the glycoprotein gp36 has been demonstrated to be necessary for the infection to occur, being able to destabilize the membranes to be fused. In this study, we report a physicochemical characterization of the interaction process between an eight-residue peptide, named C8, modeled on that gp36 region and some biological membrane models (liposomes) by using calorimetric and spectroscopic measurements. CD studies have shown that the peptide conformation changes upon binding to the liposomes. Interestingly, the peptide folds from a disordered structure (in the absence of liposomes) to a more ordered structure with a low but significant helix content. Isothermal titration calorimetry (ITC) and differential scanning calorimetry (DSC) results show that C8 binds with high affinity the lipid bilayers and induces a significant perturbation/reorganization of the lipid membrane structure. The type and the extent of such membrane reorganization depend on the membrane composition. These findings provide interesting insights into the role of this short peptide fragment in the mechanism of virus-cell fusion, demonstrating its ability to induce lipid segregation in biomembranes.

3) Berisio R, Squeglia F, Ruggiero A, Petraccone L, **Stellato MI**, Del Vecchio P.

Differential thermodynamic behaviours of the extra-cellular regions of two Ser/Thr PrkC kinases revealed by calorimetric studies.

Biochim Biophys Acta. 2015;1854(5):402-9.

Abstract

Eukaryotic-type Ser/Thr protein-kinases are critical mediators of developmental changes and host pathogen interactions in bacteria. Although with lower abundance compared to their homologues from eukaryotes, Ser/Thr protein-kinases (STPK) are widespread in gram positive bacteria, where they regulate several cellular functions. STPKs belong to the protein kinase family named as one-component signal transduction systems, which combine both sensing and regulating properties. Thermodynamic investigations of sensing extra-cellular portions of two important Ser-Thr kinases, PrkC, from Staphylococcus aureus and Bacillus subtilis were conducted by differential scanning calorimetry (DSC) and circular dichroism (CD) melting measurements, coupled with modelling studies. The study of thermodynamic properties of the two domains is challenging since they share a modular domain organization. Consistently, DSC and CD data show that they present similar thermodynamic behaviours and that folding/unfolding transitions do not fit a two-state folding model. However, the thermal unfolding of the two proteins is differentially sensitive to pH. In particular, their unfolding is characteristic of modular structures at the neutral pH, with independent contributions of individual domains to folding. Differently, a cooperative unfolding is evidenced at acidic pH for the B. subtilis member, suggesting that a significant interaction between domains becomes valuable

4) Stellato MI, Lombardi L, Petraccone L, D'Errico G, Falanga A, Galdiero S, Del Vecchio P.

Physical-chemical characterization of the interaction of the antimicrobial peptide *Myxinidin* and its mutant WMR with liposomes mimicking *P. aeruginosa* and *E. coli* cell membranes.
In preparation